KARADENİZ TECHNICAL UNIVERSITY

THE GRADUATE SCHOOL OF APPLIED SCIENCES

ELECTRICAL-ELECTRONICS ENGINEERING DEPARTMENT

DESIGN AND OPTIMIZATION OF A FUZZY LOGIC BASED MAXIMUM POWER POINT TRACKER FOR PV PANEL

MASTER OF SCIENCE THESIS

Electrical-Electronics Eng. Adem KOCABAŞ

JUNE 2017

TRABZON

KARADENİZ TECHNICAL UNIVERSITY

THE GRADUATE SCHOOL OF NATURAL AND APPLIED SCIENCES

ELECTRICAL-ELECTRONICS ENGINEERING DEPARTMENT

DESIGN AND OPTIMIZATION OF A FUZZY LOGIC BASED MAXIMUM POWER POINT TRACKER FOR PV PANEL

Electrical-Electronics Eng. Adem KOCABAŞ

This thesis is accepted to give the degree of

"MASTER OF SCIENCE"

By

The Graduate School of Natural and Applied Sciences at
Karadeniz Technical University

The Date of Submission : 30 / 05 /2017

The Date of Examination : 22 / 06 /2017

Supervisor : Assoc.Prof.Dr. Halil İbrahim OKUMUŞ

Trabzon 2017

KARADENİZ TECHNICAL UNIVERSITY

THE GRADUATE SCHOOL OF NATURAL AND APPLIED SCIENCES

ELECTRICAL-ELECTRONICS ENGINEERING DEPARTMENT

Adem KOCABAŞ

DESIGN AND OPTIMIZATION OF A FUZZY LOGIC BASED MAXIMUM POWER POINT TRACKER FOR PV PANEL

Has been accepted as a thesis of

MASTER OF SCIENCE

after the Examination by the Jury Assigned by the Administrative Board of the Graduate School of Natural and Applied Sciences with the Decision Number 1705 dated

06 / 06 / 2017

Approved By

Chairman	:	**Prof.Dr. Saadettin AKSOY**	.....
Member	:	**Assoc.Prof.Dr. Halil İbrahim OKUMUŞ**	.....
Member	:	**Asst.Prof.Dr. Hakan KAHVECİ**	.....

Prof. Dr. Sadettin KORKMAZ

Director of Graduate School

ACKNOWLEDGEMENTS

I would like to express my gratitude to my supervisor, Assoc. Prof. Dr. Halil İbrahim OKUMUŞ, whose expertise, knowledge and farsightedness guided me during my researches. I applaud his wide knowledge in many areas and his friendliness.

Also, I would like to thank to my colleagues, Türk Telekom Family, who have always supported me throughout my studies.

Lastly, I would like to express my thankfulness to my dear mother and father, who have brought me to the present. They have always encouraged and inspired me all my life. I dedicate this thesis to my departed brother in law Dr. Harun ÖZDEMİR. May he rest in peace.

Adem KOCABAŞ

Trabzon 2017

THESIS STATEMENT

I hereby declare that all the information contained in this master thesis titled ‘Design and Optimization of a Fuzzy Logic Based Smart Solar Power Maximum Power Point Tracker’ is a result of my works under the supervision of Assoc. Prof. Dr. Halil İbrahim OKUMUŞ and with accordance with academic rules and ethical conduct. I also declare that, as required by these rules and conduct, I have fully acknowledged and cited all the material and results that are not originating directly from this work. 22.06.2017

Adem KOCABAŞ

TABLE OF CONTENTS

Yüksek Lisans Tezi

ÖZET

PV PANELLER İÇİN BULANIK MANTIK TABANLI MAKSİMUM GÜÇ NOKTASI İZLEYİCİSİ TASARIMI VE OPTİMİZE EDİLMESİ

Adem KOCABAŞ

Karadeniz Teknik Üniversitesi
Fen Bilimleri Enstitüsü
Elektrik-Elektronik Mühendisliği Anabilim Dalı
Danışman: Doç. Dr. Halil İbrahim OKUMUŞ
2017, 92 Sayfa

Günümüzde fosil yakıt kaynaklarının sınırlı miktarda olması, küresel ısınma ve yüksek ham petrol fiyatlarından dolayı araştırmalar ve yatırımlar yenilenebilir enerji üretim sistemleri üzerinde yoğunlaşmıştır. Güneşten gelen enerji sonsuzdur ve bir bedeli yoktur. Bu nedenle tüm yenilenebilir enerji üretimi yöntemleri arasında araştırmacılar tarafından en çok ilgiyi güneş enerjisi üretimi çekmiştir. Güneş enerjisi üretiminde verimlilik en önemli temel öğelerden biri olduğundan dolayı maksimum güç noktası izleyicileri güneş enerjisi üretiminde kullanılan güneş enerjisi yönetim sistemleri açısından önemli bir göreve sahiplerdir. Bu çalışma en iyi performansı elde etmek için bulanık mantık tabanlı maksimum güç noktası izleyicisinin tasarımı, geliştirilmesi ve metodolojisi hakkında bilgiler içermektedir. Maksimum güç noktası izleyicisi DA-DA dönüştürücülerin empedans dönüştürme yeteneği ile bulanık mantık teorisinin birlikte kullanılması ile değerlendirilmiştir. Bulanık mantık sonuç çıkarma sisteminin parametreleri en hızlı ve tutarlı sistem tepkilerini elde edebilmek için optimize edilmiştir. Çeşitli izleme algoritmaları tanıtılmıştır. Bulanık mantık sonuç çıkarma sisteminde kullanılan asimetrik ve simetrik üyelik fonksiyonlarının etkileri incelenmiş ve birbirleriyle karşılaştırılmıştır. Önerilen bulanık mantık tabanlı maksimum güç noktası izleyicisinin değişik çalışma koşullarındaki performansı karşılaştırılmış ve bu performansın iyileştirilmesine çalışılmıştır. Önerilen maksimum güç noktası izleyicisi sisteminin şebekeden bağımsız ve şebekeye bağlı uygulamalarda geçerliliği kanıtlanmıştır. Bulanık mantıkla maksimum güç noktası izleme işlevi artan-azaltan dönüştürücüsü ile gerçekleştirilmiştir. Benzetim çalışmaları tatbik edilmiş ve de benzetim sonuçları sunulmuştur Benzetim çalışmaları Matlab Simulink ortamında gerçekleştirilmiştir.

Anahtar Kelimeler: Maksimum güç noktası izleme, Bulanık mantık kontrol, Güneş enerjisinden elektrik üretimi.

Master Thesis

SUMMARY

DESIGN AND OPTIMIZATION OF A FUZZY LOGIC BASED MAXIMUM POWER POINT TRACKER FOR PV PANEL

Adem KOCABAŞ

Karadeniz Technical University
The Graduate School of Natural and Applied Sciences
Electrical-Electronics Engineering Graduate Program
Supervisor: Assoc. Prof. Dr. Halil İbrahim OKUMUŞ
2017, 92 Pages

Today, because of the limits of fossil fuel resources, global warming and high crude oil prices researches and investments are focused on renewable energy generation systems. Energy from the sun is almost endless and free. So that, among all renewable energy generation methods, solar power generation has attracted the most attention by the researchers. As the issue of efficiency is one of the most important fundamental of solar power generation, maximum power point tracking systems have an important duty in solar power management systems in solar power generation. This study includes study of the design and improvement of fuzzy logic based solar power maximum power point tracker, and the methodology to achieve the best system performance. Maximum power point tracker system was evaluated at the DC-DC power converters' ability of impedance conversion point of view and cooperation of fuzzy logic theory. The parameters of fuzzy inference system were optimized to obtain the fastest and accurate system responses. Various tracking algorithms were introduced. Affects of symmetrical and asymmetrical membership functions used in fuzzy inference system were examined and compared with each other. The performance of the proposed fuzzy logic based maximum power point tracker under various operating conditions were compared and improvement of this performance is dealt with. Validity of the proposed maximum power point tracking system in standalone and grid connected applications was proved. The fuzzy logic maximum power point tracking function was realized by using a buck-boost power converter. Computer simulations were practiced and simulation results were also represented. Computer simulations were carried out in the Matlab Simulink environment.

Key Words: Maximum power point tracking, Fuzzy logic control, Solar power generation.

LIST OF FIGURES

Page

LIST OF TABLES

Page

NOTATIONS

MPPT	Maximum Power Point Tracker
AC	Alternating Current
DC	Direct Current
FF	Fill Factor
FIS	Fuzzy Inference System
I	Current
INC	Incremental Conductance
MF	Membership Function
MPP	Maximum Power Point
NB	Negative Big
NS	Negative Small
PB	Positive Small
PLL	Phase Locked Loop
PO	Perturb and Observe
PS	Positive Big
PSO	Particle Swarm Optimization
PV	Photovoltaic
P-V	Power versus Voltage
PWM	Pulse Width Modulation
STC	Standard Test Conditions
UOD	Universe of Discource
V	Voltage
VSC	Voltage Source Converter
ZE	Zero
dI	Derivative of Current
dV	Derivative of Voltage
I_D	Dark current
I_0	Saturation current
V_C	Cell voltage

q	Charge of an electron
a	Diode ideality constant
k	Boltzman constant
T_{cK}	Cell temperature
I_L	Light generated current
I_D	Diode current
R_s	Series resistance
R_{sh}	Parallel resistance
G	Irradiation
G_{ref}	Reference irradiation
I_{sc}	Short circuit current
T_{ref}	Reference temperature
T_{ref}	Operating temperature
K_I	PV cell's short-circuit current temperature coefficient
V_{oc}	Open circuit voltage
P_{max}	Maximum power
V_{mpp}	Voltage at maximum power point
I_{mp}	Current at maximum power point
I_{PV}	Cell current
V_{PV}	Cell voltage
I_R	Load current
V_R	Load voltage
R	resistance
D	Duty cycle
P_{PV}	Cell power
dP_{PV}	Derivative of cell power
dV_{PV}	Derivative of cell voltage
dIpv	Derivative of cell current
Δt	Variation of time
e(t)	Error
de(t)	Derivative of error

X	Space of points
x	Generic element of X
$\mu_A(x)$	Fuzzy set A
max	Maximum
min	Minimum
z_{COG}	Output of centre of gravity method
L	Inductance
C	Capacitance
ΔP	Variation of power
ΔV	Variation of voltage
ΔI	Variation of current
Δe	Variation of error
Δd	Variation of duty cycle
ΔP_{PV}	Variation of cell power
ΔV_{PV}	Variation of cell voltage
ΔI_{PV}	Variation of cell current
S	P-V slope
ΔS	Variation of P-V slope
η	Efficiency
E	Energy
E_{max}	Maximum energy

1. GENERAL INFORMATION

1.1. Introduction

Among all supplies of power on the earth the most harmless and cleanest, plentiful one is the energy that comes from the sun. As the solar power is almost unfailing, it is going to take place as our fundamental energy supply [1,2]. It has a wide range of application area in our daily life. There are some factors that affect the performance of solar energy harvesting. These are the conditions like insolation, sunlight tilt, load variations, airmass and cell temperature. Power converter units should be associated with the PV cells in order to regulate transfer of power from cells. Maximum power point tracking systems are used to maximize power output, by the ability of continually arranging the conduction period of the switching device in the power converter unit. Algorithms that are used in MPPT systems maximize the power extractions of PV cells by controlling the conduction period of the power converter with the changing PV cell output variable combinations like changes in power versus changes in voltage etc. MPPT algorithms such as perturb and observe, incremental conductance have been evaluated until now. [3]. Unchanging units of the control signal are used in these methods. Too small steps sizes cause slow tracking process and too large step sizes cause oscillations when the highest power extraction level is reached.

Fuzzy logic tracking methods are developed to perform self adjusting step units [4-8]. Specification of fuzzy logic controllers is made according to their skill of simulating human thinking. Different than conventional controllers, fuzzy controllers have the ability to use experimental methods and their results to design variable step sizes of control signals without the need of understanding the system's mathematical model [9].

Effectiveness of the MPPT algorithm is directly related with the variables that are chosen as inputs and outputs. In general for outputs, power switch's duty ratio is selected. As input variables; various combinations of power (P) versus voltage (V)/ current (I) slope and its error, sum of conductance and increment of conductance would be selected [8].

1.2. Literature Review

In this study MPPT system is considered by the ability of adjusting the operating point of PV cell by using its voltage and current parameters; a physical tracking method not mentioned. There have been several MPPT techniques developed so far. These techniques can be listed as Incremental Conductance, Perturb and Observe, Artificial Neural Network, Fuzzy Logic Control, Particle Swarm Optimization, Genetic Algorithms. There are some advantages and drawbacks of these techniques. A review of these techniques is made below paragraphs.

Incremental conductance method basically aims to obtain PV system to work at MPP by using adaptive voltage step size changes based on PV characteristics. MPP is tracked by examining the highest point of P-V curve. This technique uses I/V and dI/dV parameters in calculations of input values. Liu et al. [48] proposed a variable step size INC method in their study. This method had an improved ability of accurate and fast responses to the changes in irradiation level. And also oscillations are eliminated when MPP reached. But in terms of the cost this method is expensive due to the need of complex sampling and speed control mechanisms. Adly et al. [49] proposed a MPPT system by combining INC method and DC-DC power converters and tested the system performance in rapid changing environmental conditions. Nearly 15% more power extraction obtained in this method. Wolfs and Li [50] proposed a MPPT method using INC. In this study they have used power converters and this topology doesn't need current sensors.

Perturb and observe method has a simple working principle. In this method PV cell/array is perturbed in the direction of irradiation change. If the power extraction increased the operating point approaches the MPP and so the voltage perturbation is continued at the same direction. If the power extraction decreased the operating point moves away from the MPP and so the direction of voltage perturbation is needed to be changed. This method's main drawback is the oscillations at the steady state. Liu et al. [51] in their study have tried the solve oscillation problem. In this method change in output power is calculated. If it is positive the operating voltage would be increased, if it is negative the operating voltage would be decreased. Al-Amoudi and Zhang [52] have proposed a method that uses variable step sizes. But this method has drawbacks because step sizes are defined previously by the operator and system can not work at desired performance due to changing operating

conditions. Suganya and Carolin Mabel [53] have improved a perturb and observation method that operates at desired performance at unchanging irradiation conditions.

Artificial neural network based techniques has better performance at changing environmental conditions and steady state. Ciabattoni et al. [54] have proposed a home energy management system using neural network. The system monitors the loads, estimates the PV energy production and home energy consumption. Sheraz and Abido [55] have achieved to overcome the rapidly changing irradiation and temperature conditions by using differential evolution and artificial neural network. Elobaid et al. [56] have studied on two stage artificial network based MPPT that has the ability to estimate the operating conditions from the current and voltage signals in order to find the MPP. This method works at desired performance at changing operating conditions and steady state. Chiu et al. [57] have studied on piecewise line segments using artificial neural network technique. This method has high response speed and low complexity. The system reacts well to the suddenly changing working conditions. Anitha and Prabha [58] tried to eliminate slow and incorrect tracking, oscillations. They have used boost converters for tracking. Back propagation feed forward trained neural networks introduced in this study.

Fuzzy logic based techniques implements fuzzy logic theory on MPPT system. Sreekumar and Benny [59] proposed a MPPT technique that uses fuzzy logic theory and boost converters. This method has a high speed of tracking but tracking can not be practiced at all ranges of P-V curve of PV cell/array. Hossain et al. [60] have studied on a method that uses fuzzy logic theory to adjust power converter's duty ratio to overcome the non-linearity characteristics of PV cell. Adly et al. [49] have compared fuzzy logic based MPPT and incremental conductance method in their study. They have used dc-dc converters in MPPT system. Wang et al. [61] have proposed a system that uses fuzzy logic theory in a hybrid electric car power supply system. Chin et al. [62] have studied on fuzzy logic based MPPT and its performance under partial shading conditions. In this this study perturb and observe method and fuzzy logic theory were combined. This method had achieved higher accuracy and response speed. Kulaksız and Aydoğdu [63] have proposed an artificial neural network based MPPT using fuzzy logic controller. They have used fuzzy theory to control duty cycle of dc-dc buck converter.

Particle swarm optimization technique aims to eliminate fluctuations when the MPP reached. It has higher performance in partial shading conditions and high fluctuations in solar irradiations. This method has higher tracking accuracy but response speed to the

instantaneous changes in environmental conditions is lower. It has a simple system configuration and faster calculations. Miyatake et al. [64] proposed a topology that is able to minimize power loss during partial shading conditions. It has divided PV system into small segments and configured the converters so that can control the unbalanced current flow through the segments. Phimmasone et al. [65] had improved this method by adding a term that has a repulsive force to the PSO agent to estimate the best voltage at operating conditions. That has improved the efficiency and the accuracy of MPPT system. Isaque [66] had modified the classical PSO method. In this study maximum change in velocity limited to a predetermined value. This method has more accurate and fast tracking ability compared to the classical PSO method, and in partial shading conditions system works more efficiently.

Ramaprabha and Mathur [67] studied on a MPPT system using genetic algorithm for partial shading conditions. This algorithm basically uses genetic and evolution biological behavior.

1.3. Purpose of the Study

This study aims to eliminate PV systems' power extracting dependency to varying load conditions and develop a MPPT method by using fuzzy control theory that has the capabilities;

- Rapid tracking response to the changing load and environmental conditions
- Capability of tracking the MPP for wide ranges of solar radiation and temperature
- Accuracy and no oscillation around the MPP
- Ease of implementation
- Low cost

In this study, PV maximum power point tracking systems were analyzed under two main topics: firstly, the influence of the dc-dc converter on the tracking quality was considered. The effect of solar radiation, temperature and load variations are considered and the tracking performance of Buck, Boost and Buck-Boost converters were compared. Secondly, tracking algorithms using different types of membership functions were introduced. The advantages concerning the proposed method come from the simplicity, low

cost, digital implementation, fast tracking response, accuracy and very small oscillations around the MPP on steady state.

1.4. Solar Energy Generation

1.4.1. Relationship Among PV Cell, Module and Array

PV cells are the electrical devices that have the ability to convert energy from the sunlight to the electricity. PV cell groups are connected serial and parallel to form PV module and arrays, by this way the desired current and voltage levels are obtained. Power extraction performance of a PV cell depends on some conditions. These are; the radiation, the temperature, the spectral characteristics of sunlight, shadows conditions, and the dirt [23,24]. The relation among PV cell, module and array is shown in Figure 1 [9].

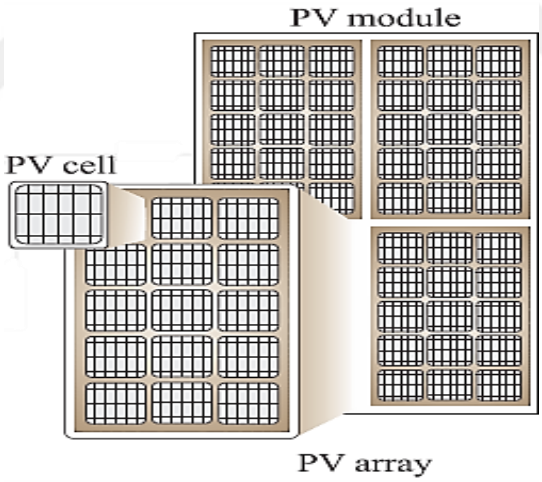

Figure 1. The relation between PV cell, module and array.

1.4.2. PV Cell Efficiency

Efficiency of PV cell is a performance index that indicates the percentage of the power produced by the PV cells and the potential power that can be generated from the sunlight. The higher efficiency means that the higher ability of conversion of light energy into electricity with using same surface area. Most of the commercial PV cells at the market have the efficiency value between 15 % and 22 %. To determine the efficiency, the panels are

tested at Standard Test Conditions. STC determines that a temperature of 25°C and an irradiance of 1000W/m^2. This is the equivalent of a sunny day with the incident light hitting a sun-facing 37°-tilted surface. Under these test conditions, a solar cell of 15% efficiency with a 100 cm^2 surface area would produce 1.5 W.

There are basically three types of solar panels, which differ in efficiency and cost.

- Thin-film solar panels
- Monocrystalline cells
- Polycrystalline cells

Monocrystalline solar cells have a efficiency rate between 20 % and 22 % and they are produced from very pure silicon.

Polycrystalline cells have a efficiency rate between 14 % and 16 %. They are also called multicrystalline cells.

Thin-film cells have a efficiency rate between 7 % and 12 %. They are produced from amorphous silicon.

A lot of investments and researches have been made so far to increase the efficiency rates of solar cells. In the last three years this rate has been enhanced from 5 % to 17 %. By the year 2015 the Fraunhofer Institute for Solar Energy Systems ISE, declared that they have achieved to produce PV cells which has a efficiency of 44.7 % As solar power becomes more popular, it is estimated that in the near future the goal of 50% efficiency will be reached [35].

1.4.3. PV Cell Model

In solar cells P-N unions are used. These P-N unions' characteristics are very similar to those of the diodes. So that we can use the equation of Shockley (1) to determine the characteristics of a solar cell [10].

$$I_D = I_{0.}\left(e^{\frac{V_{c.}.q}{a.k.T_{cK}}} - 1 \right) \tag{1}$$

where;

- "I_D" is dark current (A),
- "I_0" is saturation current of the diode (A),
- "V_C" is cell voltage (V),
- "q" is the charge of an electron,
- "a" is the diode ideality constant,
- "k" is the Boltzmann's constant
- "T_{cK}" is the cell temperature.

The relation among the net current I, light generated current I_L and the normal diode current I_D is defined by the equation (2).

$$I = I_L - I_D \tag{2}$$

In addition equation (3) presents the simplified model as shown in Figure 2.

$$I = I_L - I_{0.}\left(e^{\frac{(V+I.R_S).q}{a.k.T_{CK}}} - 1 \right) \tag{3}$$

So that equivalent circuit of a ideal solar cell can be represented as shown in Figure 2 with an ideal current source in anti-parallel with a diode.

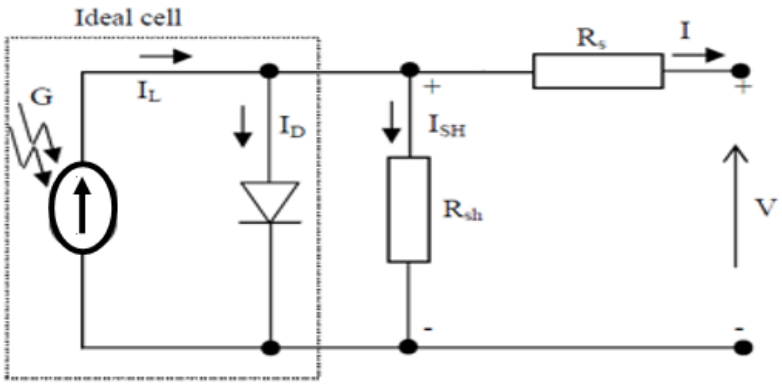

Figure 2. Equivalent circuit for PV modules.

In practice solar cells have some losses. These losses occur because of the resistance in series (R_s) and another in parallel (R_{sh}). The final model is as shown in Figure 2.

If we take account these resistances equation (3) can be written as (4).

$$I = I_L - I_{0.}\left(e^{\frac{(V+I.R_S).q}{a.k.T_{CK}}} - 1 \right) - \frac{V + IR_s}{R_{sh}} \tag{4}$$

The photocurrent mainly depends on the solar insolation and cell's working temperature, which is described as [11,12]

$$I_L = \left[I_{SC} + K_I \left(T_C - T_{ref} \right) \right] \frac{G}{G_{ref}} \tag{5}$$

where I_{sc} = solar cell short-circuit current, G_{ref} = reference solar insolation in W/m^2, T_{ref} = cell's reference temperature, T_c= operating temperature, K_I = cell's short-circuit current temperature coefficient, and G = solar insolation in W/m^2.

There is another important characteristic of PV cells, which is called fill factor (FF). PV cells usually have a FF somewhere between 0.4 and 0.8; ideal PV panels have a Fill Factor of 1.0. The Fill Factor (FF) is the ratio of the maximum power point (P_{max}) divided by open circuit voltage V_{oc} and short circuit current I_{sc} [13].

$$FF = \frac{P_{\max}}{V_{OC}.I_{SC}} \tag{6}$$

Figure 3 shows the current-voltage (I-V) characteristics of a typical silicon PV cell operating under STC. The power delivered by a solar cell is the product of current and voltage (I x V). If the multiplication is done, point for point, for all voltages from short-circuit to open-circuit conditions, the power curve above is obtained for a given radiation level [14].

When the solar cell open circuited no current flows between the two terminals of the solar cell and the voltage across the cell is at maximum. This is called open circuit voltage V_{oc}. When the solar cell is short circuited the voltage across the cell is at its minimum (zero) but the current flowing out of the cell reaches its maximum, known as the solar cells short

circuit current, or I_{sc}. In the short circuit and open circuit conditions electrical power is not being generated. But these values determine the ranges of I-V curves.

There is another term that is called maximum power point. At this point solar cell generates maximum power. At maximum power point the current and voltage values are defined as I_{mpp} and V_{mpp}.

At MPP, $V_{mpp} \cong (0.8–0.90)V_{oc}$ and $I_{mp} \cong (0.85–0.95)I_{sc}$. The MPP varies with the changing temperature and irradiance levels.

In a PV array several cells are connected parallel and serial. The I-V characteristic of a PV array is shown in Figure 4.

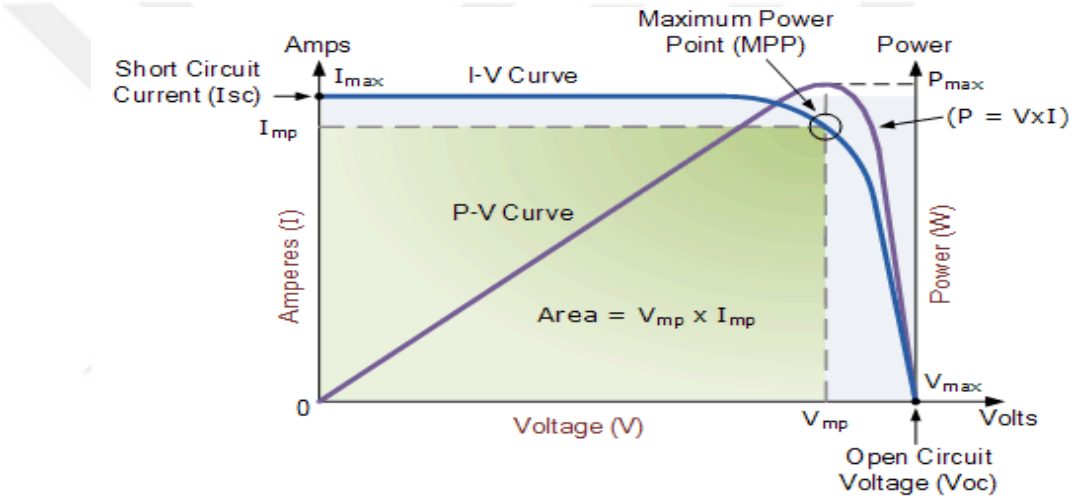

Figure 3. Current-voltage (I-V) characteristics of a typical silicon PV cell.

To increase the power generation capacity, solar cells are connected in serial and parallel. When they are connected in serial, the voltage is increases and when they are connected in parallel the current produced is increases. By both two ways the power generation is being increased.

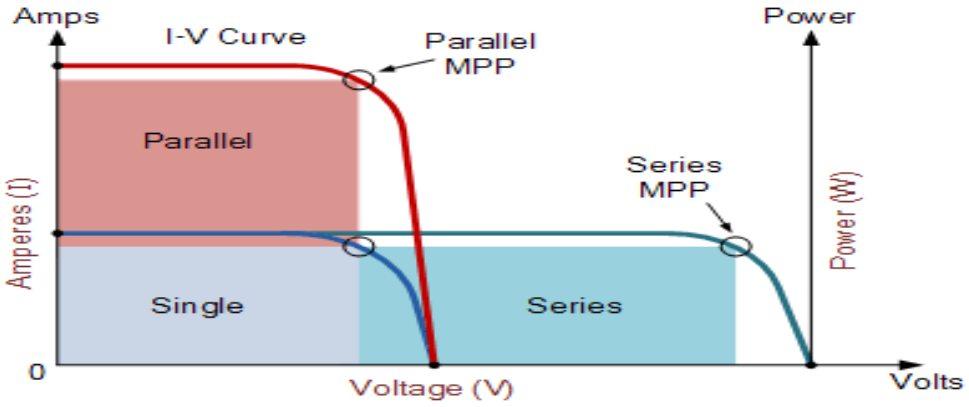

Figure 4. I-V curve of a PV panel composed of series and parallel connected cells.

I-V and P-V characteristics of any given PV cell at different temperature and irradiance conditions are shown below.

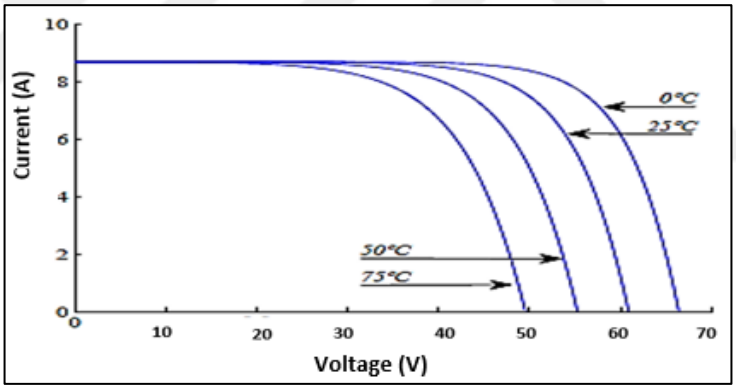

Figure 5. I-V characteristics for the temperature variation between 0 and 75ºC.

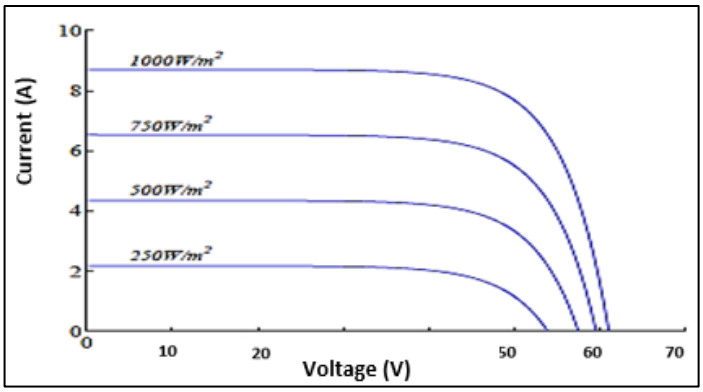

Figure 6. I-V characteristics for various conditions of solar radiation.

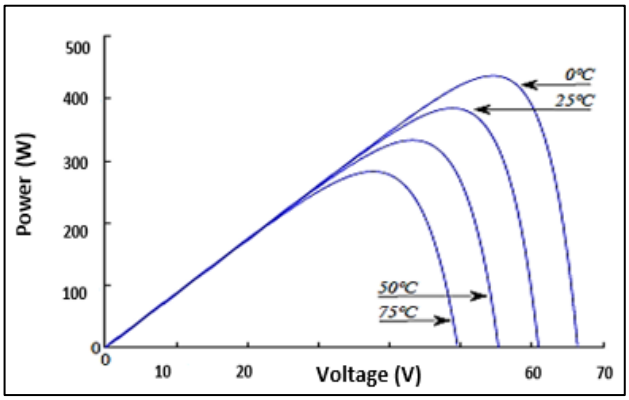

Figure 7. P-V characteristics for the temperature variation between 0 and 75ºC.

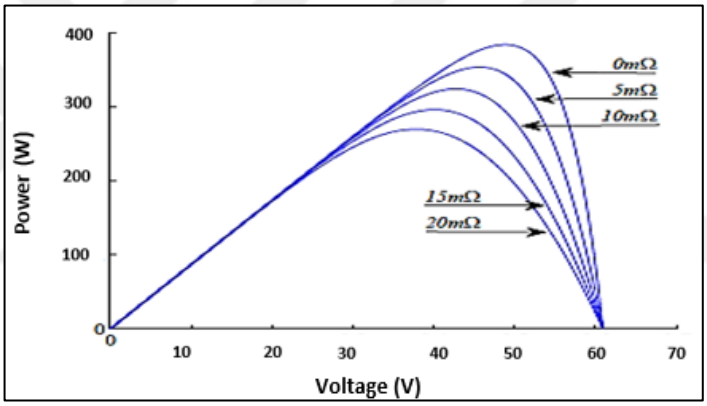

Figure 8. P-V characteristics for the R_s variation.

1.5. Solar Maximum Power Point Tracking System

Conversion of the energy from the sun to the electricity is maximized when PV device operates at the maximum power point. The operating point varies along the I-V plan of the solar cell because of changing radiation and temperature levels as shown in Figure 9.

We need special circuits to make the PV system operate at the MPP dynamically with the changing irradiation and temperature levels. These circuits are known as Maximum Power Point Trackers (MPPT) [18,19].

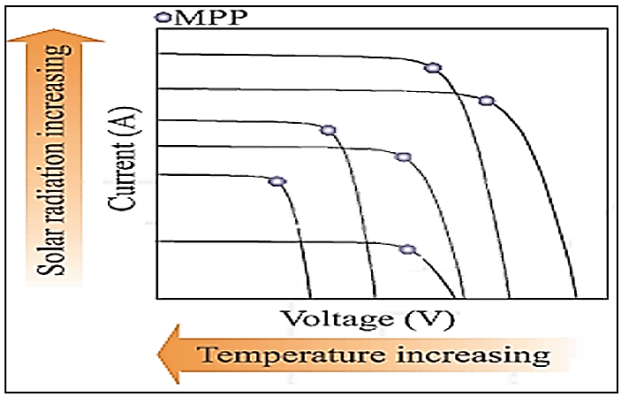

Figure 9. MPP on the I-V plan with changing solar radiation and temperature levels.

Studies about MPPT systems concern two side of the problem. One is the hardware, dc-dc converters and load types and the other one is the software that is about tracking algorithm.

1.5.1. Maximum Power Point Tracking System Combining DC-DC Power Converters

The operating point of PV system is the intersection point of the I-V curve and load curve. As shown in Figure 10, to understand operating point, first of all we will work with a resistive load.

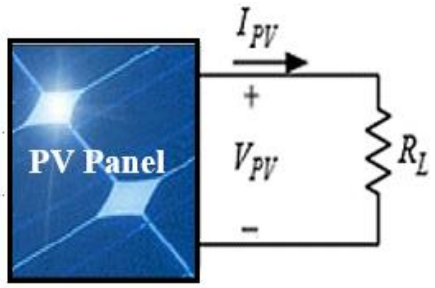

Figure 10. PV system with resistive load

The load curve is derived from the Ohm's law with the equation (7). PV I-V curve and load curve are represented in Figure 11.

$$I_{PV} = \frac{V_{PV}}{R} \tag{7}$$

We can not be sure that maximum power transfer to the load for a long period of time is guaranteed, even if the load curve and I-V curve intersects at the MPP, becuse the MPP changes when the irradiation and temperature changes [15-18].

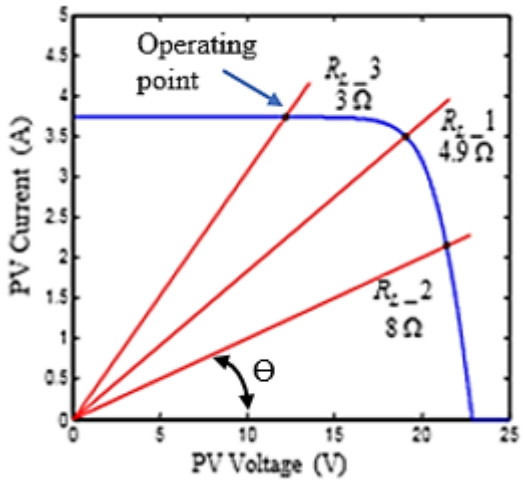

Figure 11. Operating points of the system.

To overcome this issue and set the operating point to the MPP continually, the load curve is needed to be rearranged according to the irradiation and temperature changes. This is possible when a smart system is placed between the load and the PV device. By using a dc-dc power converter and changing its duty cycle a variable load can be emulated from the PV device's terminals. The topology shown in Figure 12, composed by a PV module, a dc-dc converter and a load, defines the hardware of a maximum power point tracking system.

There is an important point, the tracking systems behaves differently because of the dc-dc converter and load types features. In this study buck, buck-boost, boost, Cuk, SEPIC and zeta converters will be examined in association with resistive load-types.

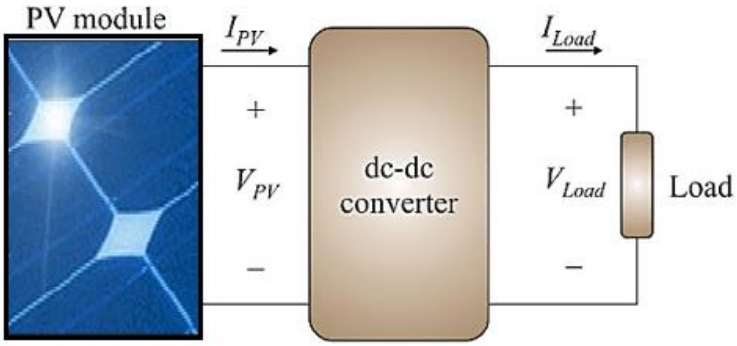

Figure 12. Maximum point tracker system.

1.5.2. Examinations for Resistive Load-Type

When a resistive load is connected to the dc-dc converter, Figure 12 may be redrawn as Figure 13 and equation (8) can be derived.

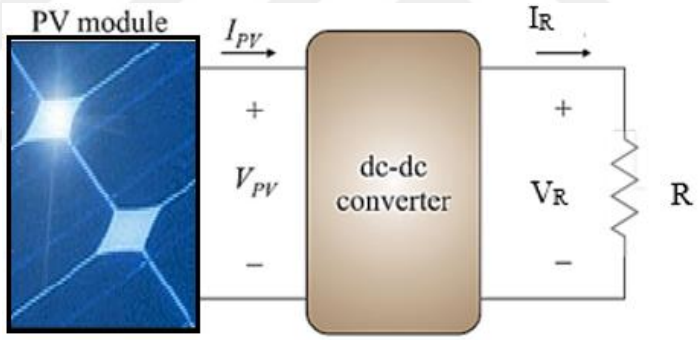

Figure 13. MPPT with resistive load.

$$V_R = R.I_R \tag{8}$$

If the static gain of the converter is G, the relationship between V_{PV}/I_{PV} and V_R/ I_R is defined as (9) and (10) [15-18].

$$G = \frac{V_R}{V_{PV}} \tag{9}$$

$$G = \frac{I_{PV}}{I_R} \tag{10}$$

We can derive equation (11) by rearranging equations (9) and (10).

$$\frac{V_{PV}}{I_{PV}} = \frac{R}{G^2} = R_{eff.} \tag{11}$$

V_{PV}/ I_{PV} is the effective resistance, R_{eff}, that is seen from the terminals of the PV device. Thus, the dc-dc converter emulates a variable resistance. The value of this variable resistance can be adjusted by changing the the gain G. Figure 13 can be redesigned as in Figure 14 and (12) can be written.

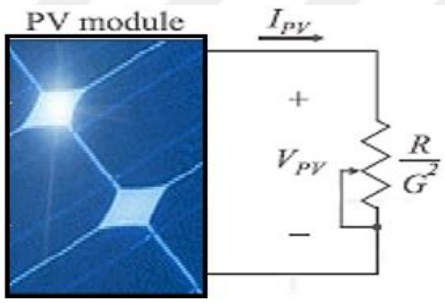

Figure 14. PV system with the effective load.

$$V_{PV} = \frac{R}{G^2} I_{PV} \tag{12}$$

Equation (12) is a straight line with an inclination angle θ. θ can be modified with the changing static gain G as in (13) [15-18].

$$\theta = \arctan\left(\frac{I_{PV}}{V_{PV}}\right) = \arctan\left(\frac{G^2}{R}\right) \tag{13}$$

Static gain is represented as a function of the duty cycle D in Table 1. By replacing static gain with the values in Table 1, the inclination angle θ can be written as in Table 2.

Table 1. Static gains of different types of dc-dc converters.

DC-DC Power Converter	Static Gain
Buck	G=D
Boost	G=1/(1-D)
Buck-boost, Cuk, SEPIC and zeta	G=D/(1-D)

Table 2. Load curve inclination angle (in degrees) as a function of the converter duty cycle D.

DC-DC Power Converter	Effective Load Inclination Angle θ
Buck	$\theta = \arctan\left(\frac{D^2}{R}\right)$
Boost	$\theta = \arctan\left(\frac{1}{(1-D)^2 R}\right)$
Buck-boost, Cuk, SEPIC and zeta	$\theta = \arctan\left(\frac{D^2}{(1-D)^2 R}\right)$

Duty cycle varies between 0 and 1. So that the effective inclination angle is limited according to the type of dc-dc converter. For example for buck converter when duty cycle D is 0 (14) is found.

$$\theta|_{D=0} = \arctan\left(\frac{0^2}{R}\right) = 0 \tag{14}$$

If the duty cycle D=1, (15) can be written.

$$\theta|_{D=1} = \arctan\left(\frac{1}{R}\right) \tag{15}$$

If we apply these equations to all types of converters, we can obtain Table 3 and Figure 15. It can be observed from table 3 that effective load inclination angle determines the region of maximum power point tracking on the I-V plan.

The dc-dc converter can emulate a suitable effective load in this tracking region of I-V plan, so that the load curve and the I-V characteristic curve intersect at the MPP and

maximum power transfer is guaranteed. When irradiation or temperature changes, the I-V characteristic curve changes too. That's why, the effective load inclination angle must be changed in order to reach MPP. This is possible if the new MPP is in the tracking region, else the operating point would be set out of MPP.

Table 3. The minimum and maximum values of effective load inclination angle.

DC-DC Power Converter	**Mininum Effective Load Inclination Angle θ**	**Maximum Effective Load Inclination Angle θ**
Buck	$\theta \mid_{D=0} = 0$	$\theta \mid_{D=1} = \arctan\left(\frac{1}{R}\right)$
Boost	$\theta \mid_{D=0} = \arctan\left(\frac{1}{R}\right)$	$\theta\mid_{D=1}=90°$
Buck-boost, Cuk, SEPIC and zeta	$\theta \mid_{D=0} = 0$	$\theta\mid_{D=1}=90°$

From the graphical results shown in Figure 15 it is understood that buck-boost, Cuk, SEPIC and zeta converters are more suitable than the other types for tracking function. Because they have the ability to track at every point of the I-V plan. This can be proved by using the converters shown in Figure 16. [19,20].

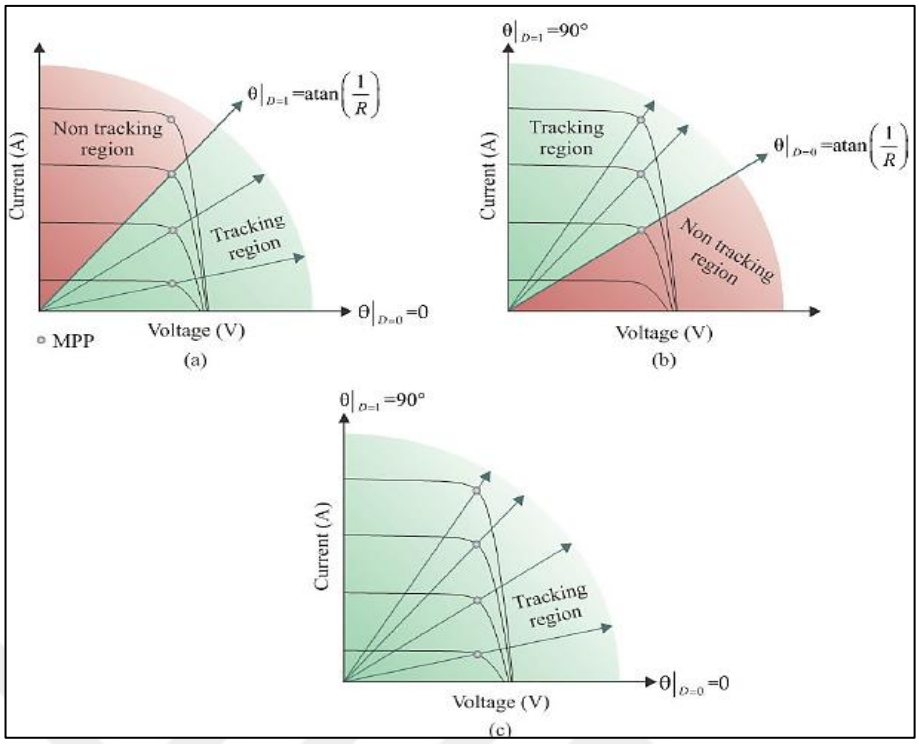

Figure 15. Tracking regions of: (a) buck converter; (b) boost converter and (c) buck-boost, Cuk, SEPIC and zeta converters [20].

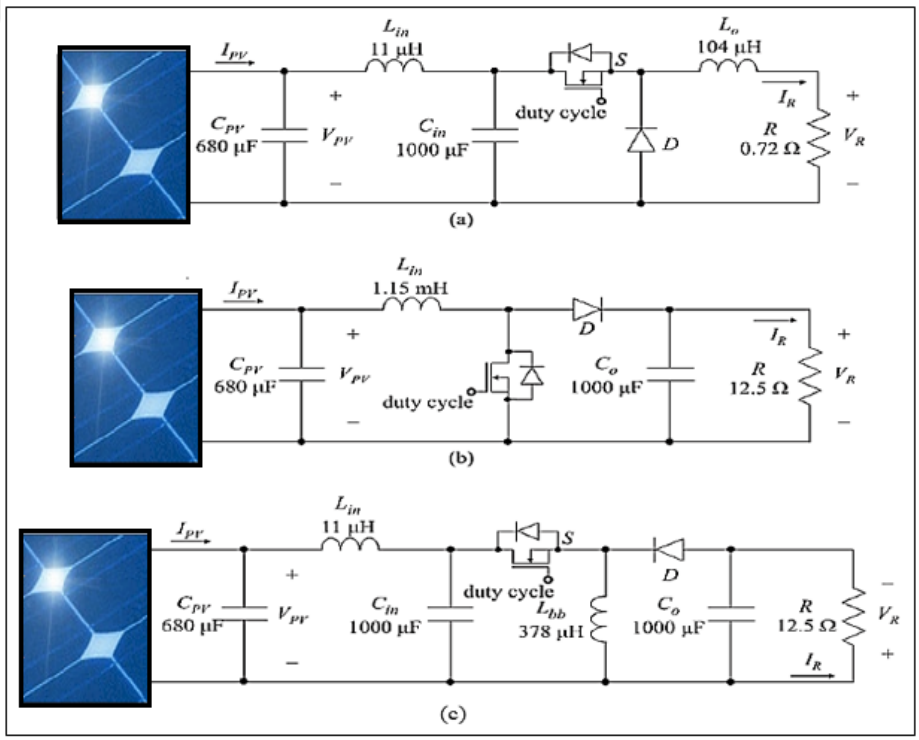

Figure 16. a) buck (b) boost and (c) buck-boost power converters.

1.5.3. Maximum Power Point Tracking Algorithms

The efficiency of the tracking function is directly related with the quality of tracking algorithm. In the tracking algorithm as inputs generally PV module current and voltage values are used. By this way duty cycle of the power converter is adjusted to set the operating point to the MPP.

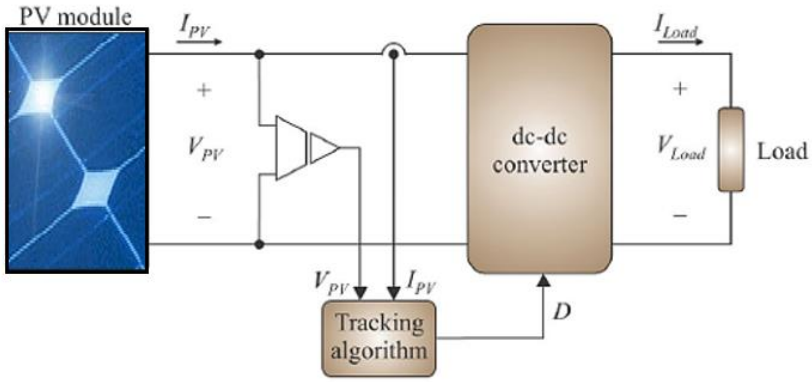

Figure 17. General MPPT system topology.

The irradiation and temperature changes dynamically so that in practice this algorithm must have the ability of fast and accurate tracking. Several tracking algorithms have been developed so far to improve the tracking speed and accuracy. The ease of implementation and the efficiency of the tracking algorithms differ from type to type.

1.5.3.1. Constant Voltage

This method aims to keep the voltage across the terminals of the PV device at a constant value at which the maximum power transfer is possible [21]. In this method a single voltage sensor is needed, so that it has the property of low cost and ease of implementation. But when irradiation or temperature changes the operating point shifts away from the MPP.

1.5.3.2. Incremental Conductance

The Incremental Conductance (IncCond) method has an acceptable performance of tracking speed and accuracy. In this algorithm V_{PV} and I_{PV} are measured to calculate output power P_{PV}. Then the partial derivative dP_{PV}/dV_{PV} is calculated to determine whether the duty cycle of the power converter is needed to be increased or decreased. By this way operating point is set to MPP. This method can be implemented digitally and the derivative is calculated by the microcontrollers by using equation (16).

$$\frac{dP_{PV}}{dV_{PV}} = I_{PV}(n) + V_{PV}(n)\frac{I_{PV}(n-1) - I_{PV}(n)}{V_{PV}(n-1) - V_{PV}(n)} \tag{16}$$

It can be inferred from (16) that;

- if $(dP_{PV}/dV_{PV})<0$ (the operating point is at the left of MPP), the duty cycle is in order to approach to zero,
- if $(dP_{PV}/dV_{PV})>0$ (the operating point is at the right of MPP), the duty cycle is changed in reverse direction in order to approach zero,
- if $(dP_{PV}/dV_{PV})=0$ (at MPP), then the duty cycle is unchanged.

This method has high tracking speed and accuracy but it has a complex procedure of implementation because of the calculation of derivative in real time [21].

1.5.3.3. Perturb and Observe

Perturb and Observe (P&O) method is widely used among the MPPT algorithms. This method works independently from the environmental conditions. Current and voltage sensors are needed to make calculations, so that it has a higher cost relatively [22]. Basic principle of this method is to calculate the output power P_{PV} and perturb the duty cycle by increasing or decreasing it. After every perturbation the output power is recalculated. If it is increased perturbation is repeated in the same direction otherwise direction of the perturbation reversed.

This method has some drawbacks. These are; oscillations when MPP reached at steady state because of constant perturbation, slow tracking speed and wrong decisions when fast changes happen in the irradiation or temperature.

1.5.3.4. Algorithms Combined with Fuzzy Logic Theory

The methods mentioned above chapters use step sizes that have constant values to adjust the duty ratio of power converter. Using unchanging step sizes brings some drawbacks together. Too small sizes of steps cause slow tracking and too large sizes of steps cause oscillations when the MPP point reached. The characteristics of the PV device change according to the environmental conditions so that in order to adapt to these changing environmental conditions we need to use variable step sizes in adjusting increment of duty ratio of power converter. Fuzzy logic combined MPPT techniques have advantages of application in such non-linear systems. They do not need the knowledge of complex mathematical models and system parameters. These advantages made FLC based techniques popular among all MPPT techniques [25-30]. The performance of MPPT algorithms depends on directly to the selected input and output variables of the system. MPPT techniques based on FLC usually use the error ($e(t)= Ppv(t)-Ppv(t-\Delta t)$, $dPpv(t)/dVpv(t)$ or $dPpv(t)/dIpv(t)$) and change of error ($de(t)/dt$) as inputs. But the derivative calculations make calculations complex and the small measurement noises cause large errors. So that variation of power, voltage and current can be taken as inputs. By this way calculations are made easily and accurately [31-34].

1.6. Fuzzy Logic Theory

Fuzzy logic is a method that converts expert knowledge into processable algorithms. It was first proposed by Dr. Lofti Zadeh in 1960's as a theory of uncertainty. This theory makes it possible to model the ways of human reasoning approximately with logical algorithms. Smart systems can be designed with fuzzy logic by using expert knowledge that is expressed in human language. It has been proved that fuzzy logic based smart systems have superior performances than the other conventional methods. Fuzzy logic has been widely used in system modeling, process control, military, prediction technologies,

estimation and smart machines etc. Especially it has a fame in designing control systems. Some important systems for which fuzzy logic based controllers have been extensively used are water quality control system, elevator control system, automatic train operation system, automatic transmission control, nuclear reactor control system, washing machine etc. [36].

1.6.1. Basics of Fuzzy Logic

Fuzzy logic is another kind of artificial intelligence. It has been more recently progressed than artificial intelligence applications. Fuzzy logic is based on the principle that human decision making isn't all about "ones and zeros" or "yes-no" and it is uncertain, vague and indecisive. Fuzzy logic is concerned with the problems that include uncertainty, vagueness or partial truth. Fuzzy set theory is the fundamental of fuzzy logic. Every member of a fuzzy set has a degree of membership value between 1 and 0. Different than classical Boolean logic based set theory that particular object is a member of a set (logic 1) or not a member of it (logic 0). Set operations in Boolean logic, union (OR), intersection (AND) and complement (NOT), are also used in fuzzy set theory [37-38].

1.6.1.1. Fuzzy Sets

A fuzzy set has no clearly defined boundary. It contains elements that have different degree of membership values. This is why they differ from the classical sets.

If we assume that X is a space of points (Universe of discourse) and x is a generic element of it, then we can define a fuzzy set A that has the elements as defined at (17) and (18).

$$\mu_A(x) \in [0,1] \tag{17}$$

$$A=\{(x, \mu_A(x))\}, \; x \in X \tag{18}$$

1.6.1.2. Basic Fuzzy Set Operations

Commonly used fuzzy set operations are union, intersection and complement operations. “max” and “min” operators are commonly used in engineering problems in order to model union and intersection operations.

Let A and B be two fuzzy sets in the universe of discourse *X*, which are characterized by membership functions $\mu_A(x)$ and $\mu_B(x)$. Then A∪B which is characterized by $\mu_{A\cup B}(x)$ can be designed as follows.

$$\mu_{A\cup B}(x)=\max(\mu_A(x),\ \mu_B(x)) \tag{19}$$

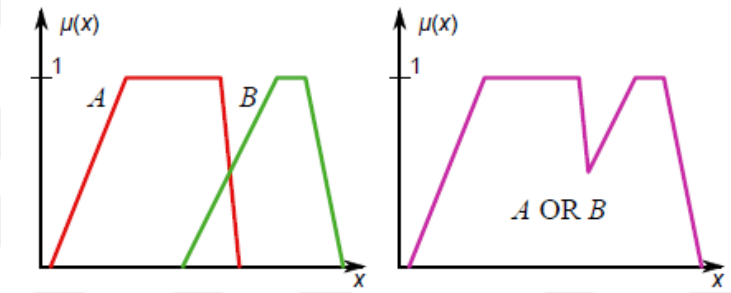

Figure 18. Fuzzy union of two fuzzy sets A and B.

Fuzzy intersection of two fuzzy sets A and B in the universe of discourse *X* is described by (20).

$$\mu_{A\cap B}(x)=\min(\mu_A(x),\ \mu_B(x)) \tag{20}$$

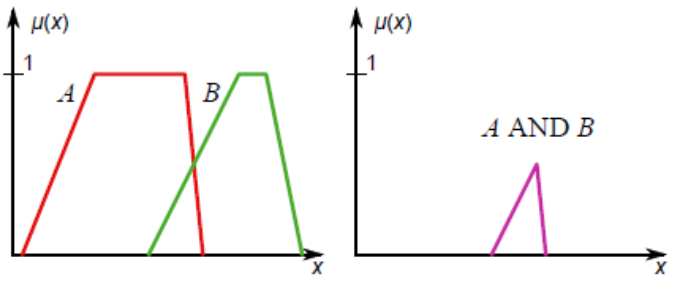

Figure 19. Fuzzy intersection of two fuzzy sets A and B

Fuzzy complement of a fuzzy set A in the universe of discourse *X* is described by (21).

$$\mu_{\tilde{A}}(x)=1-\mu_A(x) \tag{21}$$

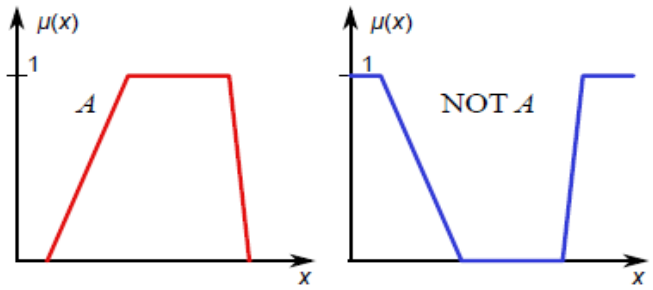

Figure 20. Fuzzy complement of a fuzzy set A.

1.6.1.3. Membership Functions

A fuzzy set is shaped by its membership functions. Since the universe of discourse mostly consists real values, defining MFs as continuous functions is convenient. Commonly used MFs are represented below.

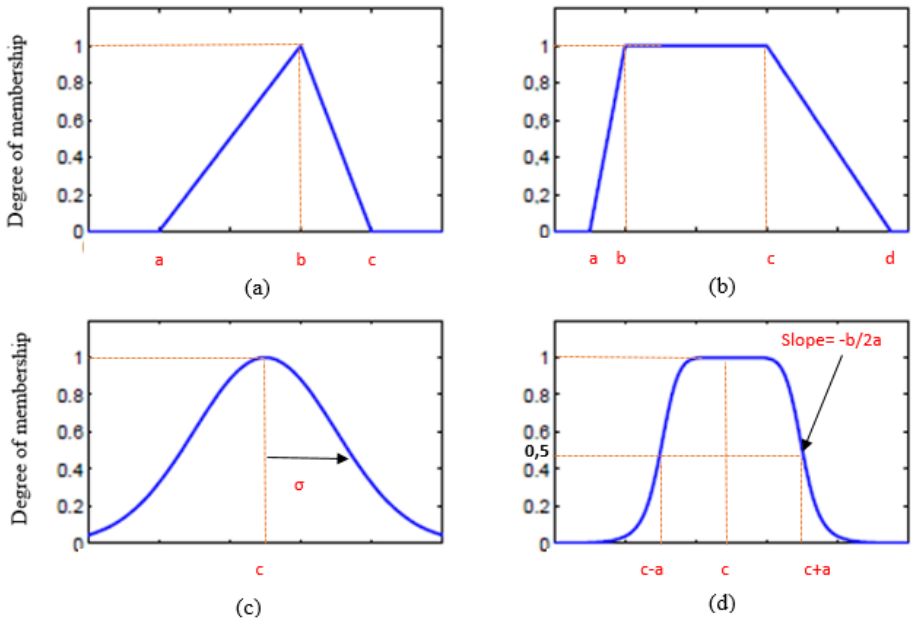

Figure 21. (a) triangular MF (b) trapezoidal MF (c) Gaussian MF (d) generalized bell MF

A triangular MF with parameters {a,b,c} can be defined as follows:

$$triangle(x;a,b,c)=\begin{cases}0, x\le a\\ \dfrac{x-a}{b-a}, a\le x\le b\\ \dfrac{c-x}{c-b}, b\le x\le c\\ 0, c\le x\end{cases} \tag{22}$$

A trapezoidal MF with parameters {a,b,c,d} can be defined as follows :

$$trapezoid\,(x;a,b,c,d)=\begin{cases}0, x\le a\\ \dfrac{x-a}{b-a}, a\le x\le b\\ 1, b\le x\le c\\ \dfrac{d-x}{d-c}, c\le x\le d\\ 0, d\le x\end{cases} \tag{23}$$

A Gaussian MF with parameters {c,σ} can be defined as follows (the parameter c represents the MF center and σ determines the MF width.):

$$gaussian(x;c,\sigma)=e^{-\frac{1}{2}\left(\frac{x-c}{\sigma}\right)^2} \tag{24}$$

A generalized bell MF with parameters {a,b,c} can be defined as follows:

$$bell(x;a,b,c)=\frac{1}{1+\left|\dfrac{x-c}{a}\right|^{2b}} \tag{25}$$

where b is usually positive (if b < 0; then the MF becomes an upside-down bell).

1.6.2. Fuzzy Rules

A fuzzy IF-THEN rule combines a condition consisting linguistic variables and fuzzy sets to define an output or conclusion. The part of IF contains a knowledge about conditions and the part of THEN contains an output or conclusion about the knowledge of conditions. These IF-THEN rules are used in fuzzy inference systems to define the degree about how much the input data matches the condition of the rule. As an example air conditioner system should be examined.

IF the temperature is LOW, THEN the heater motor should be rotated FAST.

For other input temperatures, different rules should be developed.

Fuzzy input variables can be multi-dimensional according to the type of applications. For example, in our air conditioner system, the inputs include both current temperature and the change rate of the temperature. Table 4. is an example of fuzzy control rules applied in our air conditioner system.

Table 4. An example of fuzzy rules

ΔT \ T	LOW	MEDIUM	HIGH
LOW	FAST	MEDIUM	MEDIUM
MEDIUM	FAST	SLOW	SLOW
HIGH	MEDIUM	SLOW	SLOW

The rows and columns represent input variables and the linguistic variables at the intersections of the columns and rows represent output variables. The inputs are related with the IF part and the output is related with the THEN part of the IF-THEN rule. For example, when the current temperature is LOW, and the current change rate of the temperature is also LOW, the heater motor's speed should be FAST to increase the temperature as soon as possible. This can be represented by the IF-THEN rule as

IF the temperature is LOW, and the change rate of the temperature is LOW, THEN the conclusion or output (heater motor speed) should be FAST.

Remaining rules can be formed with the same strategy. In this example 9 rules were created. According to the sensitivity of the control process inputs and outputs would be partitioned to smaller segments [40-44].

1.6.3. Fuzzy Inference Systems

The process of converting fuzzy inputs to fuzzy outputs according the fuzzy rules is defined as fuzzy inference. There are several types of fuzzy inference mechanisms.

FIS (fuzzy inference systems) have many application areas [45];

- Automatic control and robotics
- Classification and clustering
- Pattern recognition
- Decision analysis and expert systems

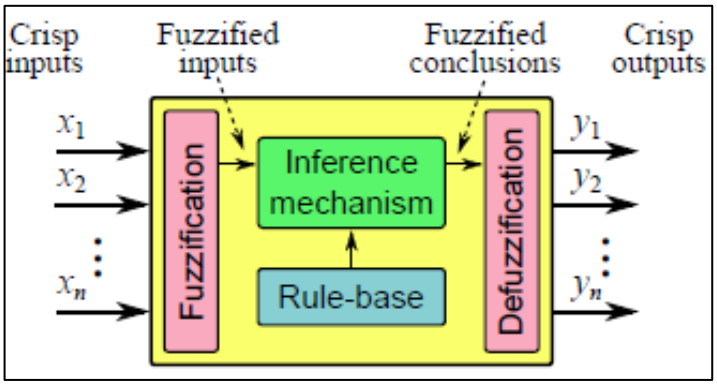

Figure 22. General FIS structure.

- Fuzzification: Transformation of crisp values to fuzzy sets
- Rule-base: contains a selection of fuzzy rules
- Inference mechanism: performs a certain inference procedure upon the rules and derives a conclusion
- Defuzzification: Transformation of output fuzzy sets to crisp values

1.6.3.1. Mamdani-Type Fuzzy Inference System

Mamdani-type fuzzy inference process has five steps:

Step 1: Fuzzify input variables
Step 2: Application of fuzzy operator
Step 3: Application of implication method
Step 4: Application of aggregation method
Step 5: Defuzzification

A simple example of "climate comfortability" can be examined to describe fuzzy inference process. According to the flowchart shown in Figure 23, as input variables temperature and humidity are chosen then processed with three IF-THEN rules to create crisp output about climate comfortability.

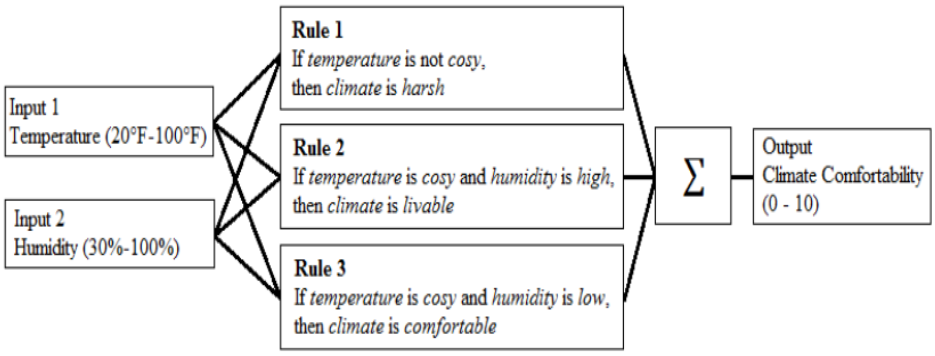

Figure 23. Flowchart of "climate comfortability" [45].

First of all crisp input variables would be converted into fuzzy inputs by using fuzzy sets defined by membership functions. In this example three IF-THEN rules are created and the inputs are defined by four different fuzzy sets "temperature is cosy " , "temperature is not cosy ", "humidity is high", and "humidity is low". Input variables are fuzzified according to these linguistic fuzzy sets. As shown in Figure 24, the temperature 80°F is located on the "temperature is cosy" fuzzy set and has the degree of membership value $\mu = 0.66$.

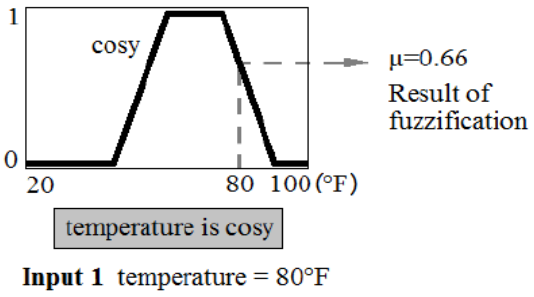

Figure 24. Fuzzifying input variable “temperature” [45].

If we examine Rule 2, we can see that the antecedent consists of two fuzzy linguistic sets. So that we need to combine these two membership values with a fuzzy operator. Most common operators are AND and OR. They are formulated with the min and max functions. Figure 25 shows the AND operation and resultant degree of membership of the fuzzy Rule 2. This process is the part of antecedent of fuzzy rule.

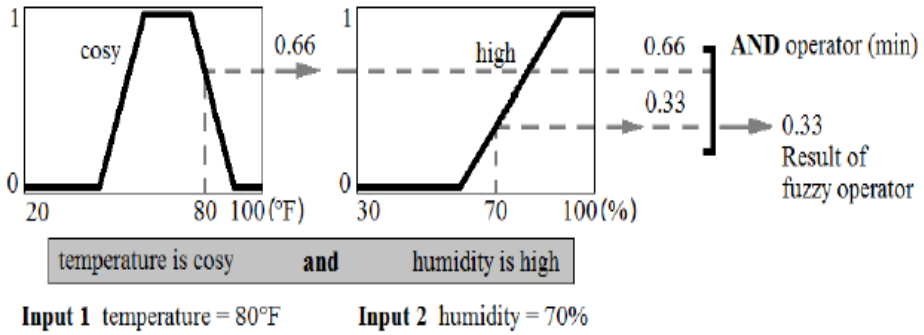

Figure 25. Applying fuzzy operator [45].

The consequent part is described by another fuzzy linguistic set. The resultant degree of membership from the antecedent part is applied, according to the inference method used, to these fuzzy linguistic set and crisp output is obtained. This process is called fuzzy implication.

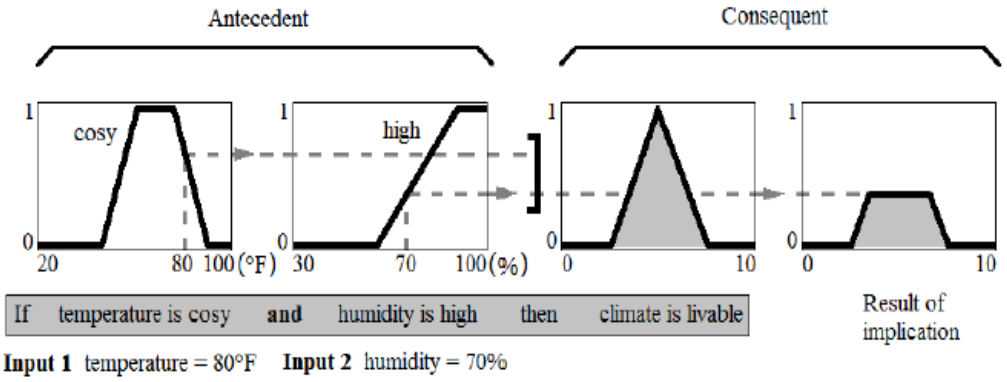

Figure 26. Applying implication method [45].

When each consequent fuzzy sets are implicated by the IF-THEN rules, now we have to combine them in order to form the output fuzzy set to make a decision. This process is called aggregation. Functions max, sum and "OR" can be applied in the aggregation process. In our example max function was used. In climate comfortability example implication of three fuzzy rules creates three new fuzzy sets. These fuzzy sets were aggregated by using max function and a fuzzy set defining output variable "climate evaluation" was created. This fuzzy set is ready for the defuzzification process.

Final step of the fuzzy inference process is the defuzzification. At this step a crisp output will be created according to the resultant fuzzy set from the aggregation operation. Defuzzification is the inverse process of fuzzification. At the beginning crisp inputs were fuzzified by using input variables' fuzzy sets and then crisp outputs were created by using this resultant fuzzy set. There are several defuzzification methods. In this thesis the Centroid Method (centre of gravity) was used. This method is defined as in (26).

$$z_{COG} = \frac{\int_z \mu_A(z).zdz}{\int_z \mu_A(z)} \tag{26}$$

here z is the crisp output variable, and $\mu A(z)$ is the membership function of the aggregated fuzzy set A with respect to z. The following figure shows the result of the climate comfortability example calculated via Centroid Method. This indicates that when temperature is 80°F and humidity reaches 70%, the fuzzy inference system rates the climate

comfortability 3.75 points, which means the climate is not appropriate for long-time living [45].

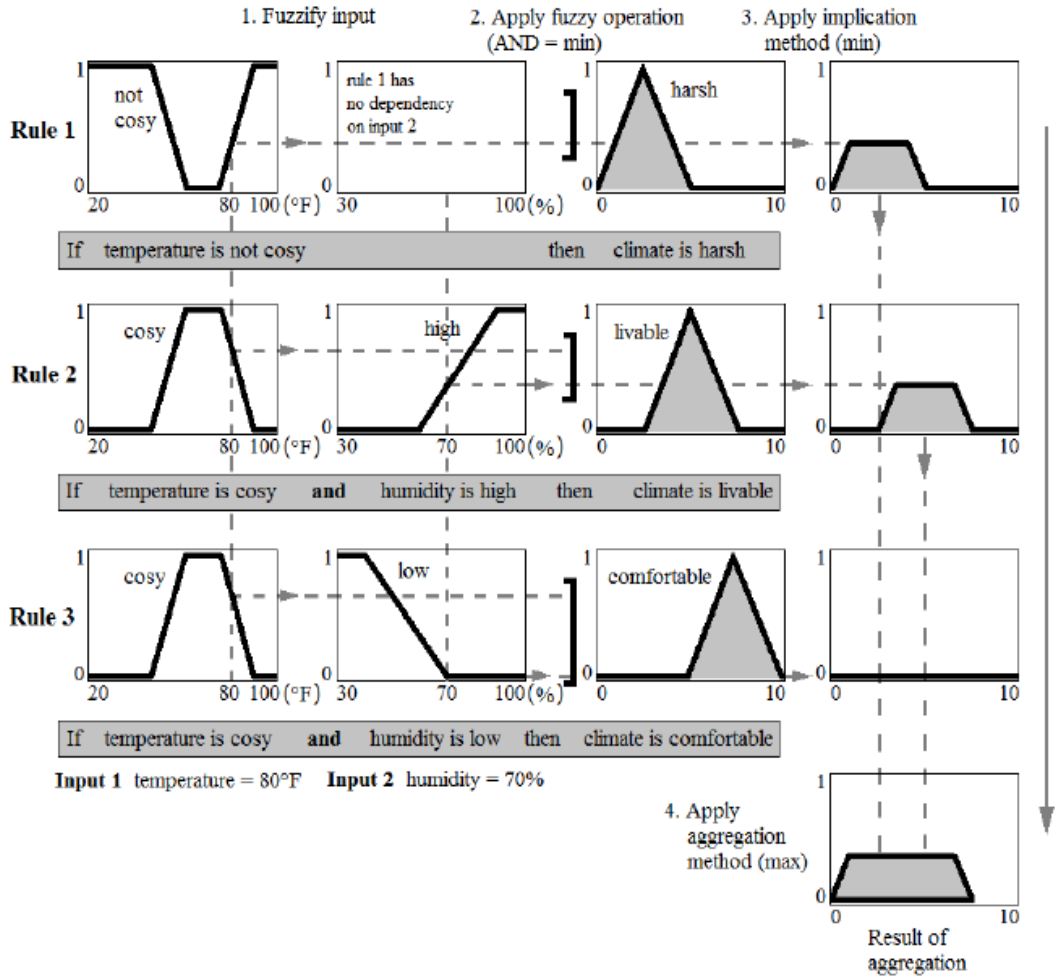

Figure 27. Applying aggregation method [45].

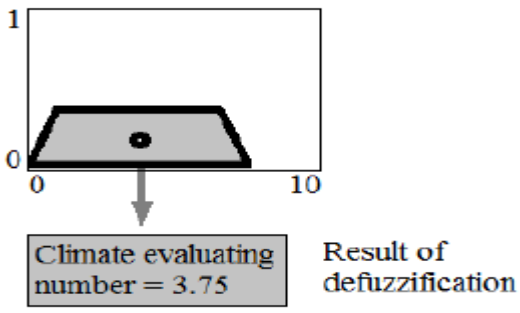

Figure 28. Applying Centroid Method for defuzzification[45].

1.7. Matlab Fuzzy Logic Toolbox Software

By using Matlab fuzzy logic toolbox users can create and edit fuzzy inference systems. Users can create these systems using graphical tools or command-line functions. And by using Simulink software users can test their fuzzy systems in a block diagram environment [46].

The following graphical tools are used to build, edit and view fuzzy inference systems:

- Fuzzy Logic Designer: Basic properties of the FIS such as number of inputs and outputs, input and output names are determined by this tool. There is no limit with the number of inputs. But the size of the memory of the users' machine may not handle to work if the number of inputs or number of membership functions too large.
- Membership Function Editor: Properties of membership functions are edited by using this tool.
- Rule Editor to edit the list of rules that defines the behavior of the system.
- Rule Viewer: FIS diagram is demonstrated by this tool. It can be to see which rules are active, or how individual membership function shapes influence the results.
- Surface Viewer to view the dependency of one of the outputs on any one or two of the inputs—that is, it generates and plots an output surface map for the system [47].

To open the fuzzy logic toolbox, users easily type "fuzzy" on the Matlab main command window and then press enter.

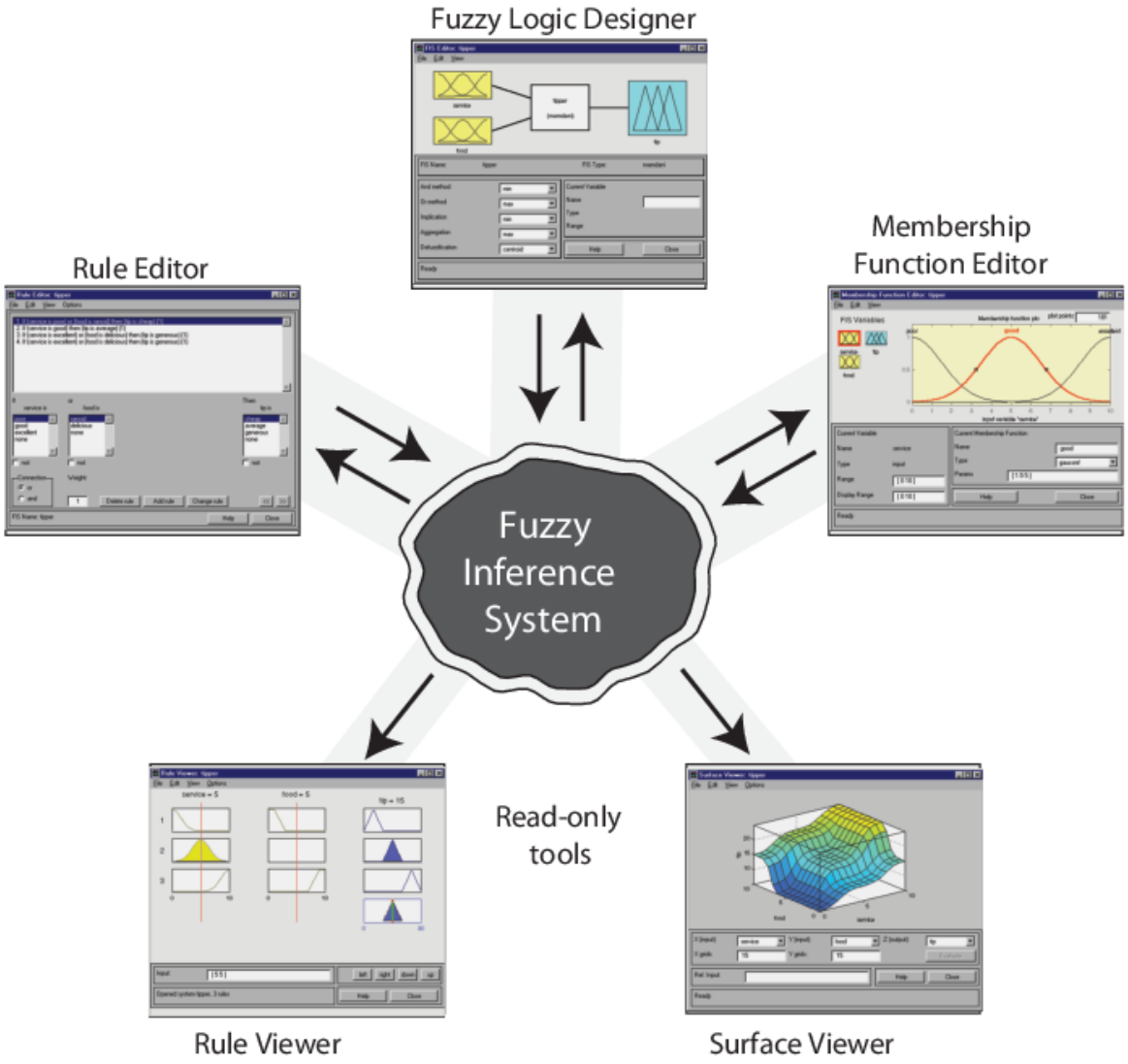

Figure 29. Main components of Matlab fuzzy logic toolbox [47].

1.7.1. The Membership Function Editor

The membership function editor allows users to display and edit membership functions. Main functions are represented in Figure 30.

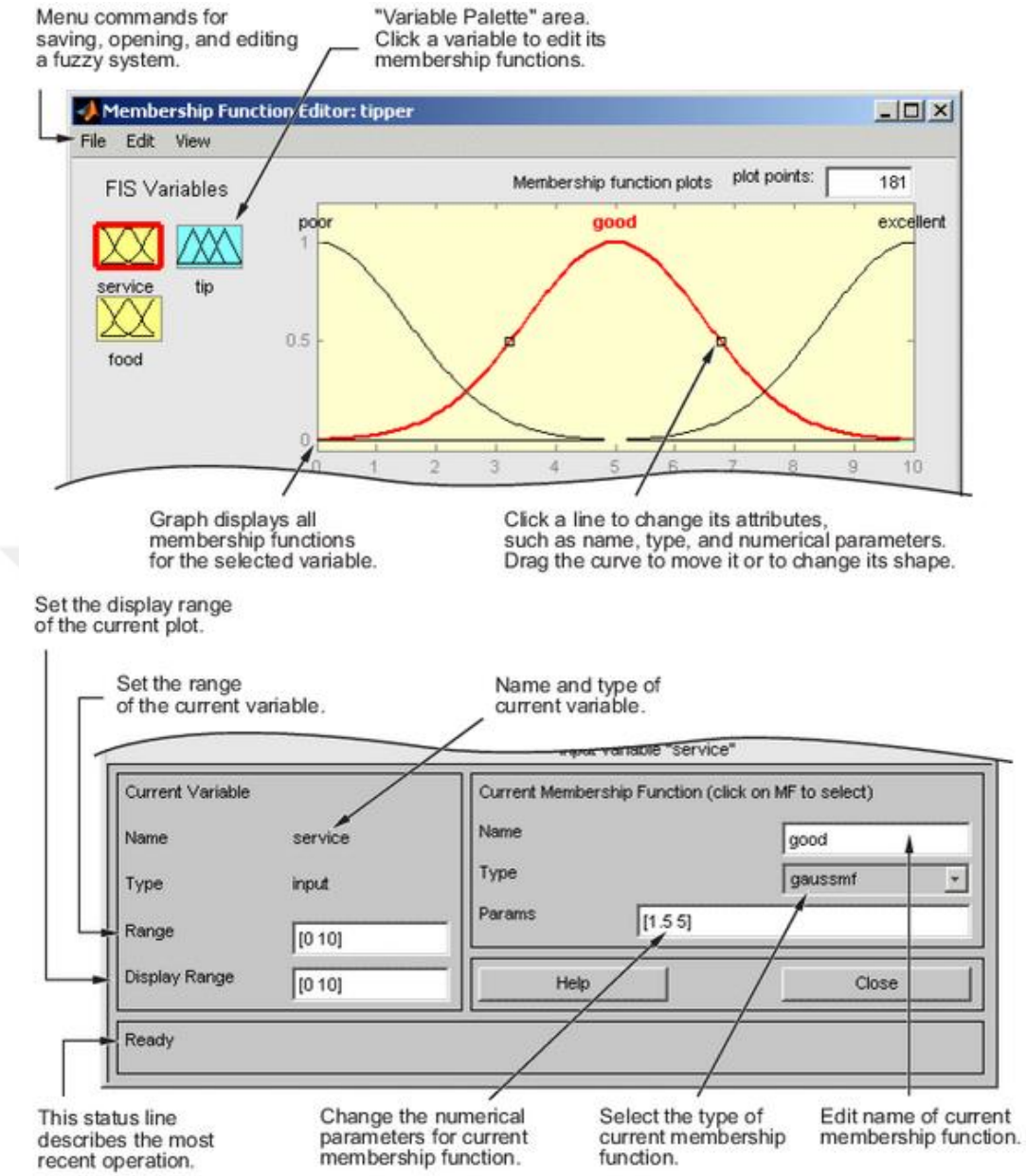

Figure 30. Basic functions of membership function editor window [47].

1.7.2. The Rule Editor

The rule editor allows users to construct the rule statements automatically as shown in Figure 31.

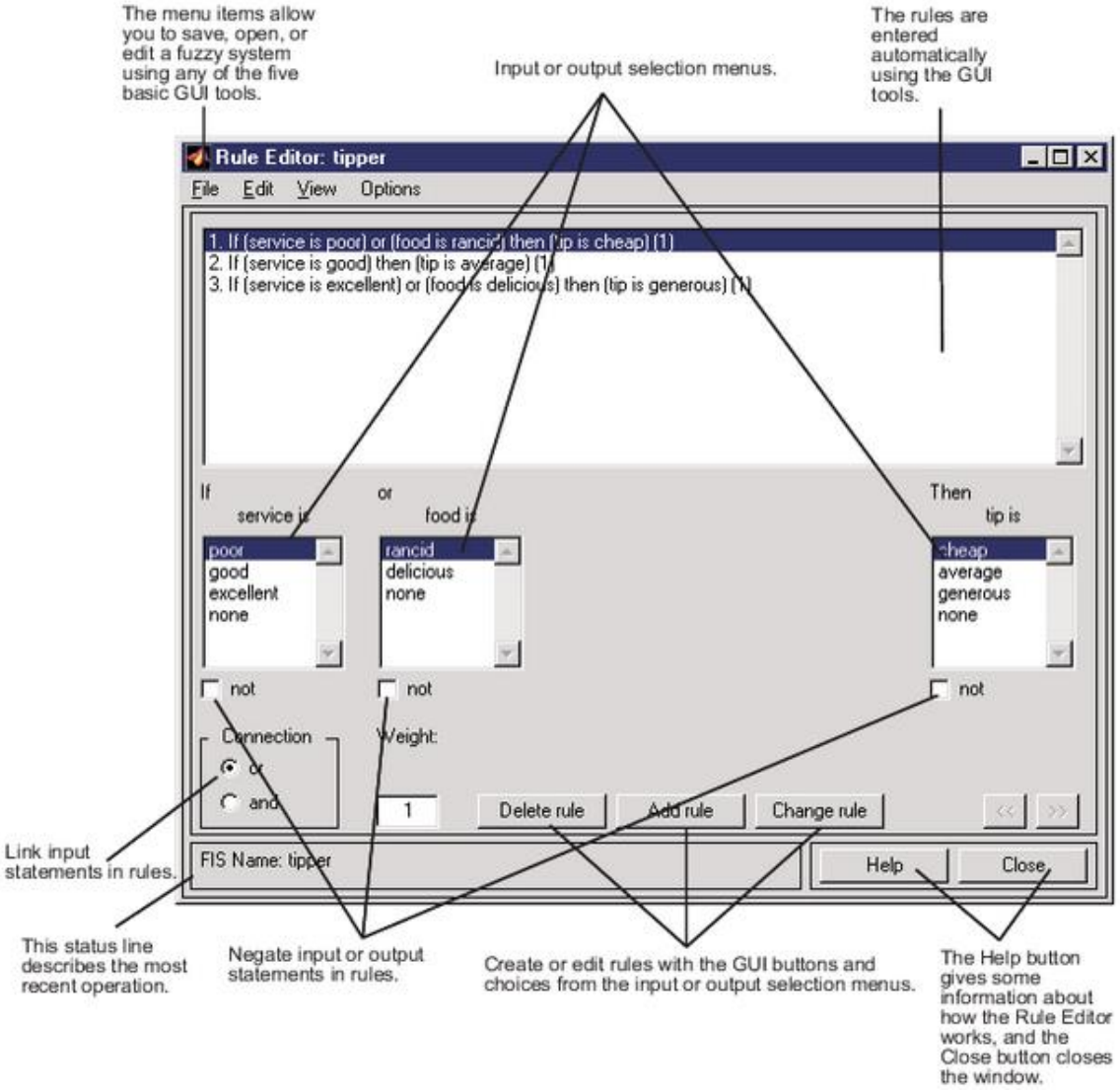

Figure 31. Basic functions of rule editor window [47].

1.7.3. The Rule Viewer

The rule viewer displays the general concepts of fuzzy inference process. The antecedent and consequent parts of the fuzzy rules are represented in three plots. The rules are represented as rows and the variables are represented as columns. By clicking on the rule

numbers users can slide the red line and change the value of the input variables and see how the output variable change simultaneously.

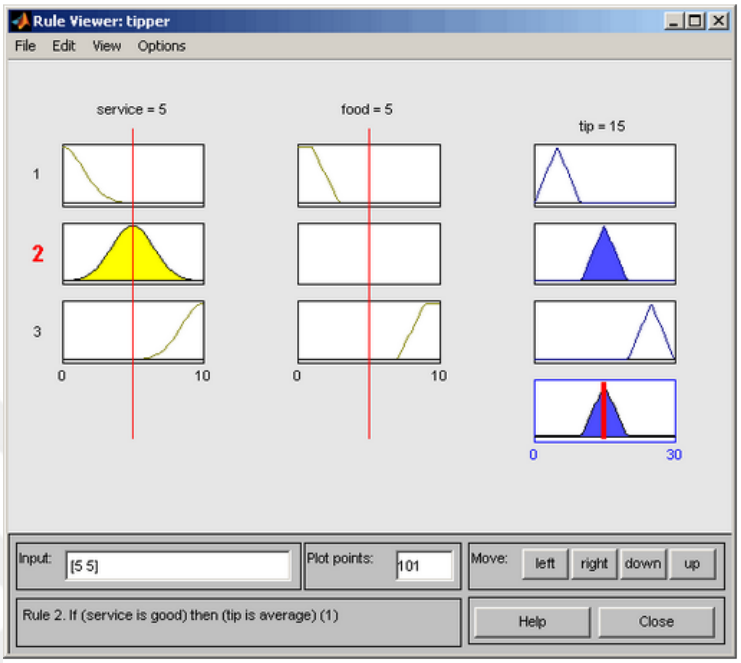

Figure 32. The rule viewer window [47].

1.7.4. The Surface Viewer

With the drop-down menus X (input), Y (input) and Z (output) users can plot nay of selected two inputs and one output. Users can grab the axes with the help of mouse and rotate the shape three-dimensionally.

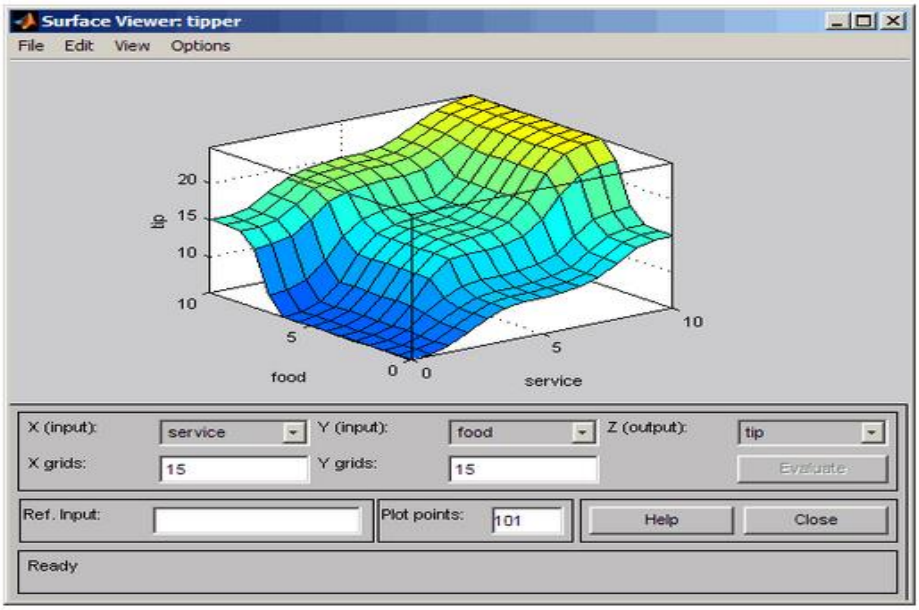

Figure 33. The surface viewer window [47].

1.7.5. Importing and Exporting Fuzzy Inference Systems

Fuzzy systems are saved as ASCII text files. The FIS files are represented with the ".fis" suffix When a fuzzy system saved to the Matlab workspace, a variable is created (whose name you choose) that acts as a Matlab structure for the FIS system. FIS files and FIS structures represent the same system [47].

2. CASE STUDY AND METHODOLOGY

The scope of this study is to design a solar MPPT system that uses fuzzy logic control theory to perform the adjustment of the duty ratio of the power switching device that is used in the dc-dc power converter circuit. Fuzzy MPPT controllers would generate fuzzy input variables needed by reading voltage and current signals from the PV panel. The fuzzy input variables would then can be used to calculate the increment of the duty ratio command for adjusting operating point of the PV panel in order to maximize the power extraction.

Figure 34 shows the block diagram of the investigated MPPT system. The system includes a PV panel, a buck-boost power converter and a fuzzy logic based MPPT controller.

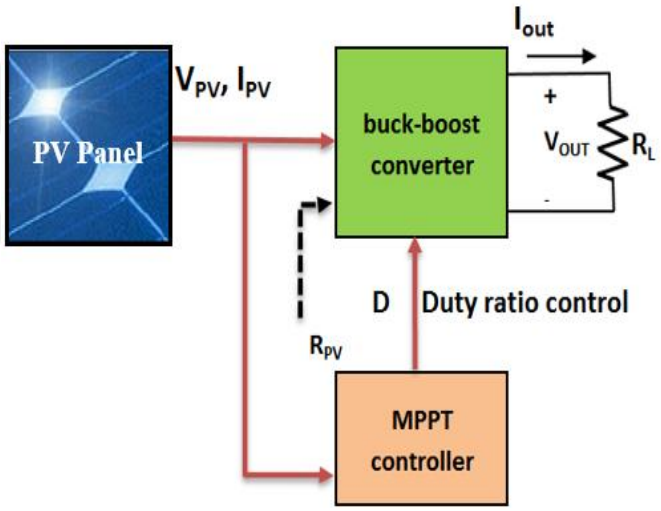

Figure 34. Solar power maximum power point tracking system.

2.1. Design of Maximum Power Point Tracking system

Sunpower SPR-305E-WHT-D (Monocrystalline Cell) (One series module and one parallel strings) PV module used for simulations in this study. The characteristics of the PV module at 25 ºC and at various irradiation levels are shown in Figure 35. The characteristics of the PV panel at 1000 W/m^2 and at various temperature levels are shown in Figure 36. Module parameters at STC are represented in Table 5.

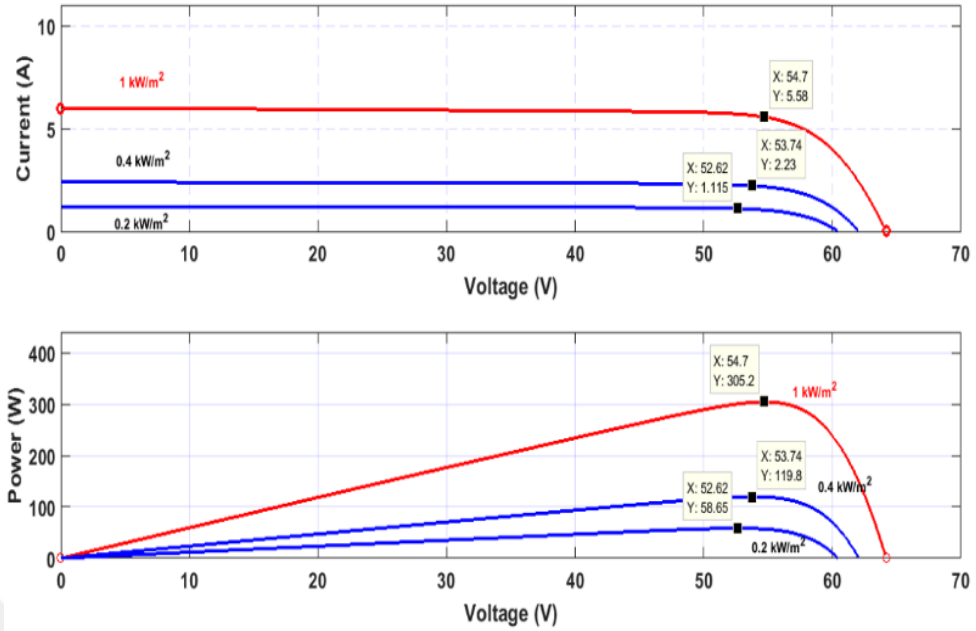

Figure 35. PV panel characteristics at 25 ºC and at various irradiation levels (the point (X,Y) refers to maximum power point).

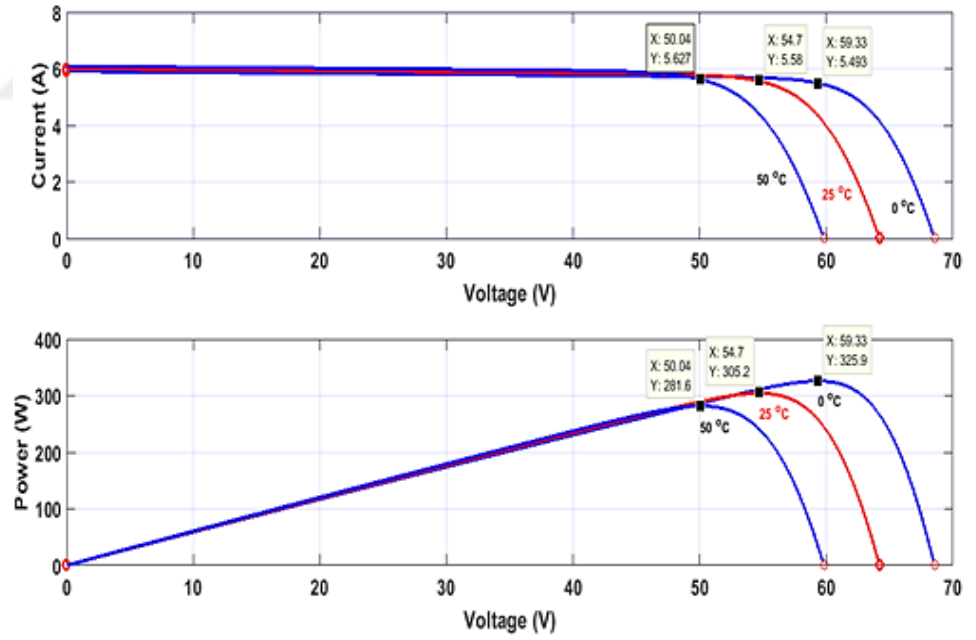

Figure 36. PV panel characteristics at 1000 W/m2 and at various temperature levels (the point (X,Y) refers to maximum power point).

Table 5. Module datasheet.

Module Parameters	
Maximum Power (W)	305,26
Open circuit voltage V_{OC} (V)	64,2
Temperature coefficient of V_{oc} (%/deg.C)	-0,27269
Cells per module	96
Short-circuit current I_{sc} (A)	5,96
Current at maximum power point I_{MP} (A)	5,58
Temperature coefficient of I_{sc} (%/deg.C)	0,061745
Light generated current I_L (A)	6,0092
Diode saturation current I_0 (A)	6,30E-12
Diode ideality factor	0,94504
Shunt Resistance R_{SH} (ohms)	269,5934
Series Resistance R_S (ohms)	0,37152

2.1.1. DC-DC Converter

As mentioned in section 1.5.2. buck-boost converters' ability of tracking at the I-V plan of the PV panel is superior than buck and boost converters. So that in this study buck-boost converters used to perform MPP tracking process.

The circuit diagram of the power converter is shown in Figure 37. The parameters of the converter are L_{in} = 11 µH, L_1 = 378 µH, C_{IN} = C_1 = 1000 µF and C_{PV} = 680 µF. The pulse width modulation (PWM) switching frequency was set to 5 kHz [20].

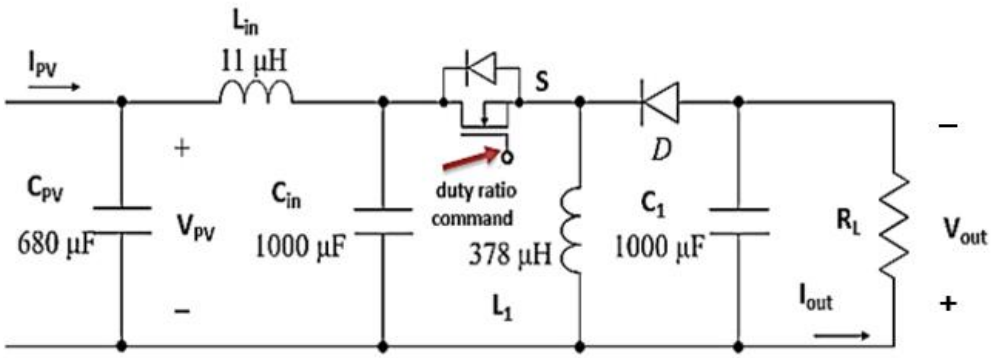

Figure 37. Circuit diagram of the power converter.

Internal resistances were ignored to obtain (27) on the converter's input and output voltage equation in steady state:

$$V_{OUT} = \frac{D}{1-D} V_{PV} \tag{27}$$

If we assume that converter operates lossless with a resistive load R_L, the value of the power obtained from this PV system would be:

$$P_{PV} = \left(\frac{D}{1-D}\right)^2 \frac{V_{PV}{}^2}{R_L} \tag{28}$$

It is demonstrated additionally, in Figure 38, that P-V curves at miscellaneous irradiation levels according (28) and miscellaneous duty ratio commands with the ohmic load 3 Ω. The intersections show the operating points of PV system.

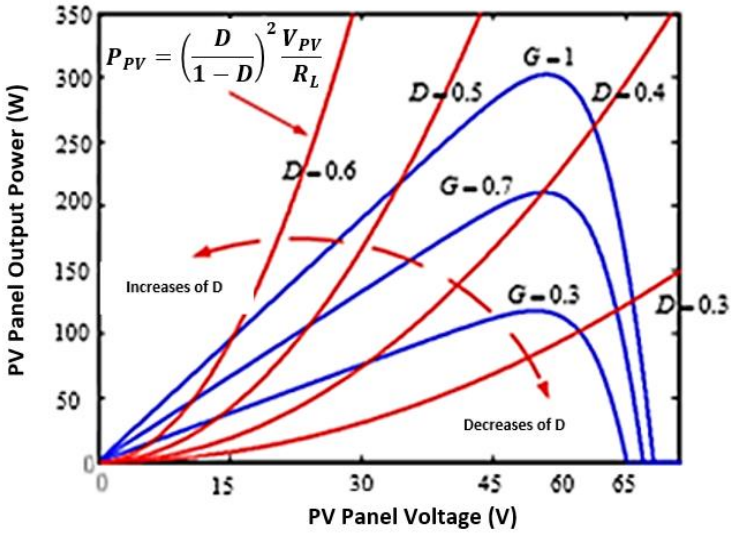

Figure 38. PV characteristics and operating points according to (28) [8].

Simulink model of the test circuit of the designed dc-dc power converter is represented in Figure 39. If we apply a ramp signal (changes the duty ratio of the switching device from 0% to 100%) as the duty ratio control command of PWM generator at 25 ºC temperature and 1000 W/m^2 irradiation level (R_L=5Ω), equations (11) and (28) are verified. Simulation results represented in Figure 40 and Figure 41.

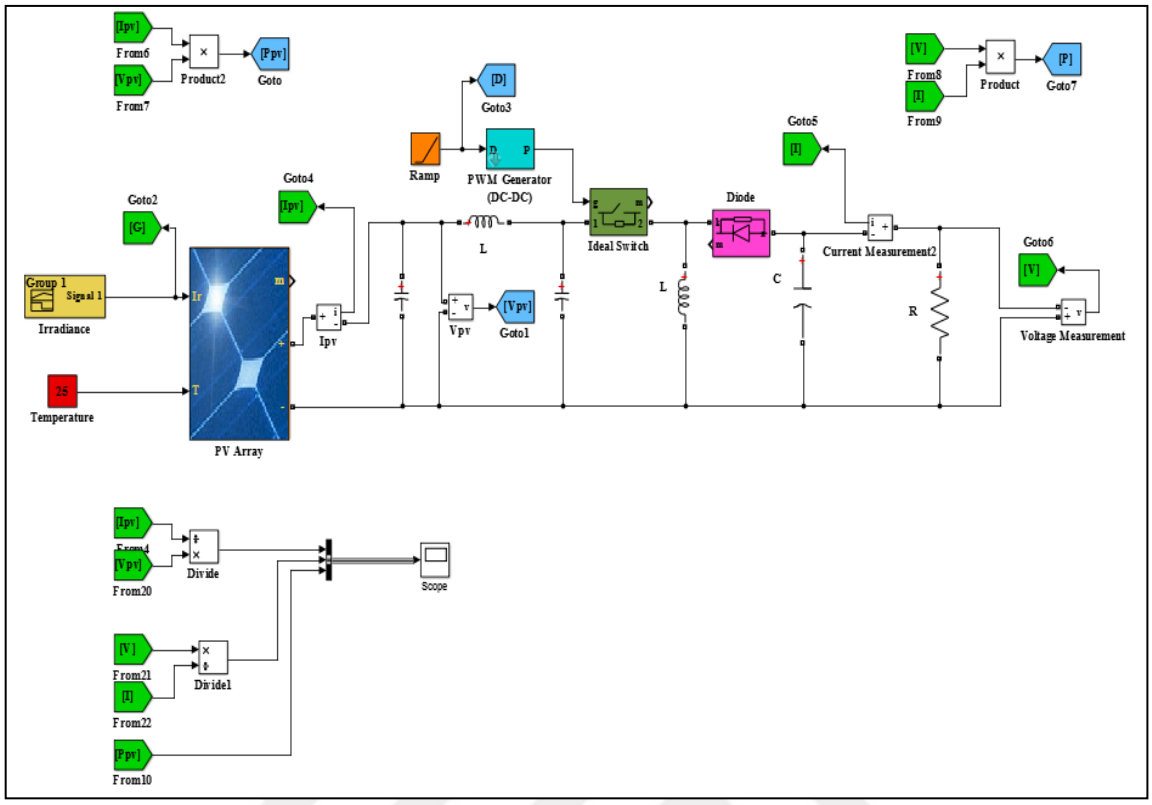

Figure 39. Simulink model of the test circuit represented in Figure 37.

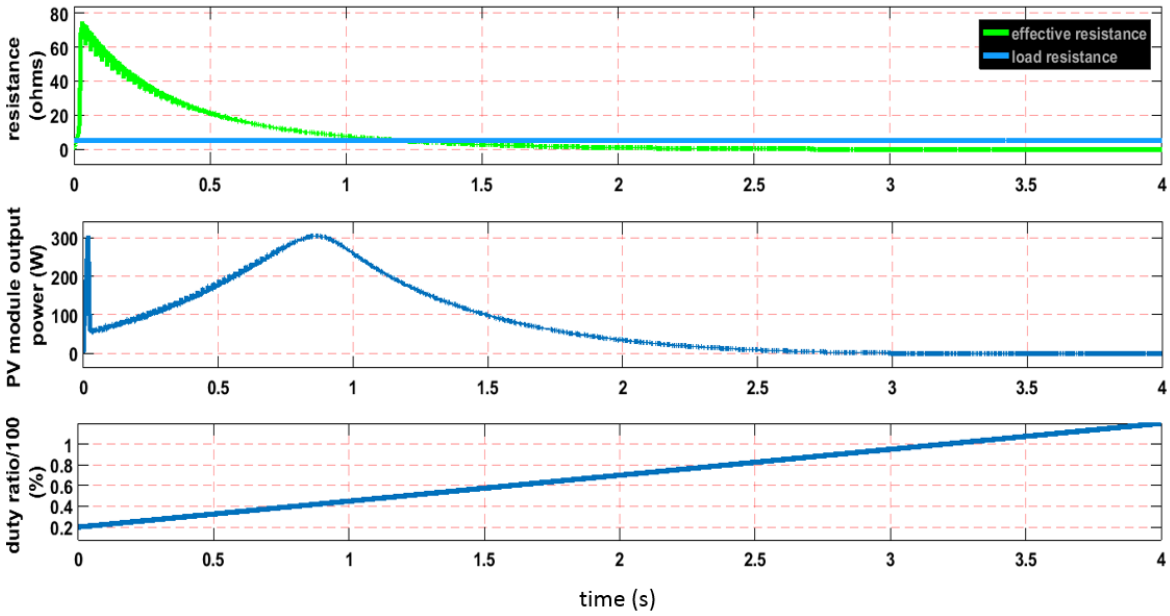

Figure 40. Simulation results when a ramp signal applied to the PWM generator as duty ratio control signal.

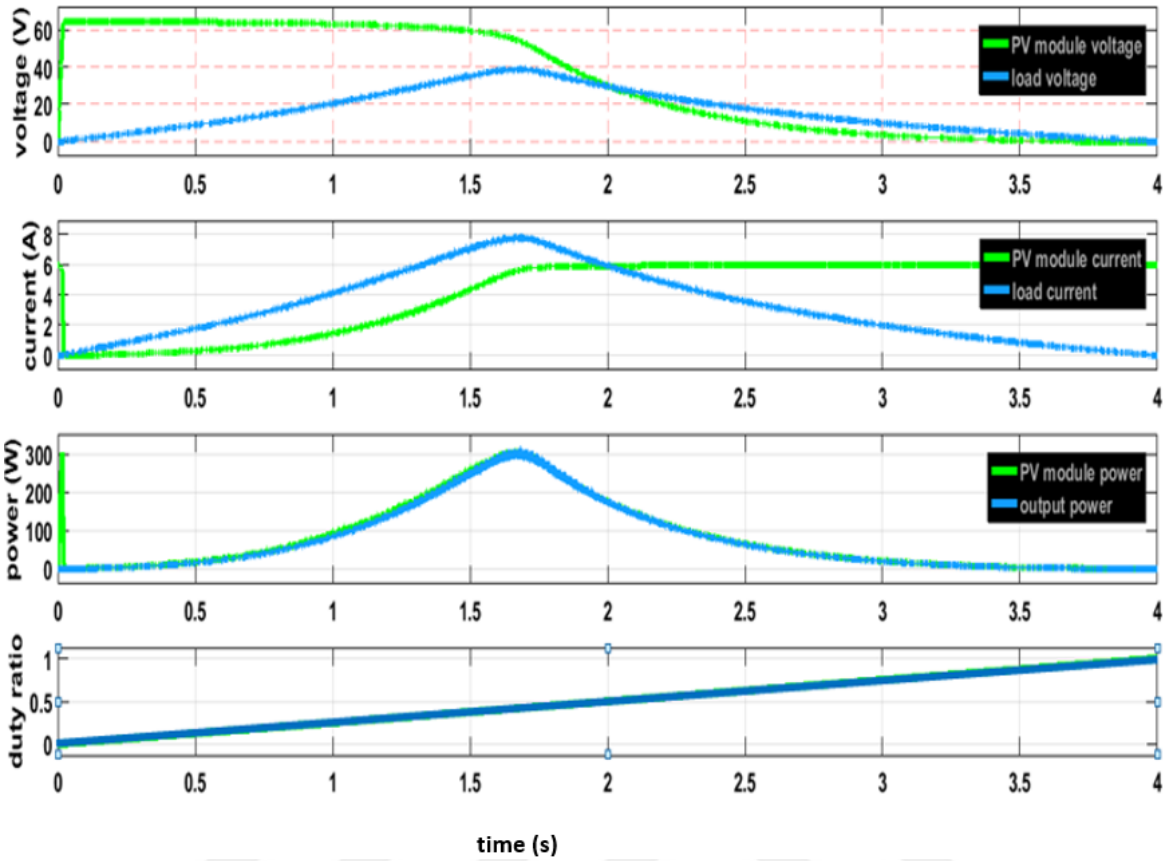

Figure 41. PV module and load waveforms with the changing duty ratio command.

We can conclude that, from the simulation results shown in Figure 40-41, by changing the duty ratio of the switching device the dc-dc power converter alters the load resistance and the effective resistance obtained from PV module terminals determines the operating point of PV module. Power extracted from the PV module and transferred to the load have almost same values and waveforms (if internal resistances ignored).

2.1.2. Design of Fuzzy Inference System

Required fuzzy input variables are generated by fuzzy MPPT controllers. The current and voltage measurements of the PV module are converted to fuzzy inputs by the fuzzy inference system. Then these fuzzy inputs can be used in the process of estimating the increment of the duty ratio. In Figure 42 the flowchart of this process is illustrated. Designs of fuzzy controllers varies according to the input variables selected. As mentioned before

as input variables, ΔP ,ΔV, ΔI and Δe can be selected, and as an output Δd was selected in this study.

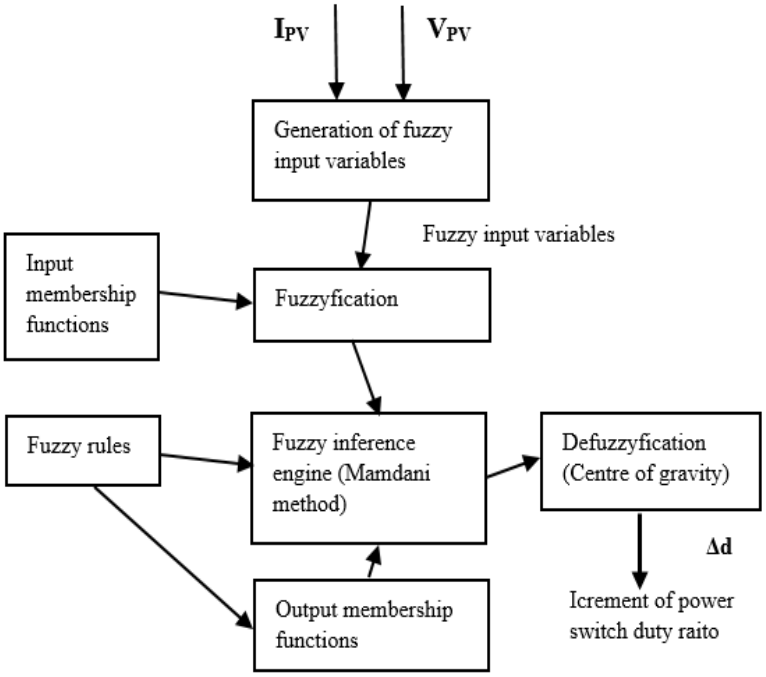

Figure 42. Flowchart of calculation process.

By using MATLAB Simulink proposed MPPT topology is implemented and universe of discourse (UOD) of input and output membership functions were determined. After determination of UOD membership functions, they were grouped with the names negative big, negative small, zero, positive small, positive big (NB, NS, ZE, PS, PB). Researchers have developed several methods in determining the UOD of the membership functions such as fuzzy clustering and particle swarm optimization. In this study the UOD of membership functions are determined by the trial and error method. This method is an empirical method. In this method system designers have to perform a lot of experiments and according to results of the experiments the boundaries of UOD of membership functions are optimized in order to achieve the best tracking performance. In this study by the help of MATLAB "histogram" function we had an idea of determining UOD of input membership functions. For example if ΔP and ΔV are selected as input variables; as shown in Figure 43 the test circuited was used to read the values of ΔP and ΔV. When the duty ratio signal, shown in Figure 44, is applied to the PWM controller (at 25 °C) values of ΔP and ΔV are read and recorded to the

workspace of MATLAB. Then by using the “histogram” function the distribution of the values of ΔP and ΔV can be evaluated. According to the histograms the UOD of membership functions can be tuned to optimize the system tracking performance.

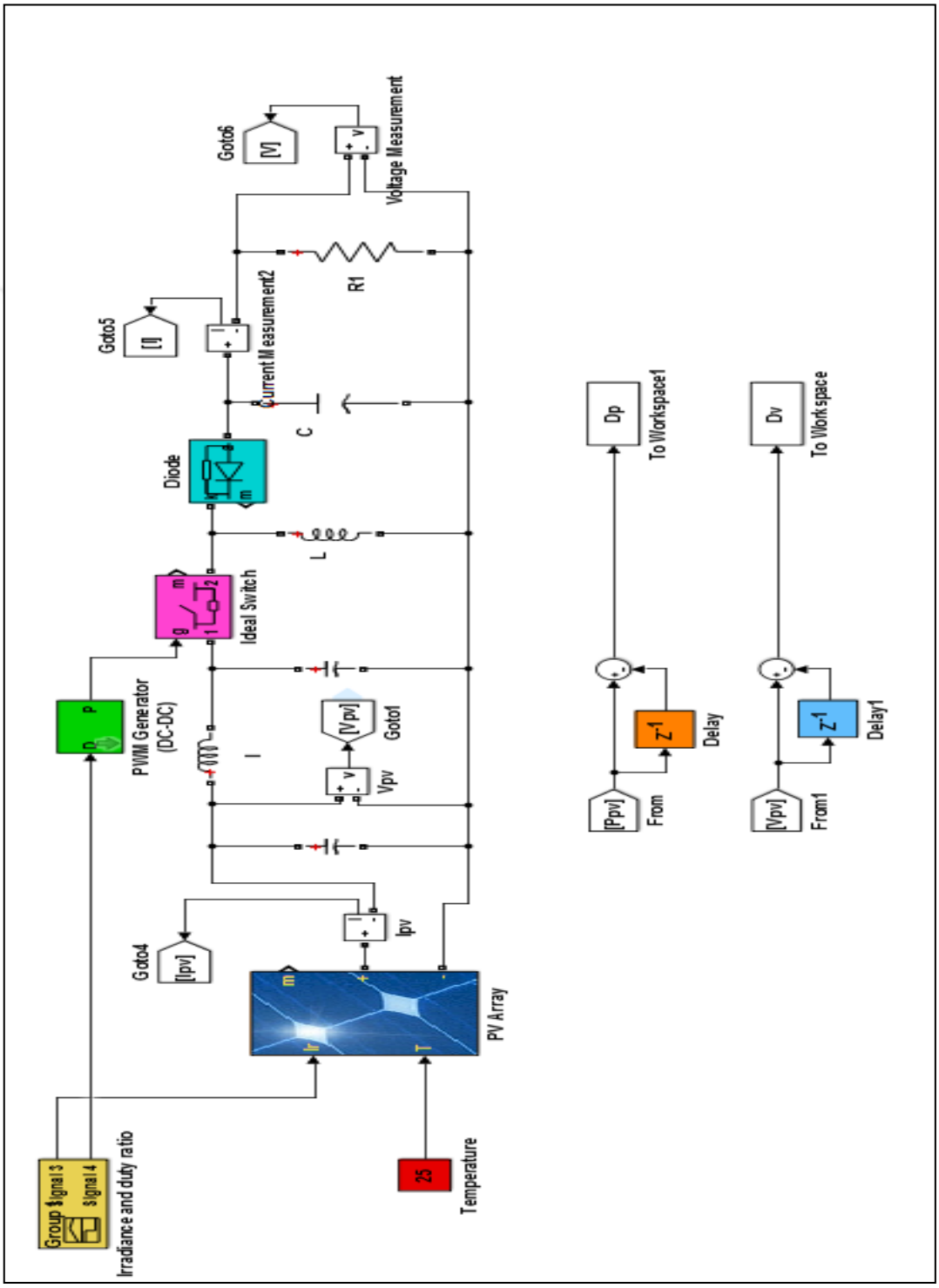

Figure 43. Simulink model of the test circuit used for the histogram calculations.

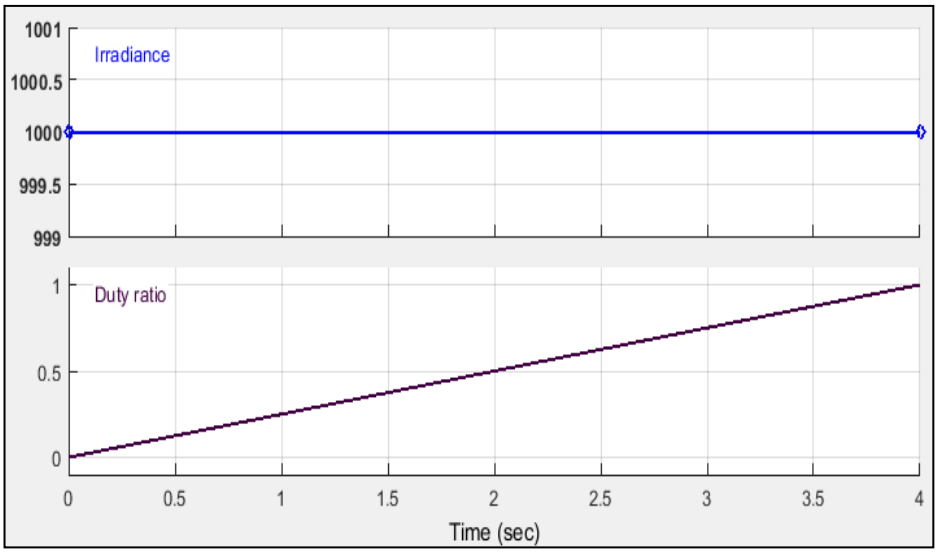

Figure 44. The duty ratio signal and the irradiance.

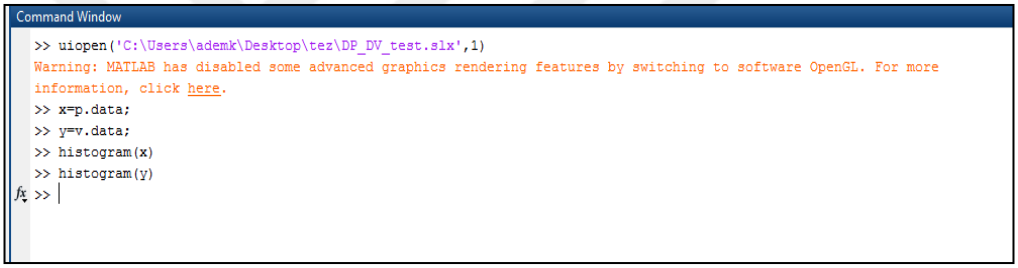

Figure 45. Matlab command window view of histogram function.

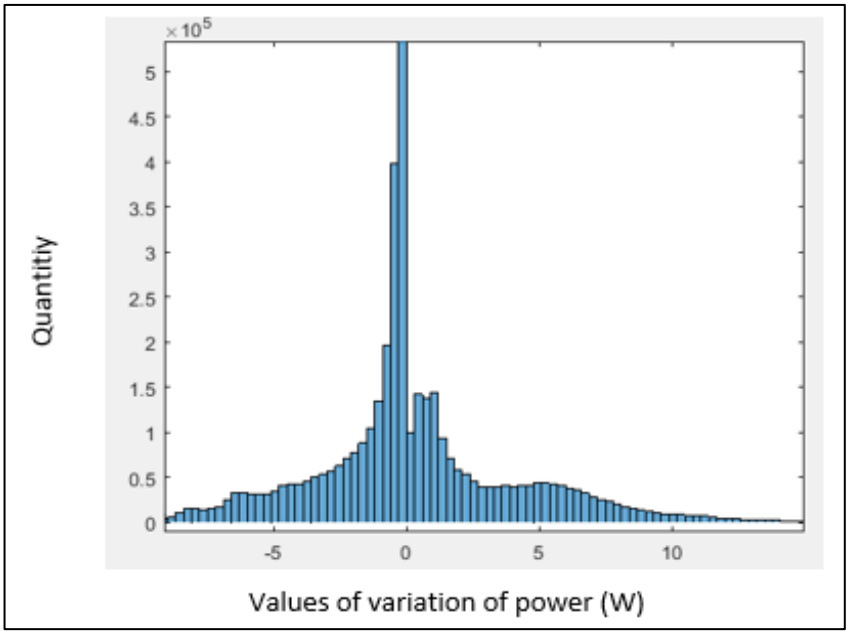

Figure 46. Histogram of ΔP.

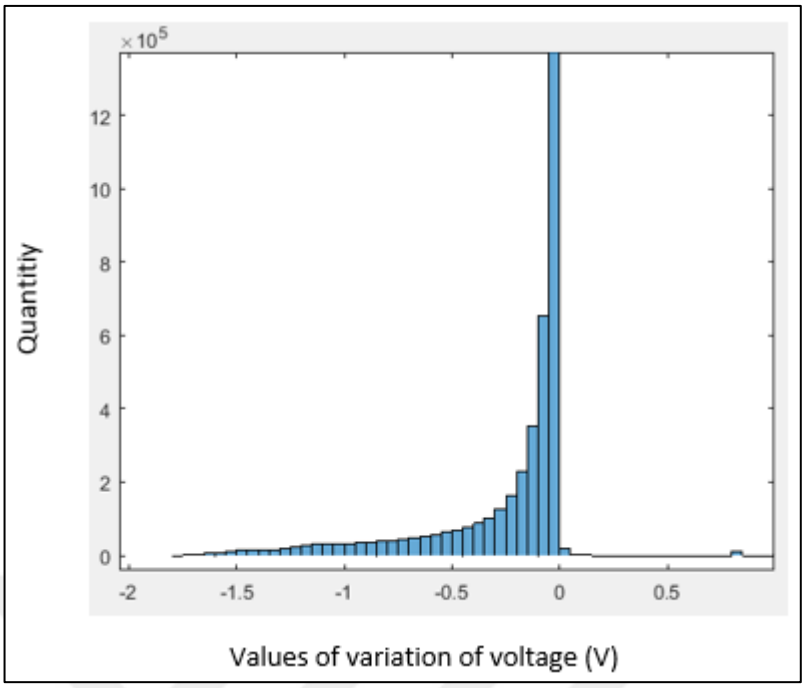

Figure 47. Histogram of ΔV.

As shown in above figures, the histograms give us information about determining the boundaries of membership functions roughly. This rough information was examined more detailed by making more experiments by changing the boundaries of membership functions and observing the change of the performance of the tracking system. Output signal generated by the fuzzy controller (increment of duty ratio) changes the PV cell's output voltage and current. When the output changes, next time values of fuzzy input variables changes too. By this way the fuzzy controller rearranges the output commands. Basically first of all boundaries of PB and NB were determined according to the input variables' characteristics. The boundaries of ZE was determined by the logic that what we expect from the MPPT when the MPP is reached and the environmental conditions change. Then PS and NS boundaries were determined.

Fuzzy rules database is shown in Figure 48. Iterations were made by moving on the P-V slope's specified regions as shown in the Figure 48.

Δd		ΔP				
		NB	NS	ZE	PS	PB
ΔV	NB	NB	NS	ZE	PS	PB
	NS	NS	NS	ZE	PS	PS
	ZE	ZE	ZE	ZE	ZE	ZE
	PS	PS	PS	ZE	NS	NS
	PB	PB	PS	ZE	NS	NB

Region 1
Region 2
Region 3
Region 4
Region 5
Region 6
Region 7
Region 8
Region 9

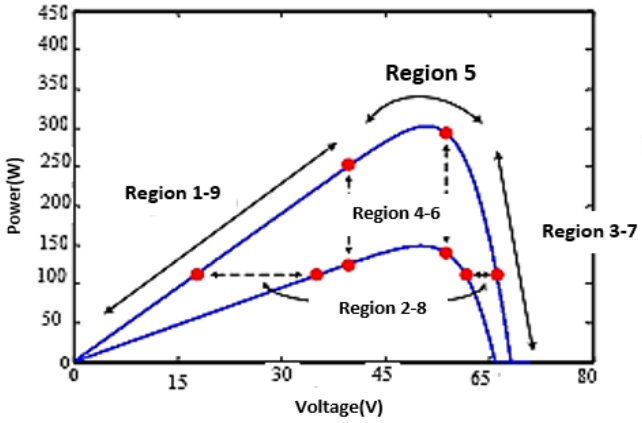

Figure 48. The rule base.

2.1.3. Fuzzy MPPT Algorithms

The experiments were carried out at the specified irradiance and temperature levels as shown in Table 6. The maximum power points are also shown in Table 6. First of all symmetric membership functions were used in the simulations and then asymmetrical membership functions were used. The performance difference was compared then. For fuzzification; Mamdani method and for defuzzification; centre of gravity methods were used in this study. Fuzzy interface system was practiced by using MATLAB Simulink fuzzy logic toolbox.

Table 6. Maximum power values of the PV panel used in the simulations at different irradiation and temperature levels.

Irradiance Level (W/m^2)	**Temperature (^oC)**	**Maximum PV output Power (W)**
1000	25	305,2
400	25	119,8
200	25	52,62
1000	0	325,9
1000	50	281,6

2.1.3.1. Change of Power (ΔP_{PV}) and Change of Voltage (ΔV_{PV}) as Inputs

The rule database was obtained by making iterations on Figure 49 and the test circuit shown in Figure 53 was used to perform experiments.

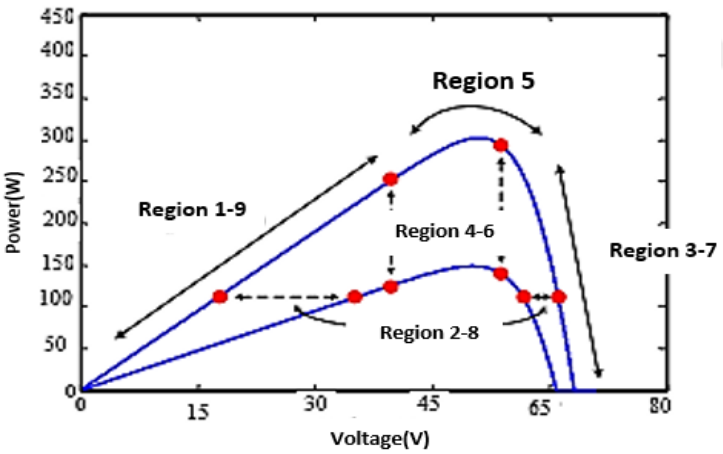

Figure 49. Change of P-V characteristic.

Δd		ΔP				
		NB	NS	ZE	PS	PB
ΔV	NB	NB	NS	ZE	PS	PB
	NS	NS	NS	ZE	PS	PS
	ZE	ZE	ZE	ZE	ZE	ZE
	PS	PS	PS	ZE	NS	NS
	PB	PB	PS	ZE	NS	NB

Region 1
Region 2
Region 3
Region 4
Region 5
Region 6
Region 7
Region 8
Region 9

Figure 50. The rule database.

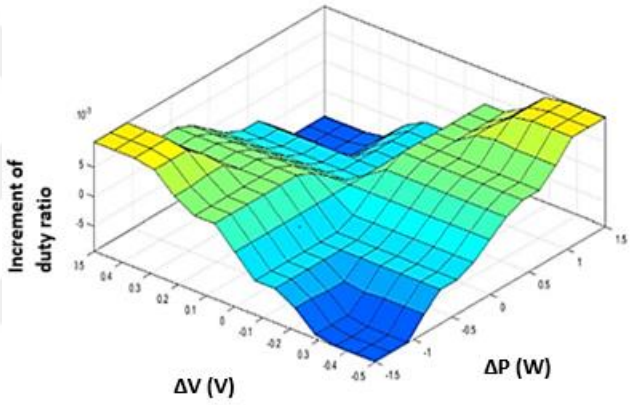

Figure 51. Fuzzy controller's input-output surface (with symmetrical membership functions).

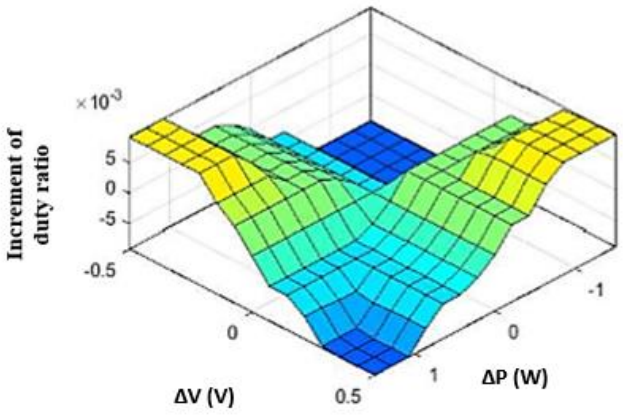

Figure 52. Fuzzy controller's input-output surface (with asymmetrical membership functions).

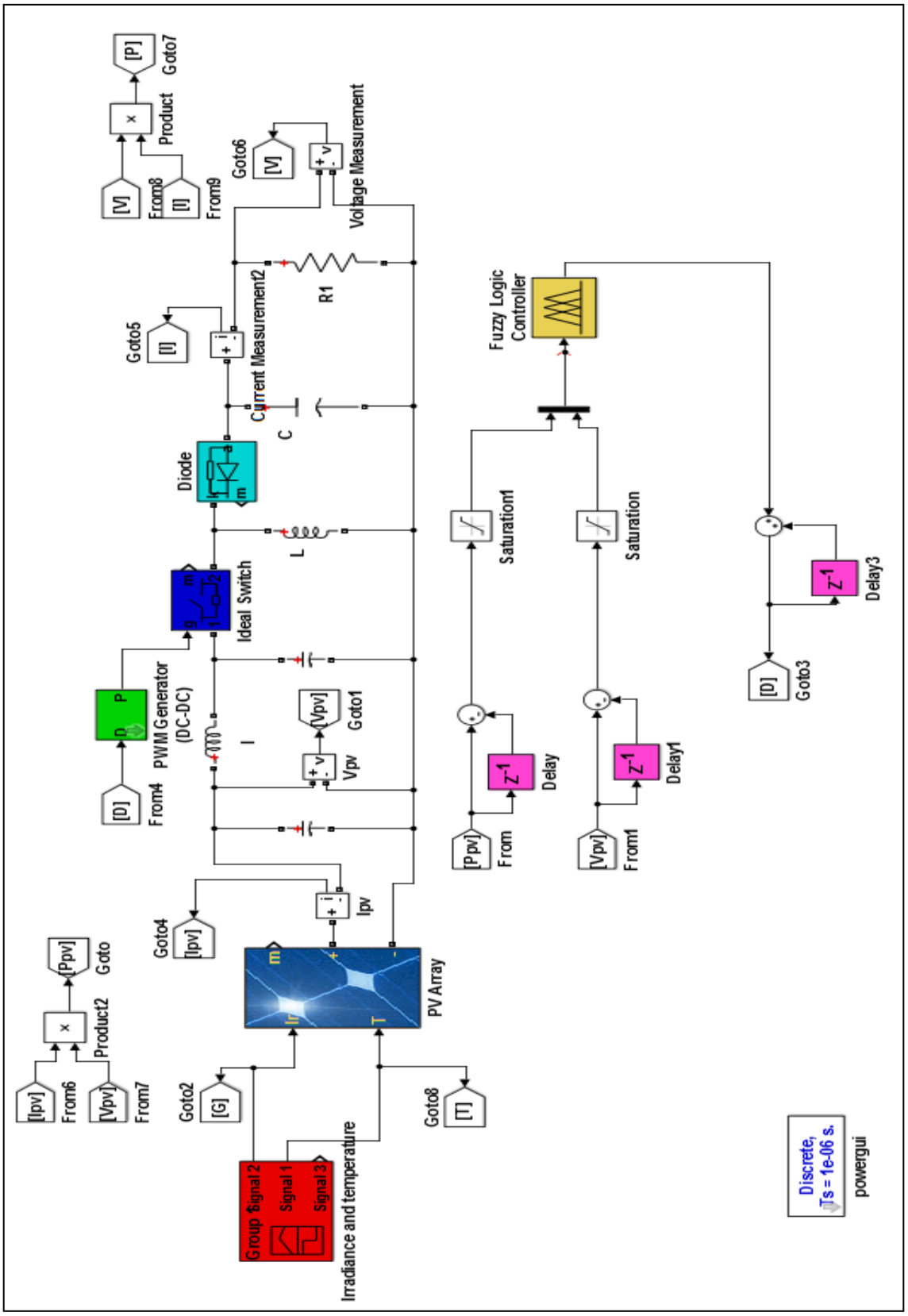

Figure 53. Simulink model of the test circuit used for the tracking algorithm change of power (ΔP_{PV}) and change of voltage (ΔV_{PV}) as inputs.

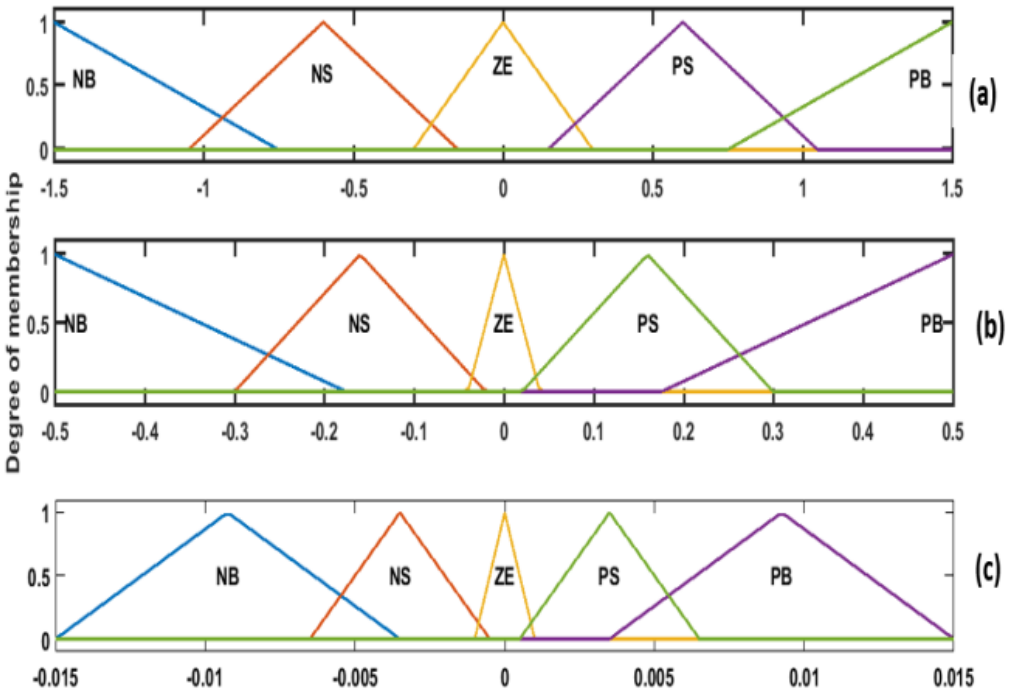

Figure 54. Symmetrical input membership functions (a) MF of ΔP_{PV} (b) MF of ΔV_{PV} (c) MF of increment of duty ratio command.

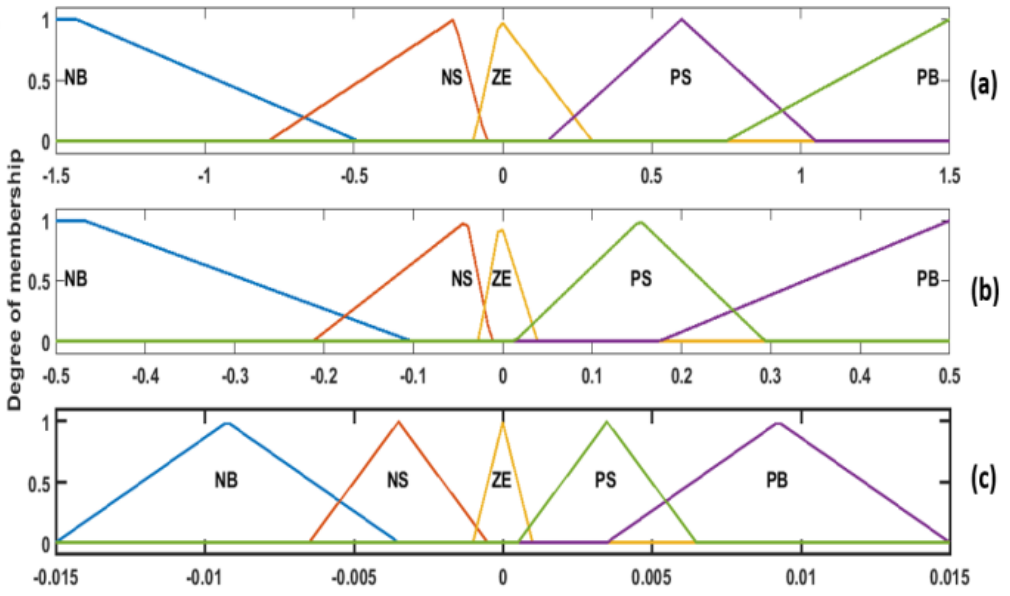

Figure 55. Asymmetrical input membership functions (a) MF of ΔP_{PV} (b) MF of ΔV_{PV} (c) MF of increment of duty ratio command.

As shown in Figure 49, the P-V characteristic curve divided into 9 regions. Now we have to determine how should the MPPT controller behave in order to reach the MPP.

At region 1: Power and voltage decrease at the same time under same irradiation level. The operating point is at the left side of the MPP. This means we need to decrease the duty ratio.

At region 2: Power doesn't change but voltage decreases. The algorithm can't determine the change in irradiation level so that the duty ratio command shouldn't be changed.

At region 3: Power increases and voltage decreases at the same irradiation level. The operating point is at the right side of the MPP. This means we need to increase the duty ratio.

At region 4: Power decreases and voltage doesn't change. The algorithm can't determine the change in irradiation level so that the duty ratio command shouldn't be changed.

At region 5: Both power and voltage don't change so that the duty ratio shouldn't be changed.

At region 6: Power increases and voltage doesn't change. The algorithm can't determine the change in irradiation level so that the duty ratio command shouldn't be changed.

At region 7: Power decreases and voltage increases under same irradiation level. The operating point is at the right side of the MPP. So that the duty ratio should be increased.

At region 8: Power doesn't change and voltage increases. The algorithm can't determine the change in irradiation level so that the duty ratio command shouldn't be changed.

At region 9: Power and voltage increase at the same time under same irradiation level. The operating point is at the left side of the MPP. This means we need to decrease the duty ratio.

Simulation results by using symmetrical and asymmetrical membership functions are shown in Figure 56 and Figure 57 respectively.

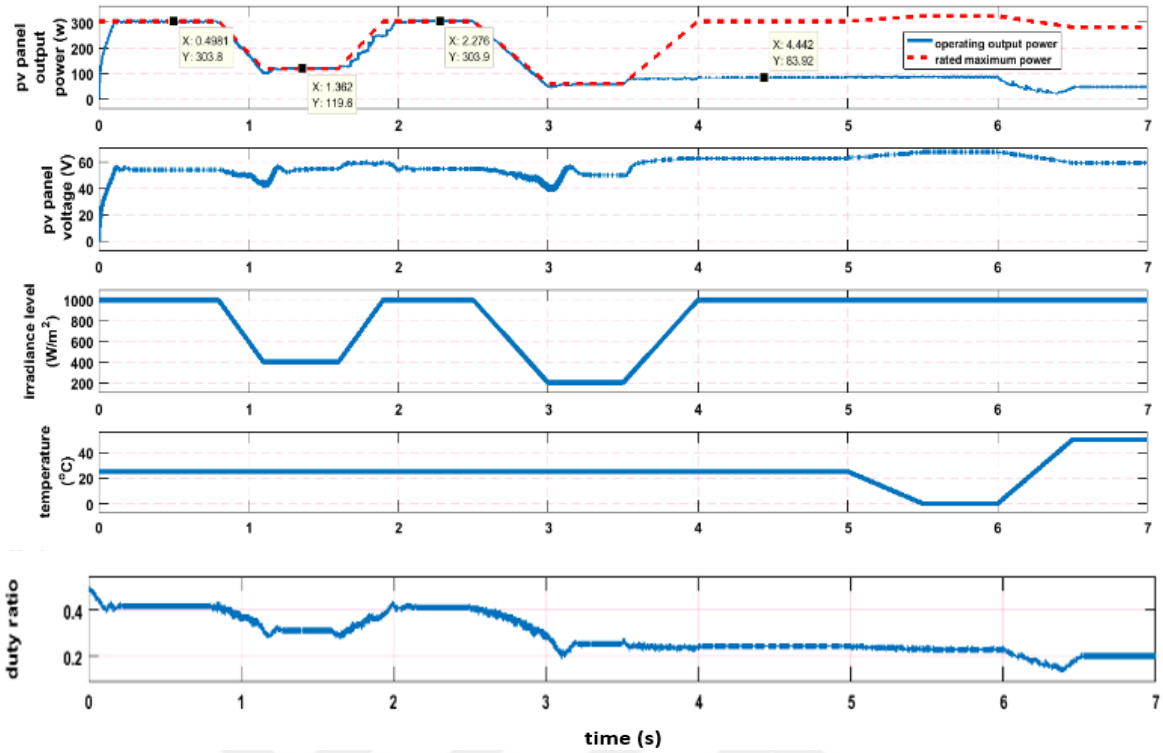

Figure 56. Simulation results (symmetrical MFs were used) (the point (X,Y) refers to maximum power point).

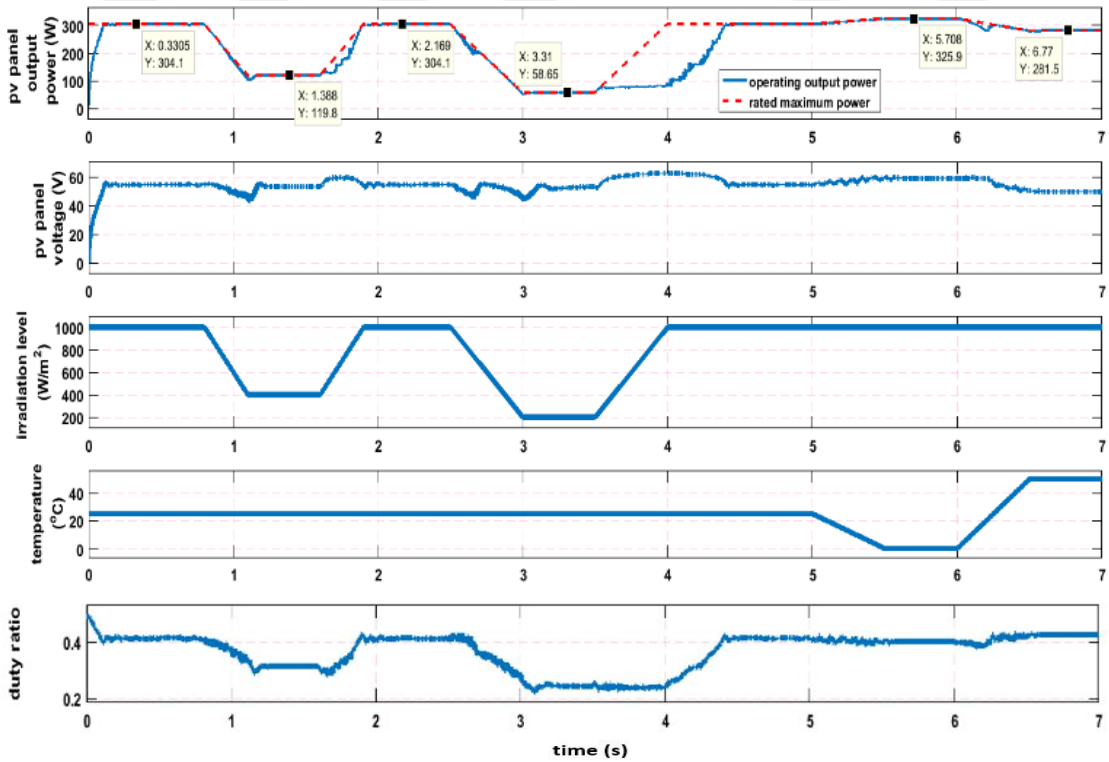

Figure 57. Simulation results (asymmetrical membership functions were used) (the point (X,Y) refers to maximum power point).

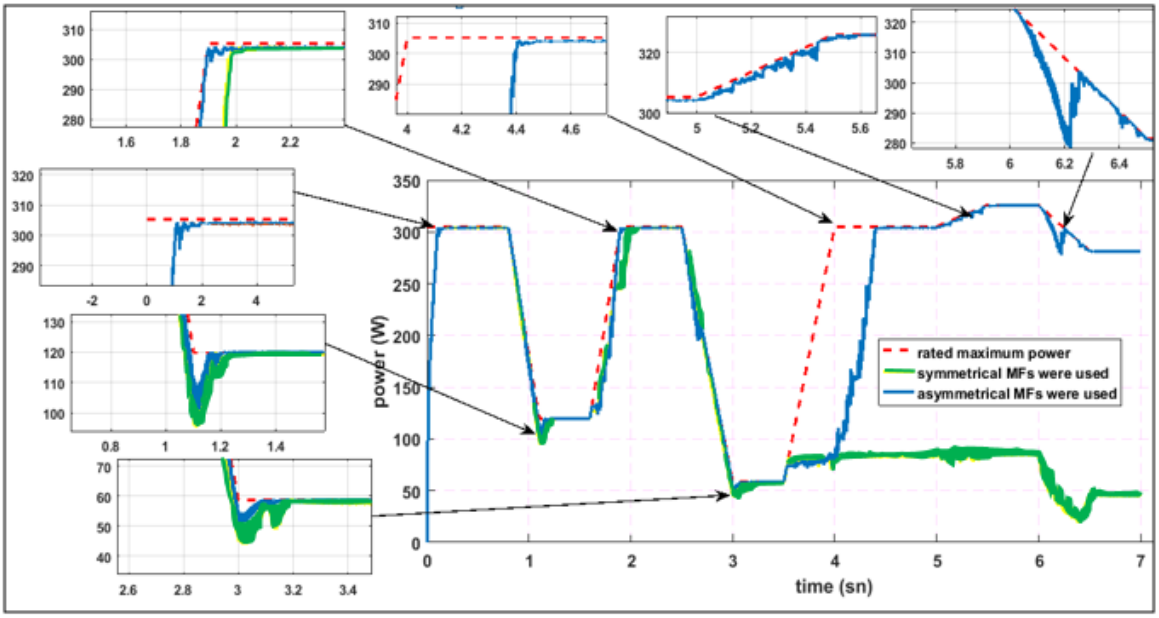

Figure 58. Detailed view of the output power of PV panel represented in Figure 56 and 57.

2.1.3.2. Change of Power (ΔP_{PV}) and Change of Current (ΔI_{PV}) as Inputs

The rule database was obtained by making iterations on Figure 59 and the test circuit shown in Figure 63 was used to perform experiments. When the operating point is at the right side of the MPP, the slope of the P-I curve is very sharp. At this region tracking operation is very sensitive to the change of increment of duty ratio.

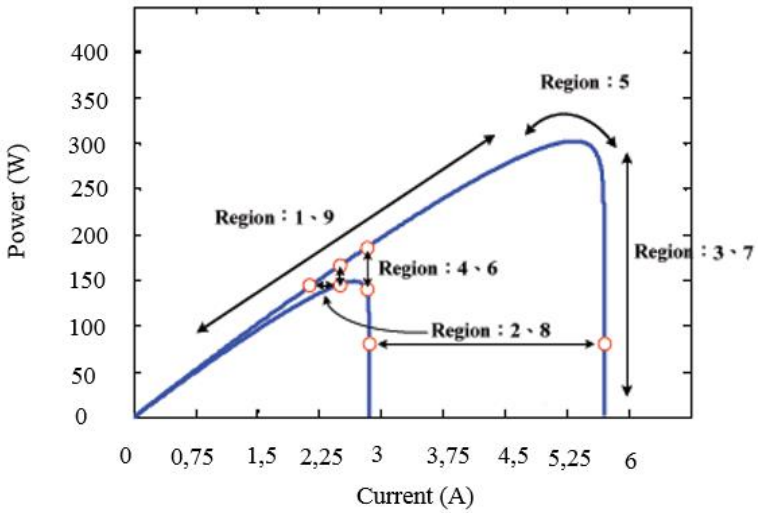

Figure 59. Change of P-I characteristic.

Δd		ΔP				
		NB	NS	ZE	PS	PB
ΔI	NB	PB	PS	ZE	NS	NB
	NS	PS	PS	ZE	NS	NS
	ZE	ZE	ZE	ZE	ZE	ZE
	PS	NS	NS	ZE	PS	PS
	PB	NB	NS	ZE	PS	PB

Region 1
Region 2
Region 3
Region 4
Region 5
Region 6
Region 7
Region 8
Region 9

Figure 60. The rule database.

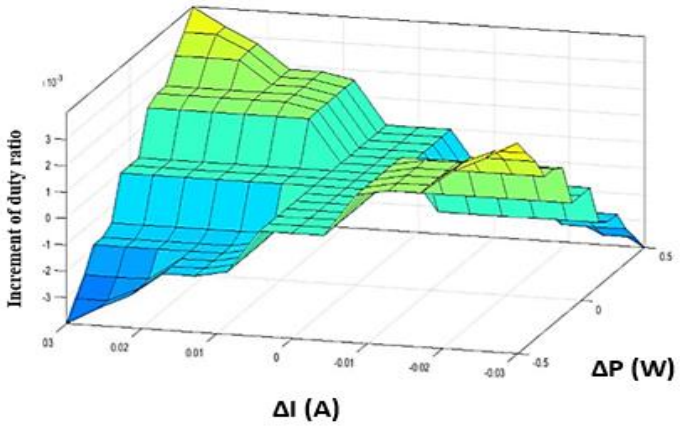

Figure 61. Fuzzy controller's input-output surface (with symmetrical membership functions).

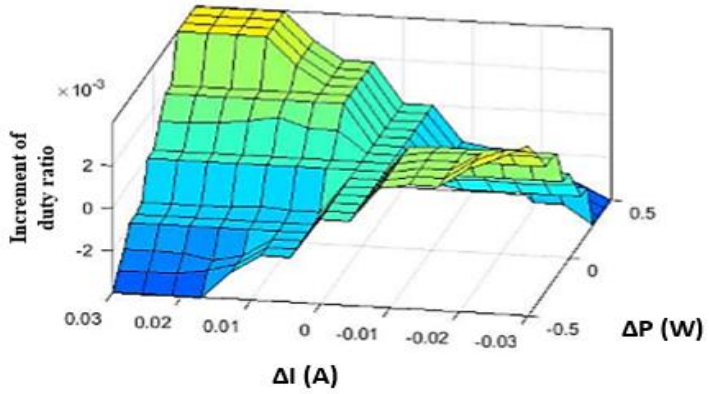

Figure 62. Fuzzy controller's input-output surface (with asymmetrical membership functions).

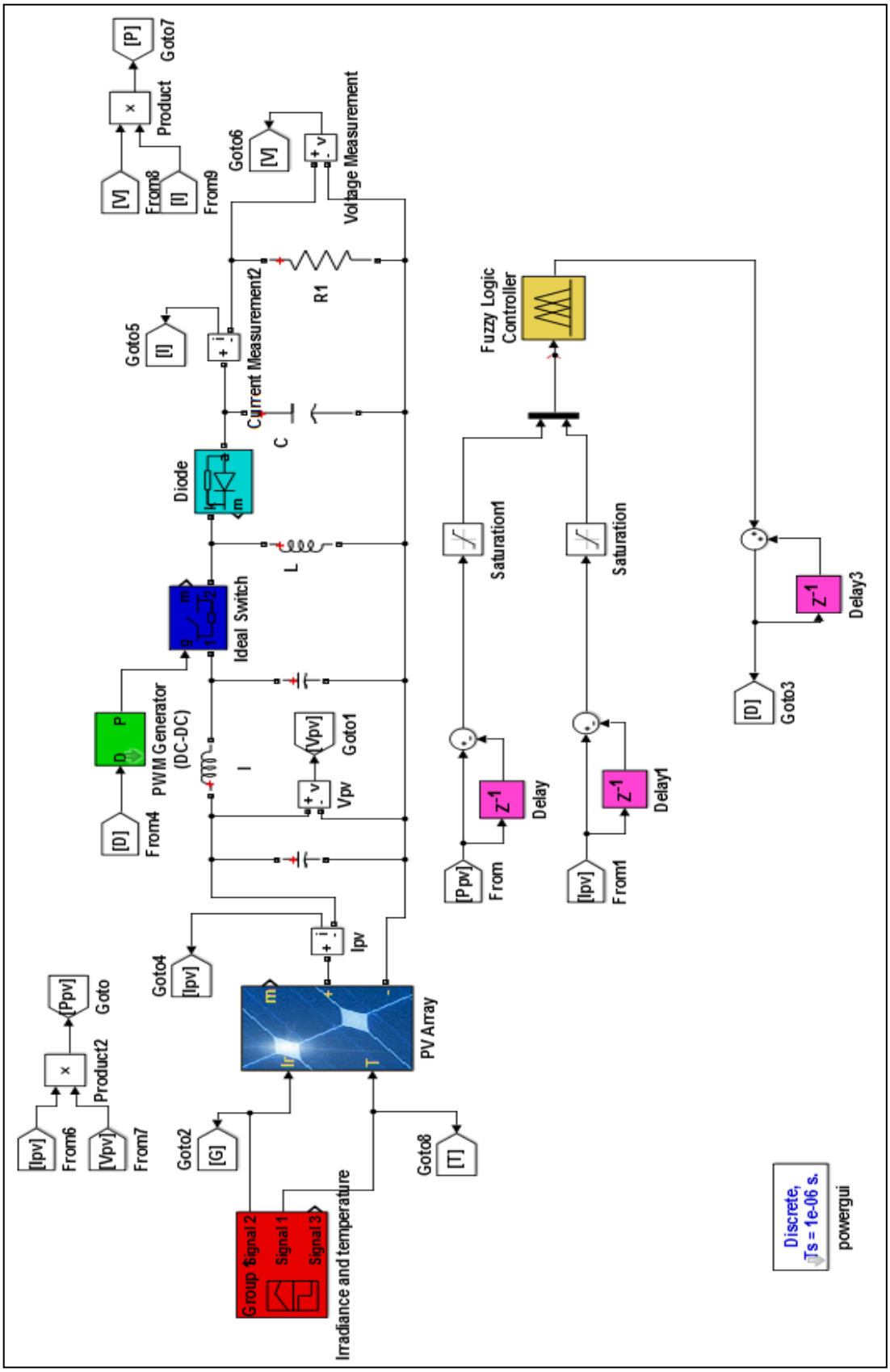

Figure 63. Simulink model of the test circuit used for the tracking algorithm change of power (ΔP_{PV}) and change of current (ΔI_{PV}) as inputs.

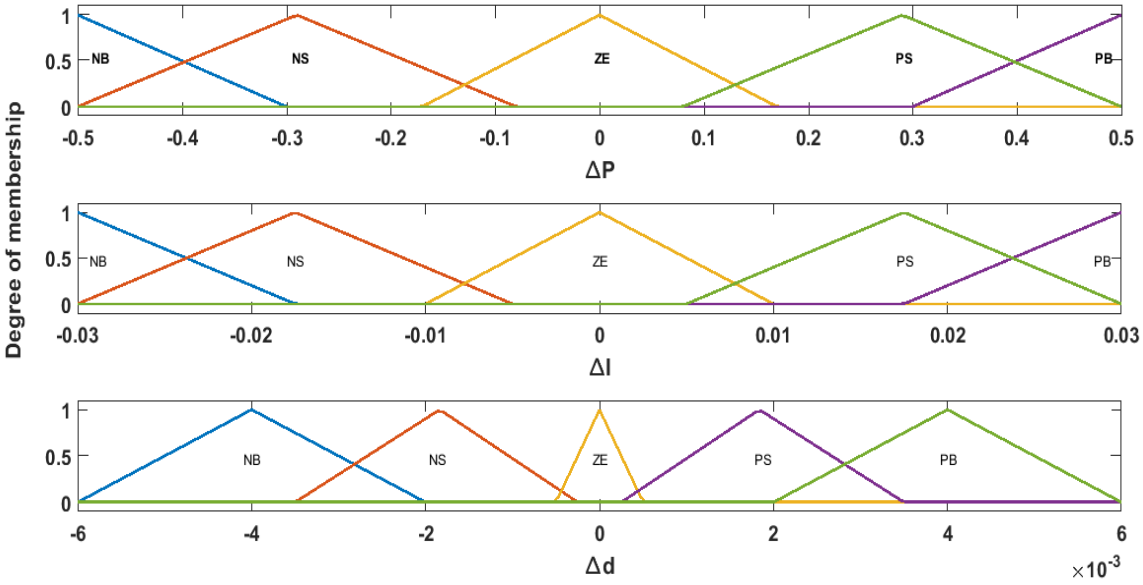

Figure 64. Symmetrical input membership functions.

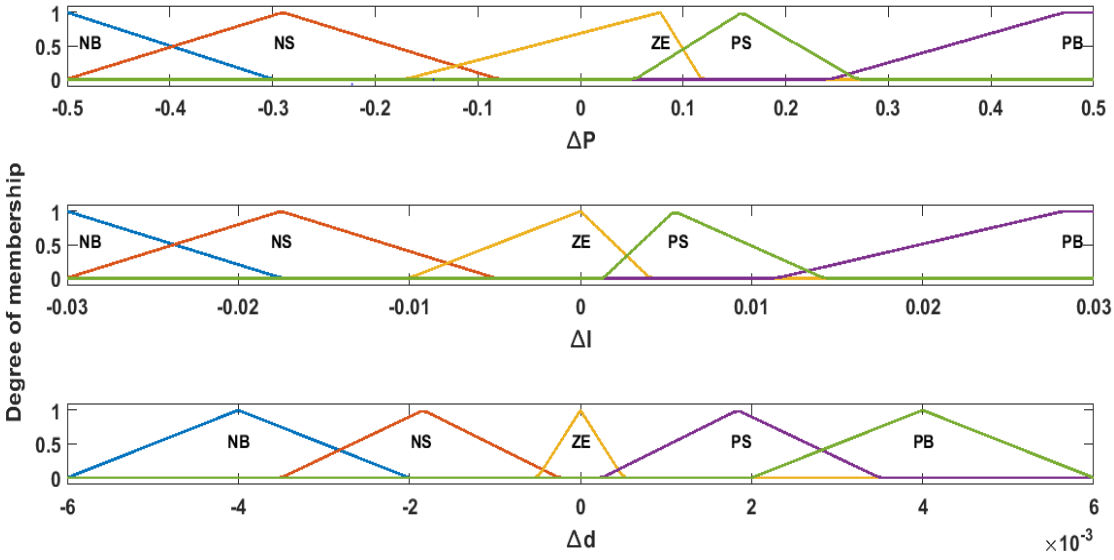

Figure 65. Asymmetrical input membership functions.

As shown in Figure 59, the P-I characteristic curve divided into 9 regions. Now we have to determine how should the MPPT controller behave in order to reach the MPP.

At region 1: Power and current decrease at the same time under same irradiation level. The operating point is at the left side of the MPP. This means we need to increase the duty ratio.

At region 2: Power doesn’t change but current decreases. The algorithm can’t determine the change in irradiation level so that the duty ratio command shouldn’t be changed.

At region 3: Power increases and current decreases at the same irradiation level. The operating point is at the right side of the MPP. This means we need to decrease the duty ratio.

At region 4: Power decreases and current doesn’t change. The algorithm can’t determine the change in irradiation level so that the duty ratio command shouldn’t be changed.

At region 5: Both power and current don’t change so that the duty ratio shouldn’t be changed.

At region 6: Power increases and current doesn’t change. The algorithm can’t determine the change in irradiation level so that the duty ratio command shouldn’t be changed.

At region 7: Power decreases and current increases under same irradiation level. The operating point is at the right side of the MPP. So that the duty ratio should be decreased.

At region 8: Power doesn’t change and current increases. The algorithm can’t determine the change in irradiation level so that the duty ratio command shouldn’t be changed.

At region 9: Power and current increase at the same time under same irradiation level. The operating point is at the left side of the MPP. This means we need to increase the duty ratio.

Simulation results shown in Figure 66,67 and 68 show us that this tracking algorithm was not able to track accurately at low irradiation levels. This is because at low irradiation levels the operating point easily shifts to the short circuit current. However there is no significant difference in the performance of MPPT by using both symmetrical and asymmetrical membership functions.

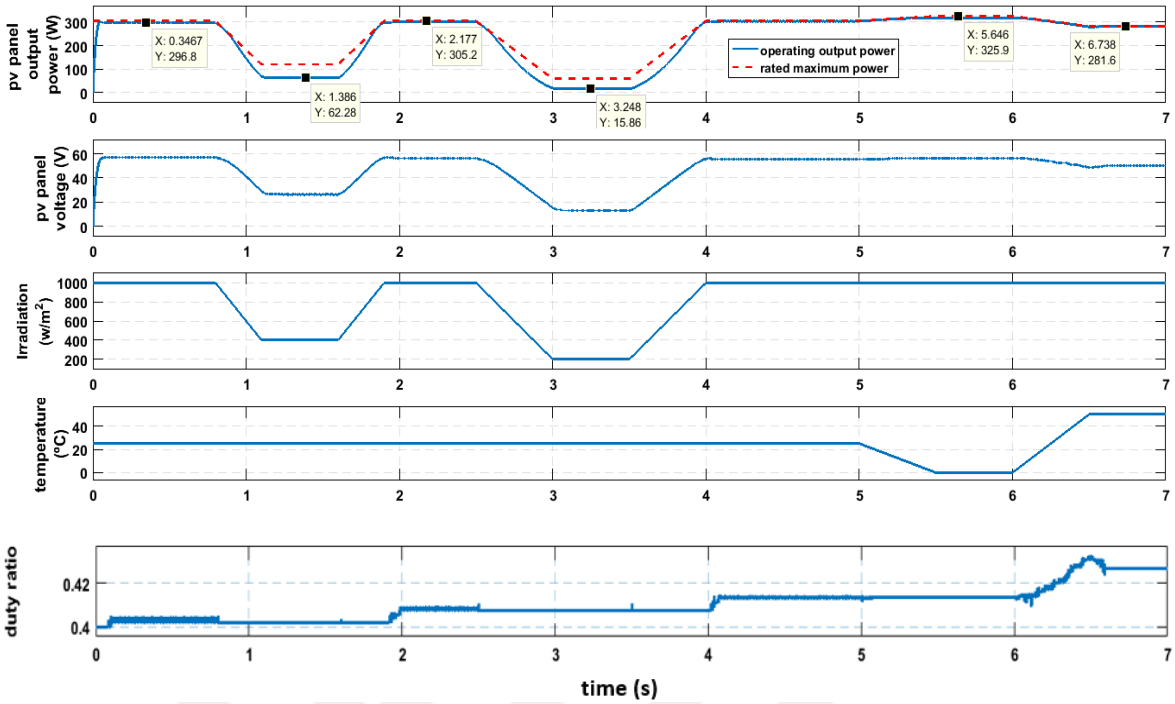

Figure 66. Simulation results (symmetrical MFs were used) (the point (X,Y) refers to maximum power point).

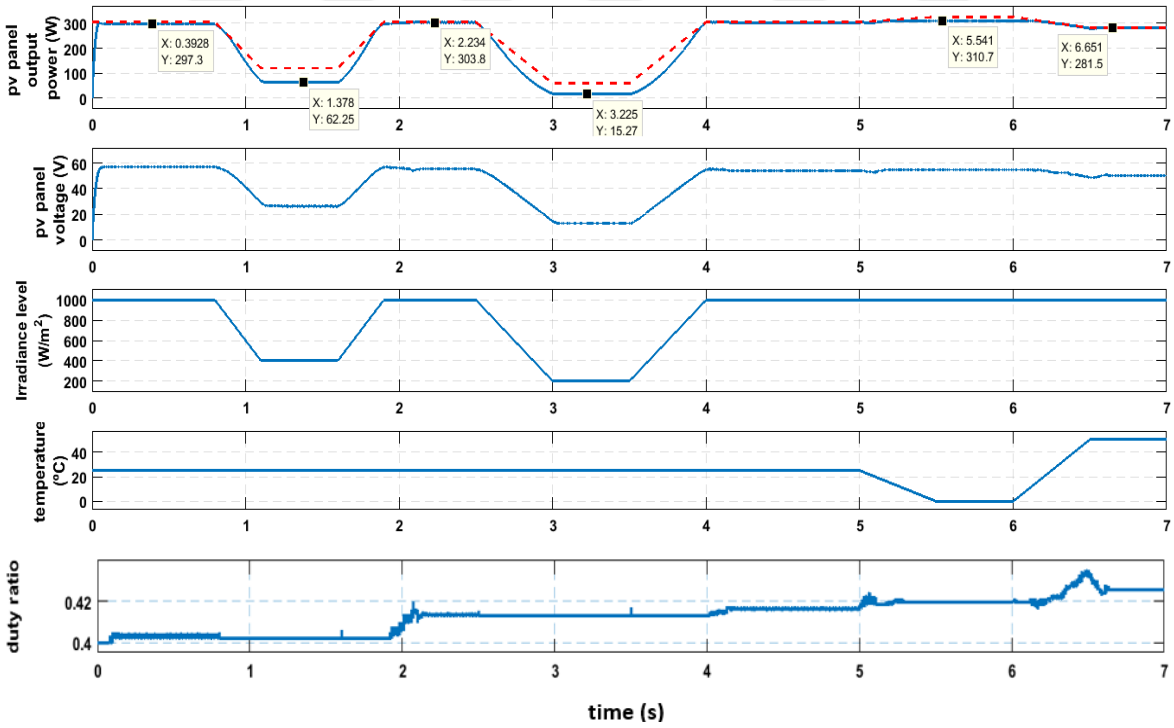

Figure 67. Simulation results (asymmetrical MFs were used) (the point (X,Y) refers to maximum power point).

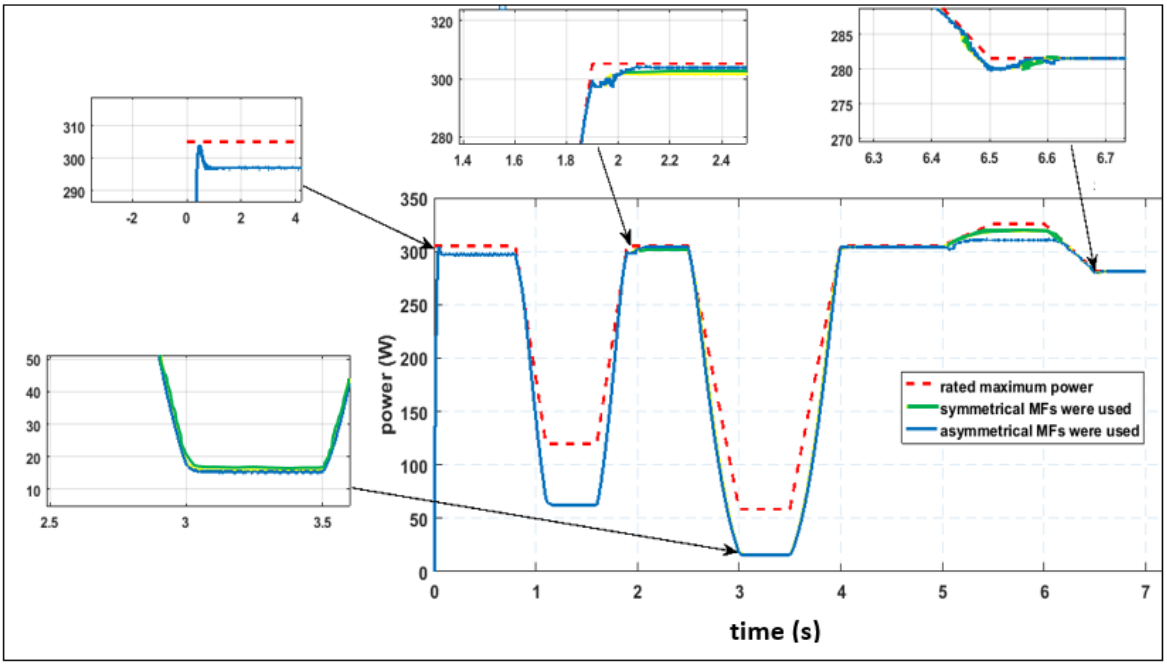

Figure 68. Detailed view of the output power of PV panel represented in Figure 66 and 67.

2.1.3.3. P-V Slope and Change of Slope as Inputs

The slope of the PV cell's P-V curve is defined as;

$$S(i) = \frac{\Delta P_{PV}}{\Delta V_{PV}} = \frac{I_{PV}(i).V_{PV}(i) - I_{PV}(i-1).V_{PV}(i-1)}{V_{PV}(i) - V_{PV}(i-1)} \quad (29)$$

$$\Delta S(i) = S(i) - S(i-1) \quad (30)$$

The rule database was obtained by making iterations on Figure 69 and the test circuit shown in Figure 73 was used to perform experiments.

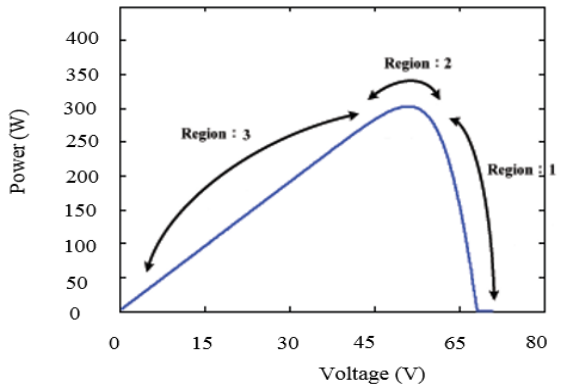

Figure 69. P-V characteristic of PV cell.

Δd		S(i)				
		NB	NS	ZE	PS	PB
ΔS(i)	NB	ZE	PB	PS	ZE	NB
	NS	PB	PS	ZE	ZE	NB
	ZE	PB	PS	ZE	NS	NB
	PS	PB	ZE	ZE	NS	NB
	PB	PB	ZE	NS	NB	ZE

Region 1
Region 2
Region 3

Figure 70. The rule database.

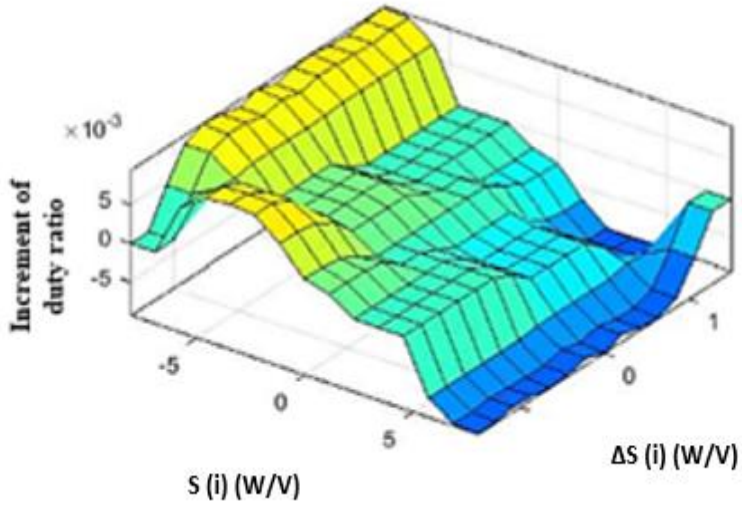

Figure 71. Fuzzy controller's input-output surface (with symmetrical membership functions).

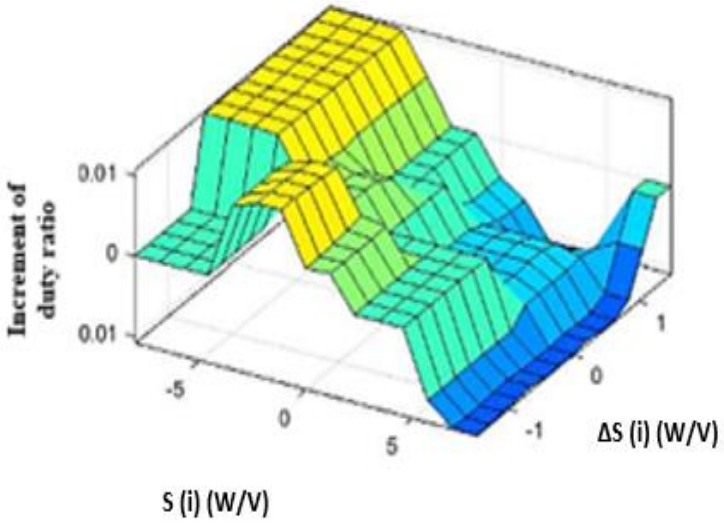

Figure 72. Fuzzy controller's input-output surface (with asymmetrical membership functions).

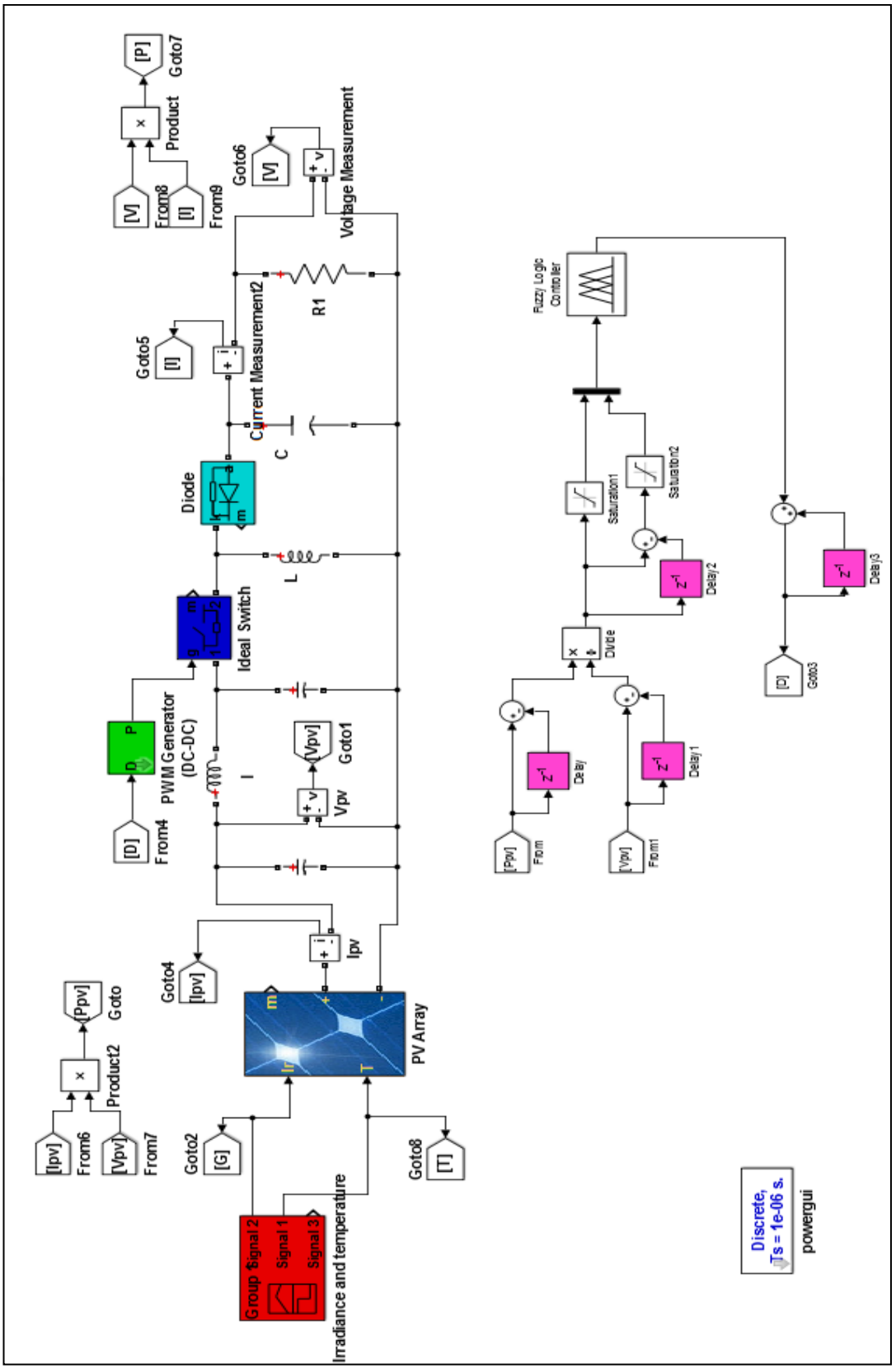

Figure 73. Simulink model of the test circuit used for the tracking algorithm P-V slope and change of slope as inputs.

As shown in Figure 69, the P-V characteristic curve divided into 3 regions. Now we have to determine how should the MPPT controller behave in order to reach the MPP.

At region 1: In this region the slope is negative, this means the operating point is at the right side of the MPP. So that the duty ratio should be increased to reach the MPP. When S(i) and ΔS(i) are both NB, this means operating point approaches or leaves the MPP rapidly. So that the output should be ZE in order to avoid wrong tracking function. When S(i) is NS and ΔS(i) is positive, this means that the operating point is approaching the MPP. So that in order not to increase the duty ratio too much and prevent oscillations the output should be ZE.

At region 2: In this region S(i) is zero. That means the operating point is near to the MPP. If ΔS(i) is NB (duty ratio decreased), the operating point approaches the MPP from left side rapidly. In order not pass the MPP the output should be PS.

If ΔS(i) is PB (duty ratio increased), the operating point approaches the MPP from right side rapidly. In order not pass the MPP the output should be NS.

At region 3: In this region the slope is positive, this means the operating point is at the left side of the MPP. So that the duty ratio should be decreased to reach the MPP. When S(i) and ΔS(i) are both PB, this means operating point approaches or leaves the MPP rapidly. So that the output should be ZE in order to avoid wrong tracking function. When S(i) is PS and ΔS(i) is negative, this means that the operating point is approaching the MPP. So that in order not to increase the duty ratio too much and prevent oscillations the output should be ZE.

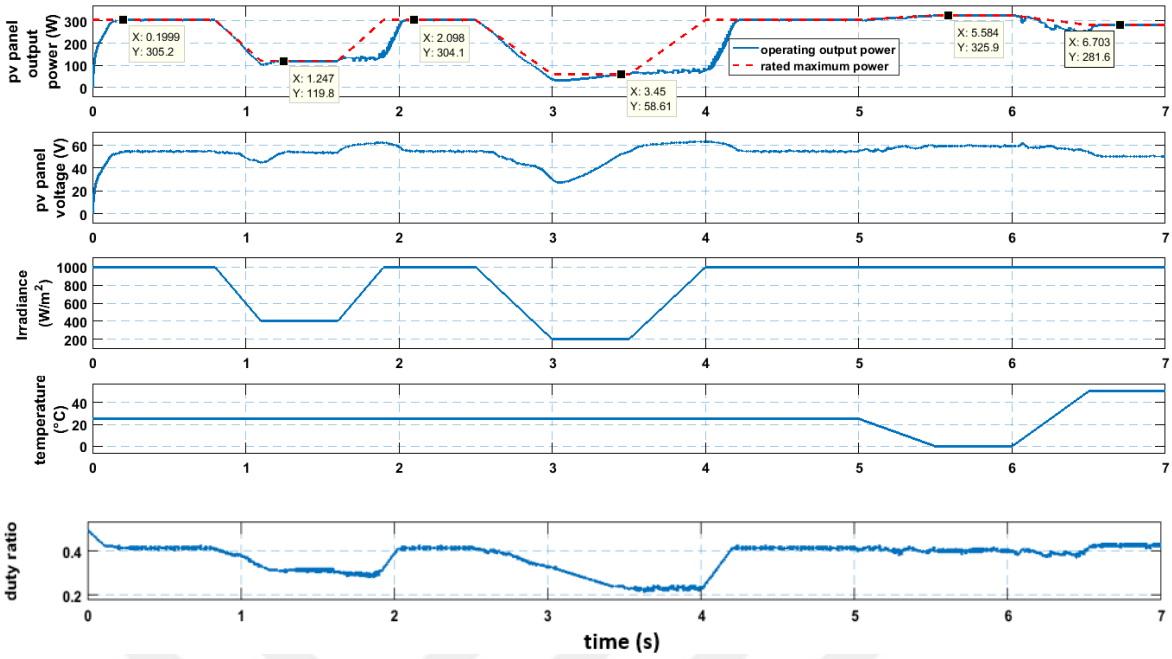

Figure 74. Simulation results (symmetrical MFs were used) (the point (X,Y) refers to maximum power point).

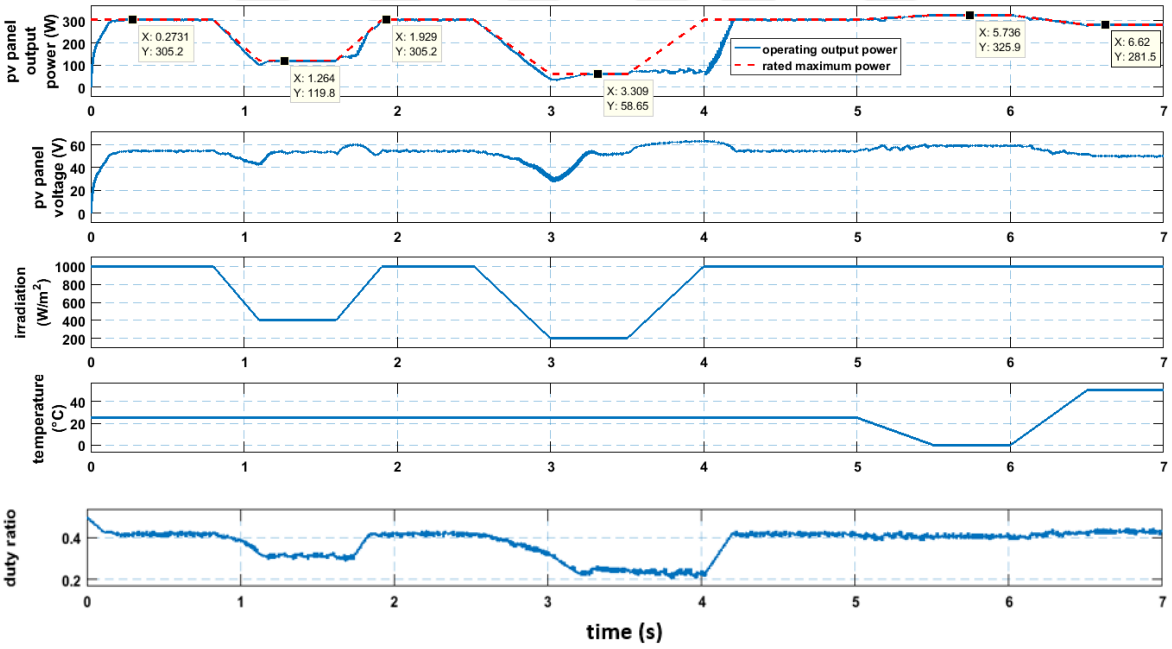

Figure 75. Simulation results (asymmetrical MFs were used) (the point (X,Y) refers to maximum power point).

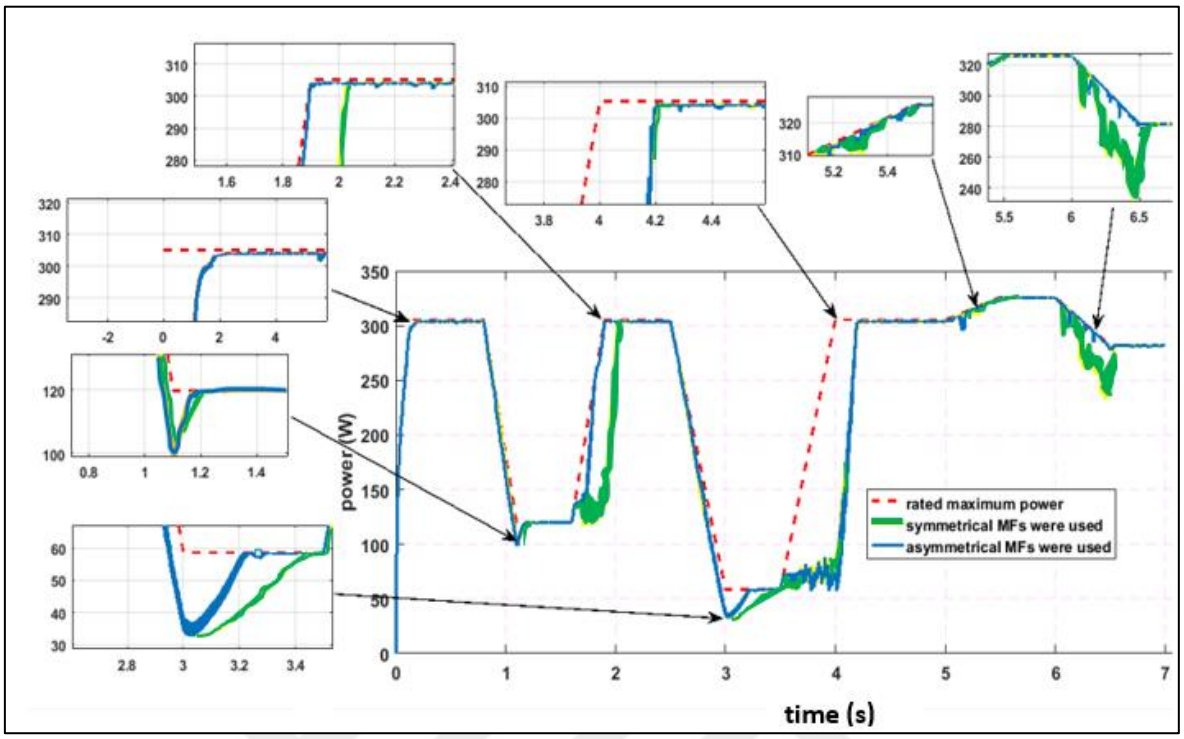

Figure 76. Detailed view of the output power of PV panel represented in Figure 74 and 75.

3. RESULTS

3.1. Simulation Results Obtained Under Changing Irradiation and Temperature Levels.

In this section the simulation results that were obtained under changing irradiation and temperature levels will be examined. Maximum power point tracking performance of the tracking algorithms that were introduced in previous section will be evaluated respectively. Simulations were carried out based on the test circuits represented in the previous section.

Table 7. Maximum power values of the PV panel used in the simulations at different irradiation and temperature levels.

Irradiance Level (W/m^2)	**Temperature (^oC)**	**Maximum PV output Power (W)**
1000	25	305,2
400	25	119,8
250	25	73,86
1000	50	281,6

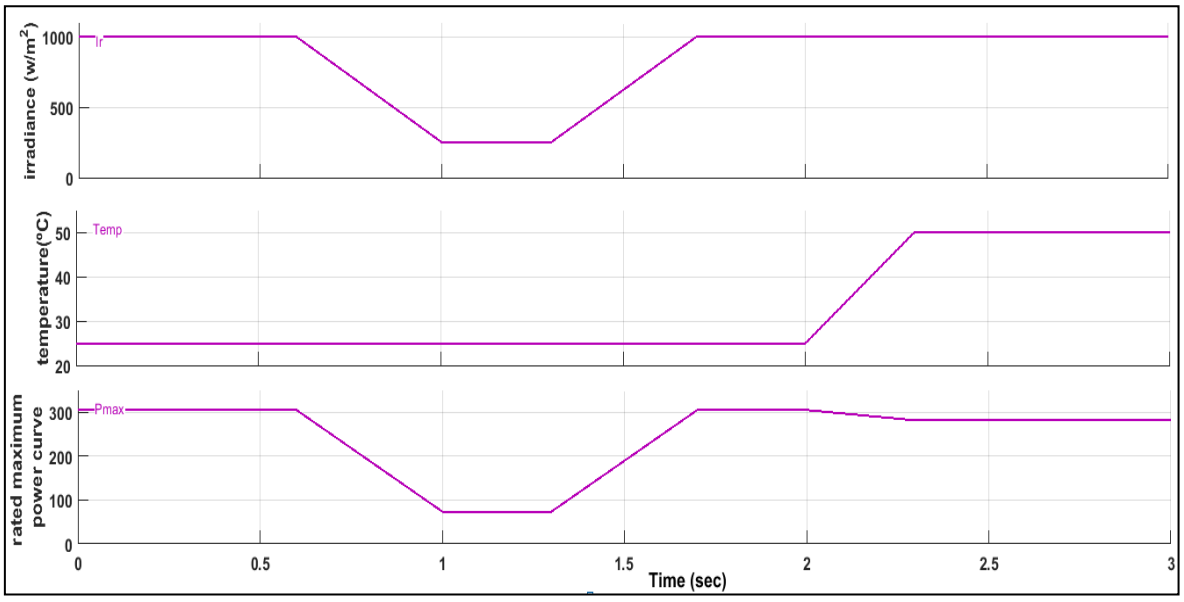

Figure 77. Operating conditions stated at Table 7.

The tracking performance will be examined according to the two criteria. These are;

- Efficiency= $\eta = \frac{E}{E_{max}} = \frac{\int_0^T P(t).d(t)}{\int_0^T P_{max}(t).d(t)}$ (31)

- Settling time: Time elapsed to reach the maximum power value

Efficiency is calculated in Matlab by using “trapz” function as fallows;

```
>> %a=the rated maximum power curve
%b=the operating power curve
x=a.data; %getting values of a
y=b.data; %getting values of be
100*trapz(y)/trapz(x) %efficiency formula

ans =

   49.0658
```

Figure 78. Calculation of efficiency in Matlab.

3.1.1. Simulation Results for Algorithm Change of Power (ΔP_{PV}) and Change of Voltage (ΔV_{PV}) as Inputs

The simulation results under operating conditions that were represented in Table 7 are shown in Figure 79.

Table 8. Tracking performances.

	Symmetrical MFs were used				Asymmetrical MFs were used			
Efficiency(%)	**49,0658**				**87,4189**			
	Region 1	**Region 2**	**Region 3**	**Region 4**	**Region 1**	**Region 2**	**Region 3**	**Region 4**
Tracked Maximum Power (W)	**303,8**	**73,6**	**87,5**	**26,7**	**304,1**	**73,1**	**303,4**	**281,1**
Rated Maximum Power (W)	**305,2**	**73,86**	**305,2**	**281,6**	**305,2**	**73,86**	**305,2**	**281,6**
Tracking Accuracy (%)	**99,5413**	**99,6480**	**28,6697**	**9,4815**	**99,6396**	**98,9710**	**99,4102**	**99,8224**
Overall Tracking Accuracy (%)	**59,3351**				**99,4608**			
Settling time (s)	**0,198**	**0,188**	**0**	**0**	**0,199**	**0,182**	**0,255**	**0,026**

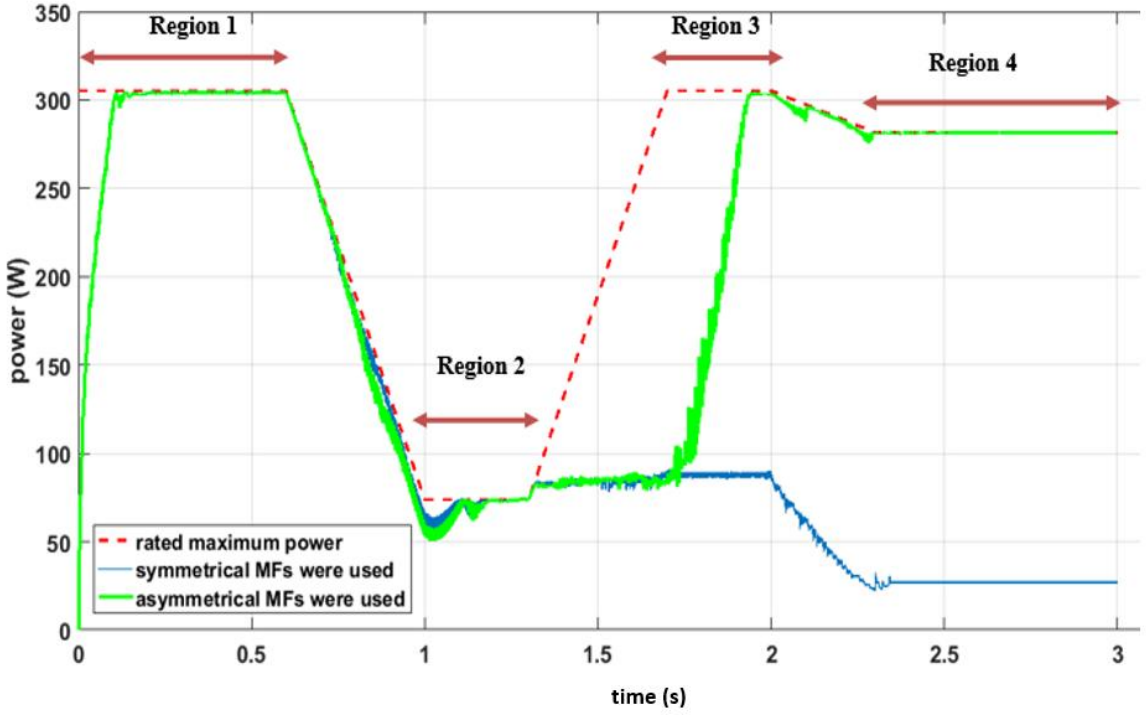

Figure 79. Simulation results under the operating conditions stated at Table 7.

3.1.2. Simulation Results for Algorithm Change of Power (ΔP_{PV}) and Change of Current (ΔI_{PV}) as Inputs

The simulation results under operating conditions that were represented in Table 7 are shown in Figure 80.

Table 9. Tracking performances.

	Symmetrical MFs were used				Asymmetrical MFs were used			
Efficiency(%)	**92,338**				**92,8166**			
	Region 1	**Region 2**	**Region 3**	**Region 4**	**Region 1**	**Region 2**	**Region 3**	**Region 4**
Tracked Maximum Power (W)	**296,8**	**25,4**	**301,1**	**281,5**	**301,4**	**24,4**	**303,8**	**281,5**
Rated Maximum Power (W)	**305,2**	**73,86**	**305,2**	**281,6**	**305,2**	**73,86**	**305,2**	**281,6**
Tracking Accuracy (%)	**97,2477**	**34,3894**	**98,6566**	**99,9645**	**98,7549**	**33,0355**	**99,5413**	**99,9645**
Overall Tracking Accuracy (%)	**82,5645**				**82,8240**			
Settling time (s)	**0,1**	**0,04**	**0,077**	**0,205**	**0,163**	**0,072**	**0,097**	**0,089**

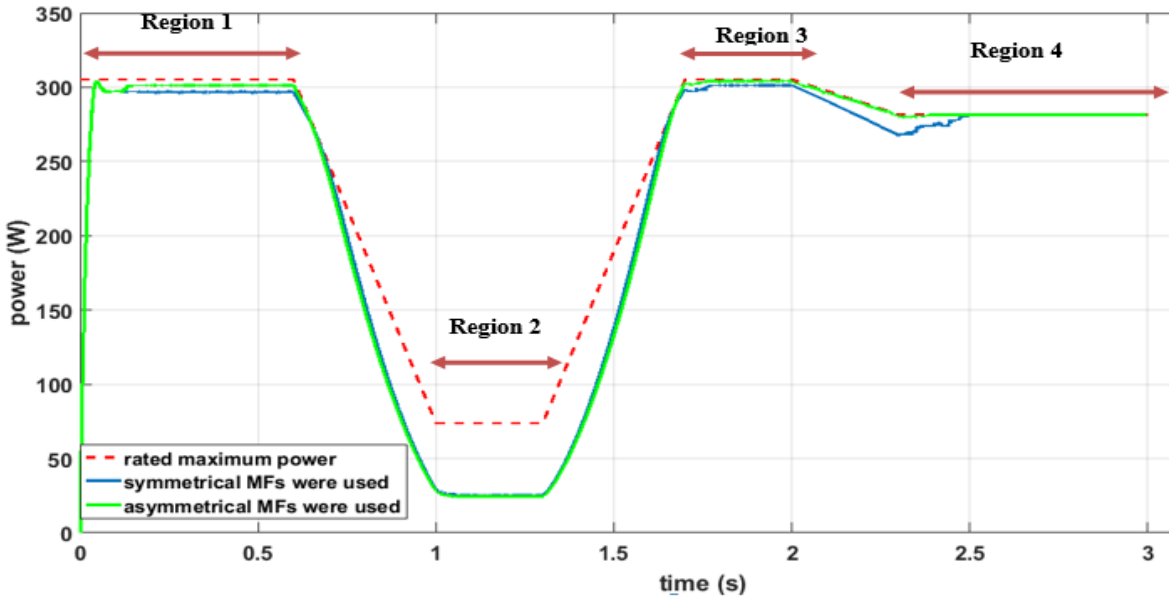

Figure 80. Simulation results under the operating conditions stated at Table 7.

3.1.3. Simulation Results for Algorithm P-V Slope and Change of Slope as Inputs.

The simulation results under operating conditions that were represented in Table 7 are shown in Figure 81.

Table 10. Tracking performances.

	Symmetrical MFs were used				Asymmetrical MFs were used			
Efficiency(%)	**88,9852**				**89,4268**			
	Region 1	**Region 2**	**Region 3**	**Region 4**	**Region 1**	**Region 2**	**Region 3**	**Region 4**
Tracked Maximum Power (W)	**304,1**	**73,2**	**304,1**	**281,5**	**304,1**	**73,8**	**304,1**	**281,5**
Rated Maximum Power (W)	**305,2**	**73,86**	**305,2**	**281,6**	**305,2**	**73,86**	**305,2**	**281,6**
Tracking Accuracy (%)	**99,6396**	**99,1064**	**99,6396**	**99,9645**	**99,6396**	**99,9188**	**99,6396**	**99,9645**
Overall Tracking Accuracy (%)	**99,5875**				**99,7906**			
Settling time (s)	**0,229**	**0,247**	**0,176**	**0,084**	**0,226**	**0,173**	**0,146**	**0,148**

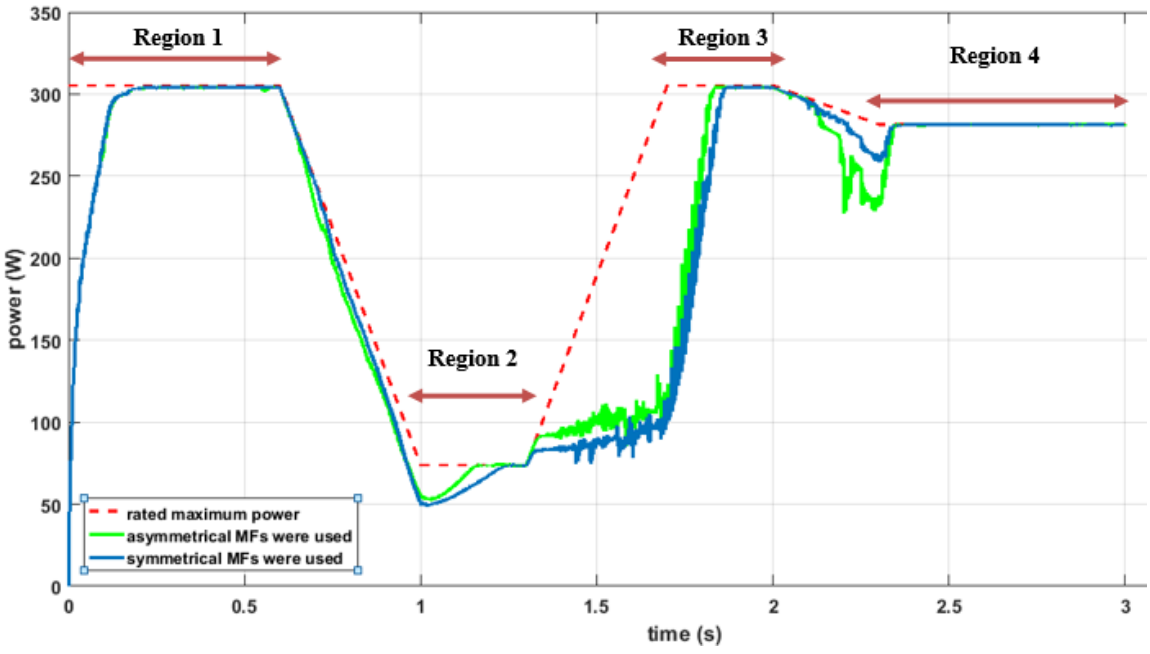

Figure 81. Simulation results under the operating conditions stated at Table 7.

3.2. Results Obtained Under Unchanging Temperature and Low Irradiation Levels.

One the most important performance criteria is the tracking performance of the MPPT system at low irradiation levels. Simulations were carried out 25 °C and 250 W/m^{2}. At these operating conditions the rated maximum power of the PV panel is 73,86 W.

Table 11. Tracking performances (Algorithm Change of Power (ΔP_{PV}) and Change of Voltage (ΔV_{PV}) as Inputs)

	Symmetrical MFs were used	Asymmetrical MFs were used
Efficiency(%)	87,1041	88,1472
Tracked Maximum Power (W)	72,63	73,72
Rated Maximum Power (W)	73,86	73,86
Tracking Accuracy (%)	98,3347	99,8105
Settling time (s)	0,433	0,514

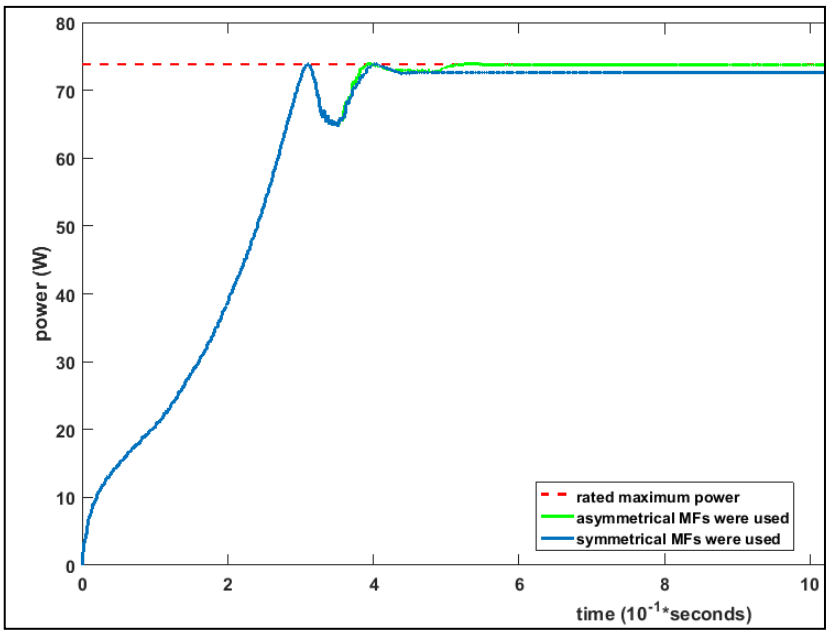

Figure 82. Simulation results (Algorithm Change of Power (ΔP_{PV}) and Change of Voltage (ΔV_{PV}) as Inputs)

Table 12. Tracking performances (Algorithm Change of Power (ΔP_{PV}) and Change of Current (ΔI_{PV}) as Inputs)

	Symmetrical MFs were used	Asymmetrical MFs were used
Efficiency(%)	33,6947	33,6947
Tracked Maximum Power (W)	25,2	25,2
Rated Maximum Power (W)	73,86	73,86
Tracking Accuracy (%)	34,1186	34,1186
Settling time (s)	0,12	0,12

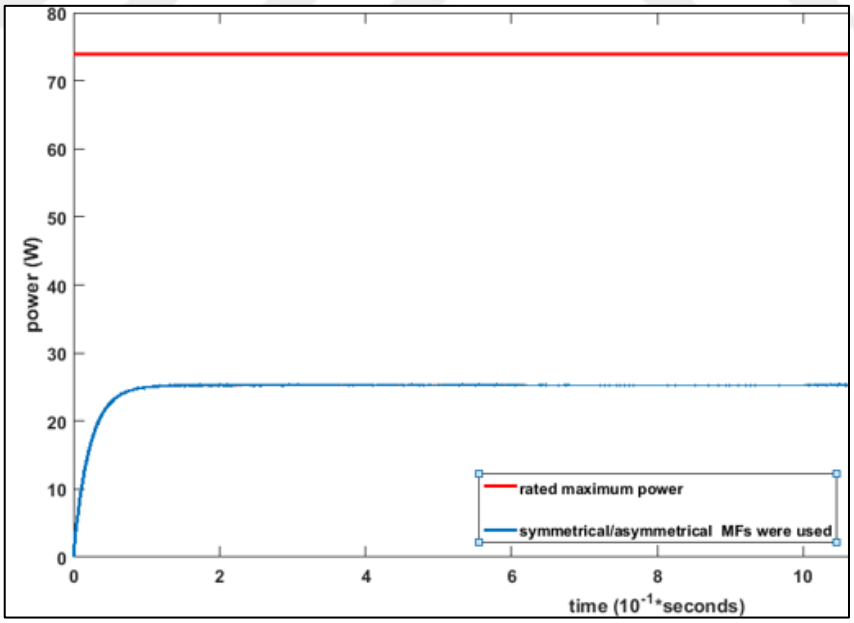

Figure 83. Simulation results (Algorithm Change of Power (ΔP_{PV}) and Change of Current (ΔI_{PV}) as Inputs).

Table 13. Tracking performances (Algorithm P-V Slope and Change of Slope as Inputs).

	Symmetrical MFs were used	Asymmetrical MFs were used
Efficiency(%)	**85,4127**	**90,6782**
Tracked Maximum Power (W)	**73,76**	**73,37**
Rated Maximum Power (W)	**73,86**	**73,86**
Tracking Accuracy (%)	**99,8646**	**99,3366**
Settling time (s)	**0,92**	**0,579**

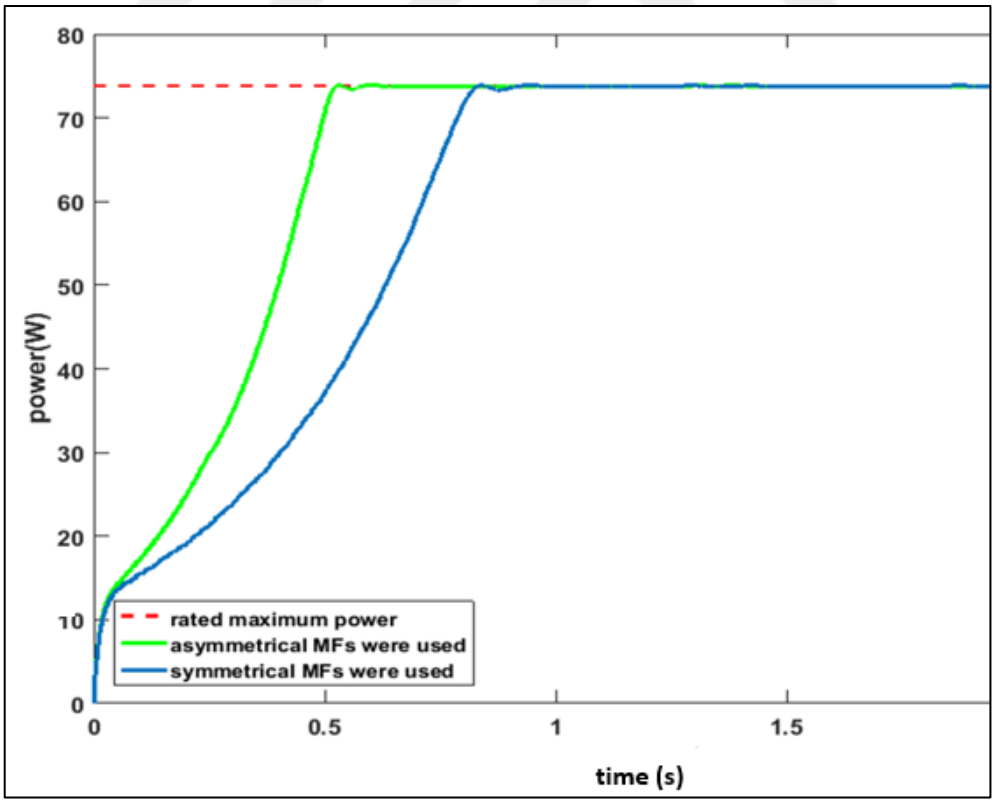

Figure 84. Simulation results (Algorithm P-V Slope and Change of Slope as Inputs).

3.3. Results Obtained Under Unchanging Temperature/Irradiation Levels and Changing Loads.

These simulations were carried out under 1000 W/m^2 irradiance and 25 ˚C temperature. In these simulations only asymmetrical membership functions were used. At the beginning of the simulation the load was 5 ohms and from 7,5th second on load changes to 100 ohms.

Table 14. Tracking Performances

	Algorithms		
	ΔP and ΔV as inputs	**ΔP and ΔI as inputs**	**P-V slope and change of slope as inputs**
Efficiency(%)	**91,6114**	**76,6514**	**89,5991**
time to re-track the maximum power point (s)	**0,333**	**unable to re-track MPP**	**0,413**

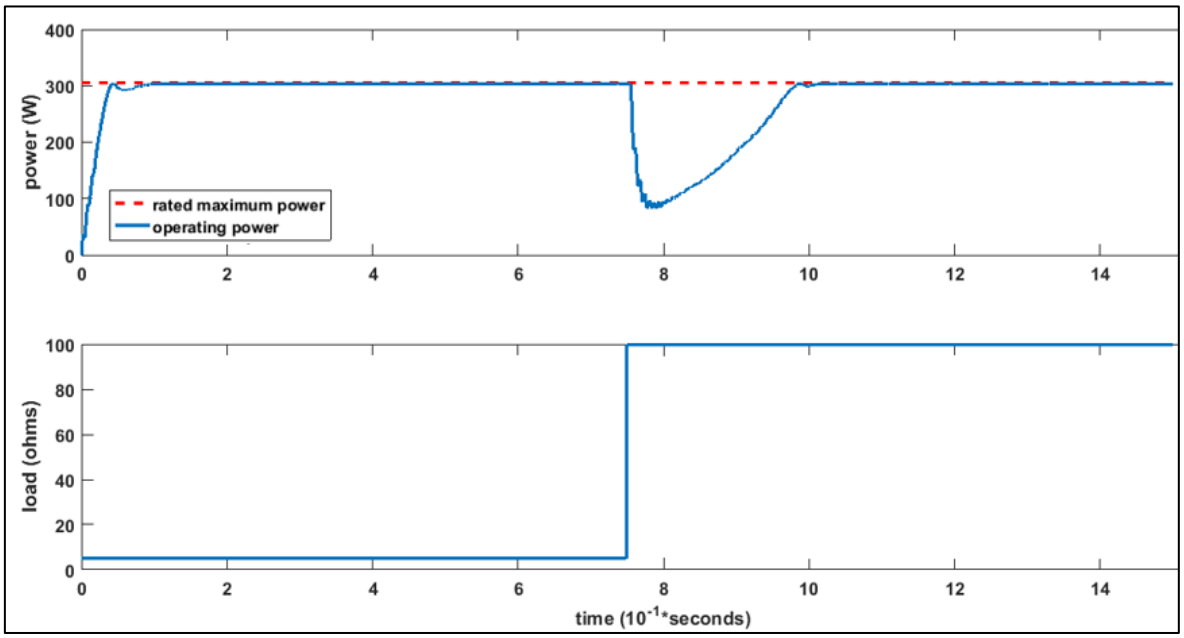

Figure 85. Simulation results (Algorithm Change of Power (ΔP_{PV}) and Change of Voltage (ΔV_{PV}) as Inputs)

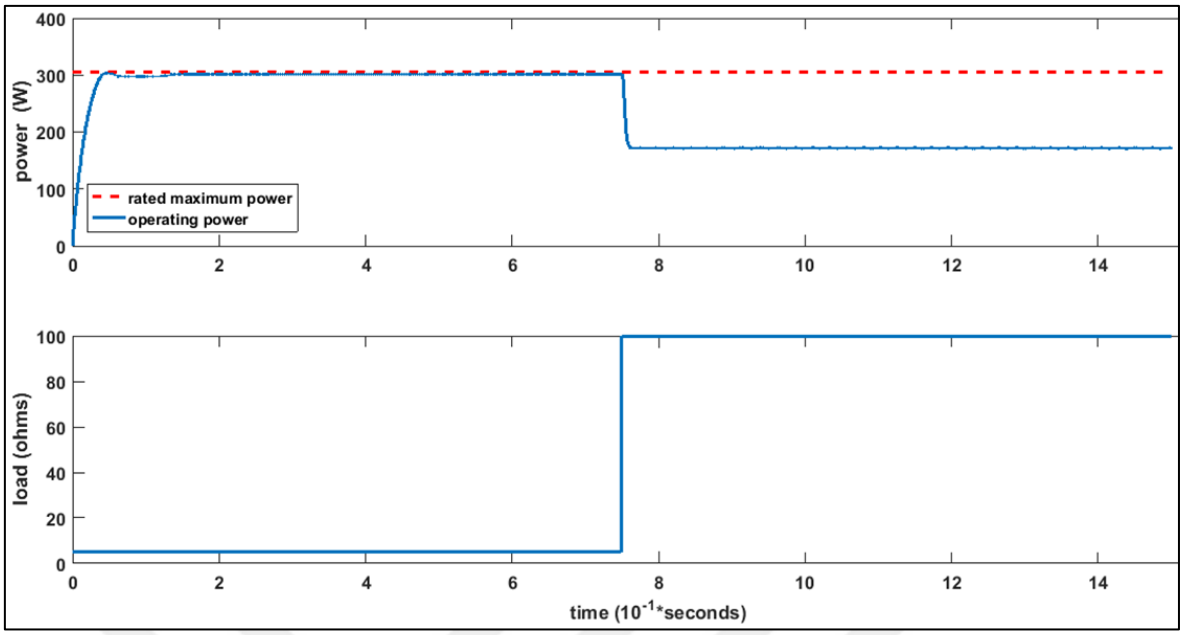

Figure 86. Simulation results (Algorithm Change of Power (ΔP_{PV}) and Change of Current (ΔI_{PV}) as Inputs).

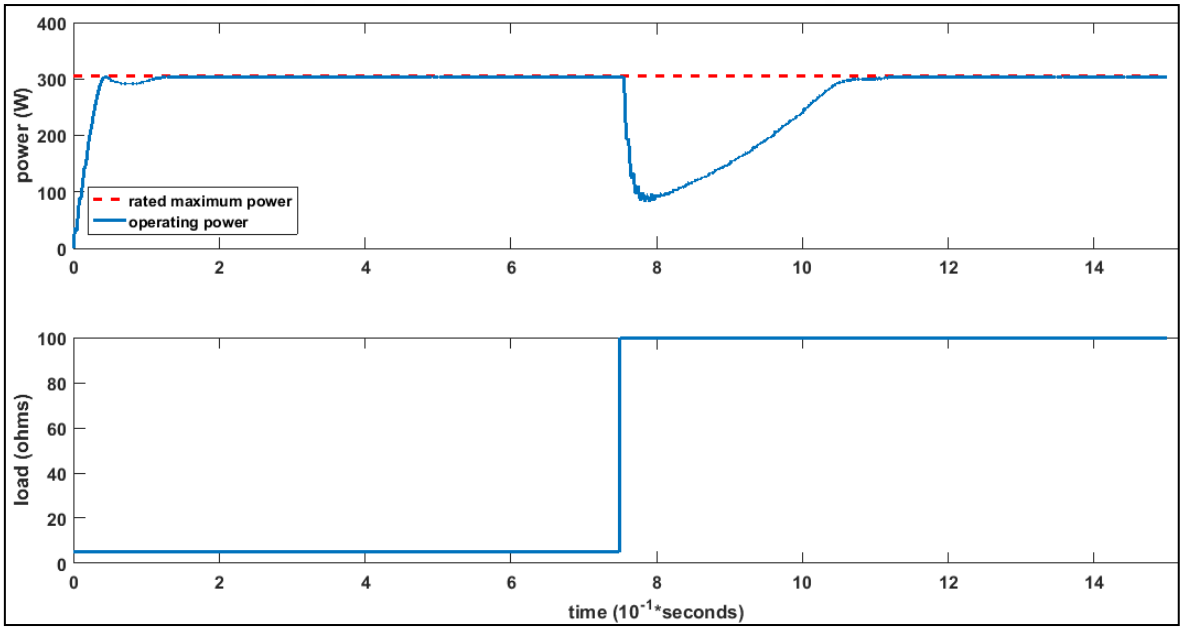

Figure 87. Simulation results (Algorithm P-V Slope and Change of Slope as Inputs).

3.4. Simulation Results Obtained when the PV Array Connected to the Grid.

Performance of the proposed MPPT system when PV array connected to the grid was examined by using the model represented at Figure 88. This model was quoted from [68]. Working principles of voltage/current controllers and phase locked loop (PLL) controllers used in this study is not going to be mentioned. For more information [68] can be reviewed.

In this model only the algorithm "P-V slope and change of slope as inputs" was used as MPPT algorithm. Boost converter that was used in [68] is replaced with buck-boost converter. The connection to the 25 kV grid is made by buck-boost converter and three-phase three-level voltage source converter (VSC). DC link voltage is regulated to 500 V and is converted to 260 V AC via VSC. Capacitor banks were used to filter harmonics. A 100 kVA 260/25 kV three phase transformer was used for coupling.

PV array consists of SPR-305E-WHT-D modules (66 parallel and 5 series connected) (66*5*305.2 W= 100.7 kW).

Table 15. Module parameters.

Module Parameters (SPR-305E-WHT-D)	
Maximum Power (W)	305,26
Open circuit voltage V_{OC} (V)	64,2
Temperature coefficient of V_{OC} (%/deg.C)	-0,27269
Cells per module	96
Short-circuit current I_{SC} (A)	5,96
Current at maximum power point I_{MP} (A)	5,58
Voltage at maximum power point V_{MP} (A)	54,7

Maximum power points of the PV array are;

At 1000 W/m^2 and 25 ˚C is 273,5 V and 100,7 kW

At 250 W/m^2 and 25 ˚C is 265,1 V and 24,4 kW

At 1000 W/m^2 and 50 ˚C is 250,2 V and 92,9 kW

Until the 0,05th second buck-boost converter and VSC were blocked. During this time three level inverter works as a rectifier and the capacitors between the terminals of the converter were charged to 500 V. After that blocking was disabled and DC voltage was

regulated to 500 V. Under these conditions the tracking efficiency was 95,21% and tracking accuracy was 99,62 %.

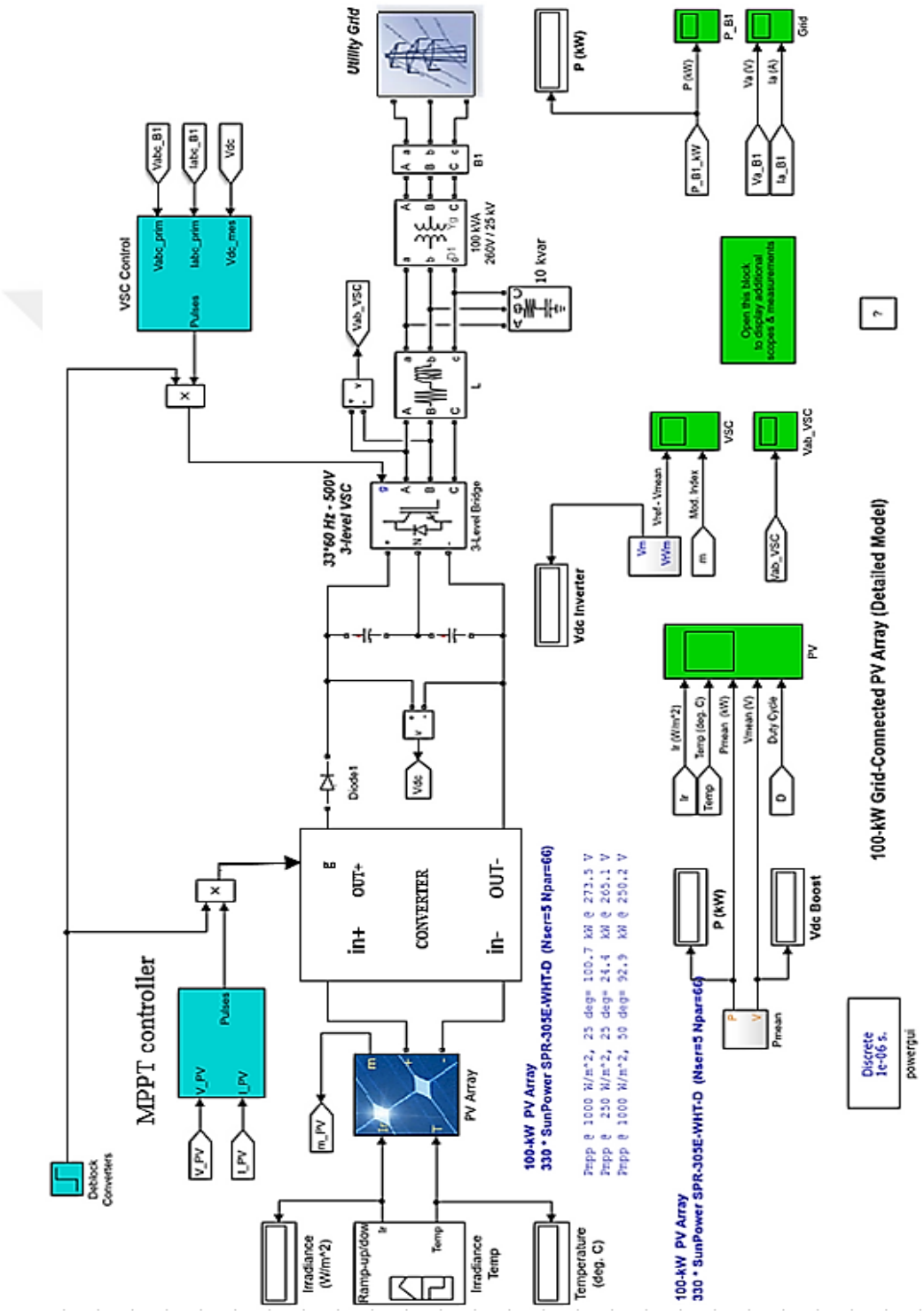

Figure 88. Simulink model of the grid connected PV system [68].

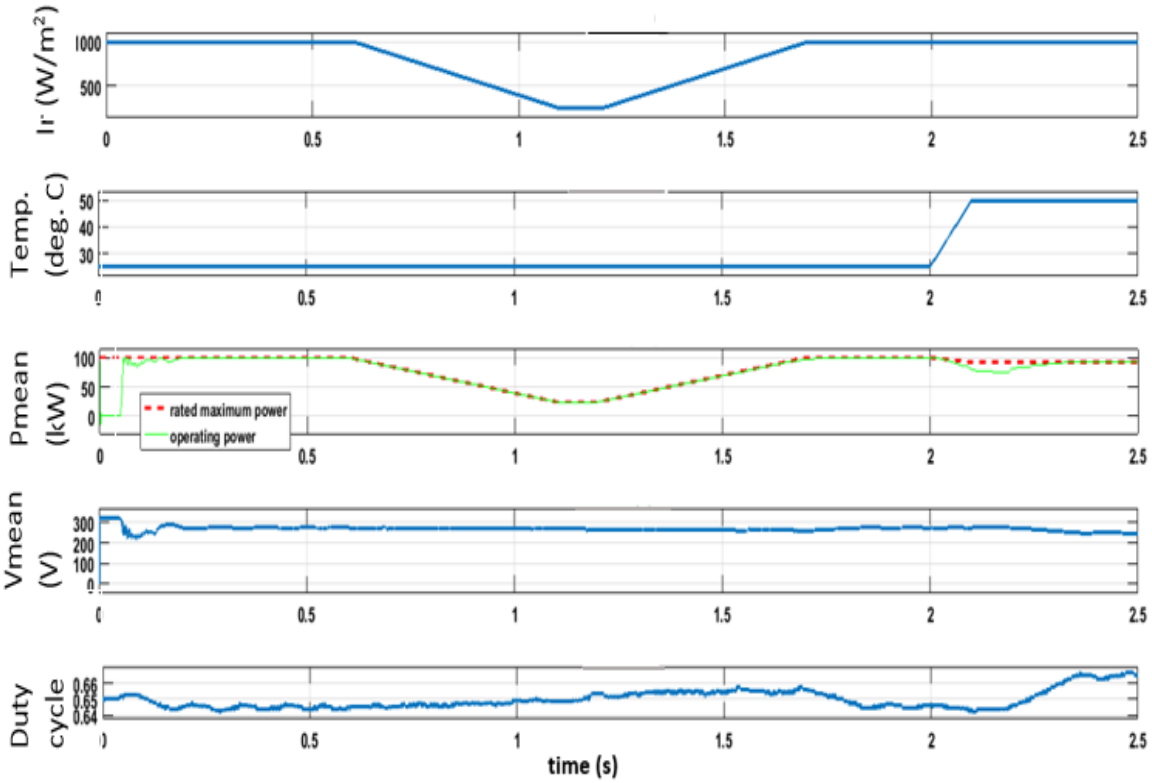

Figure 89. Operating conditions and PV generation values.

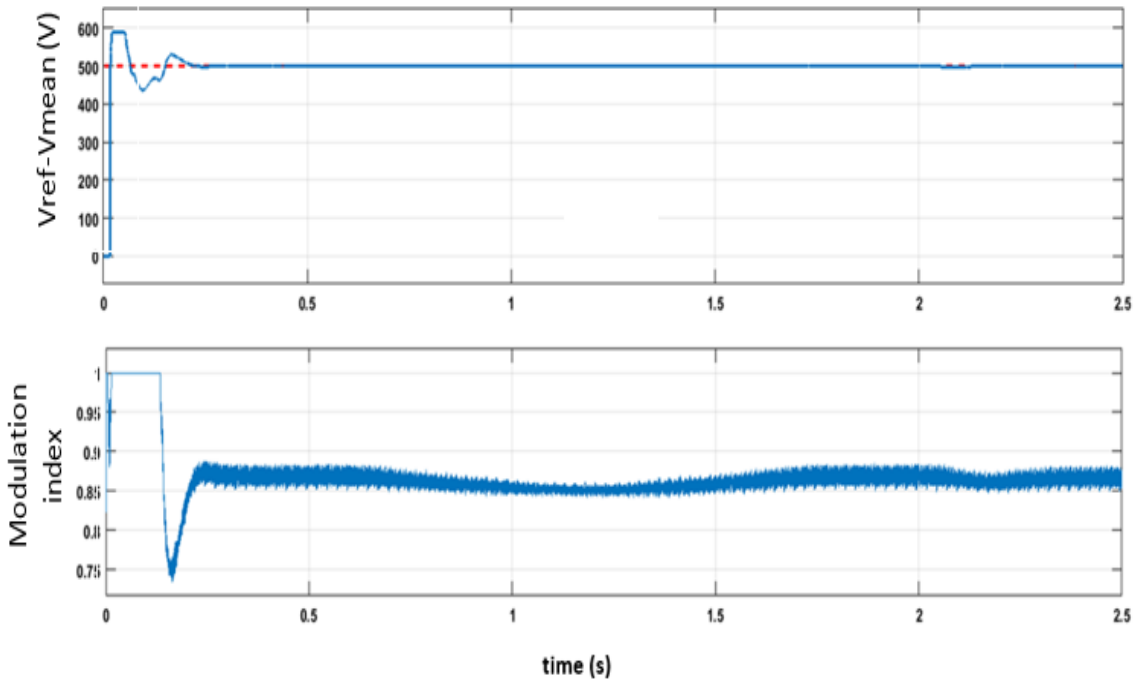

Figure 90. Reference DC voltage and regulated DC voltage.

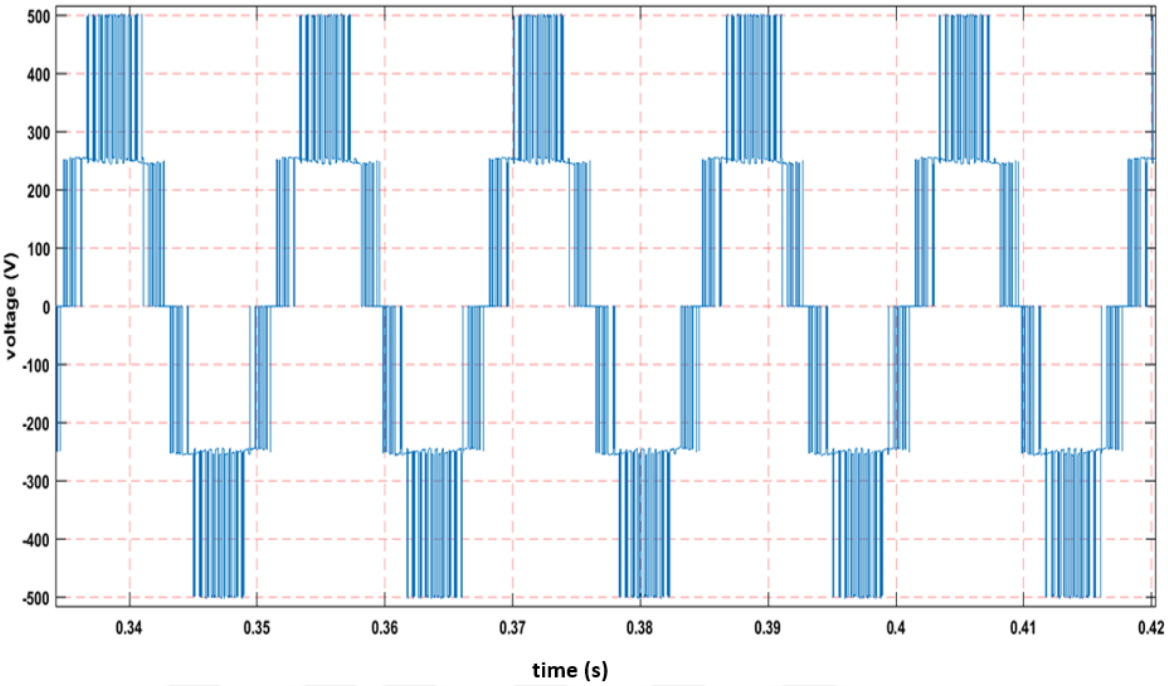

Figure 91. Output voltage of the three level inverter (phase to phase).

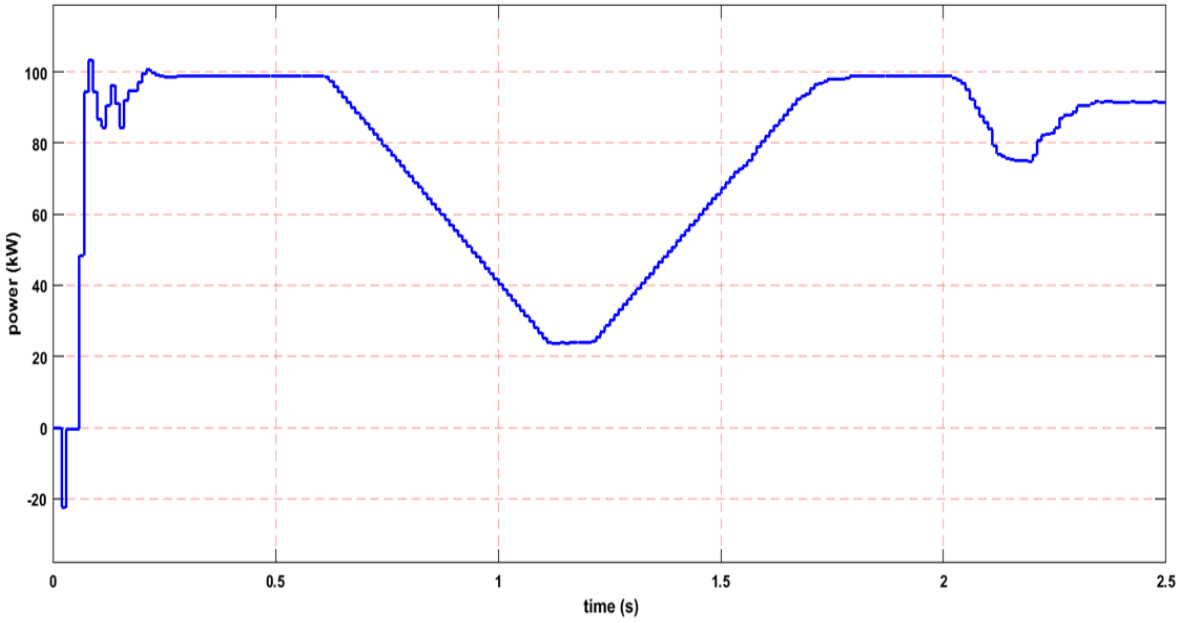

Figure 92. Power injected to the grid.

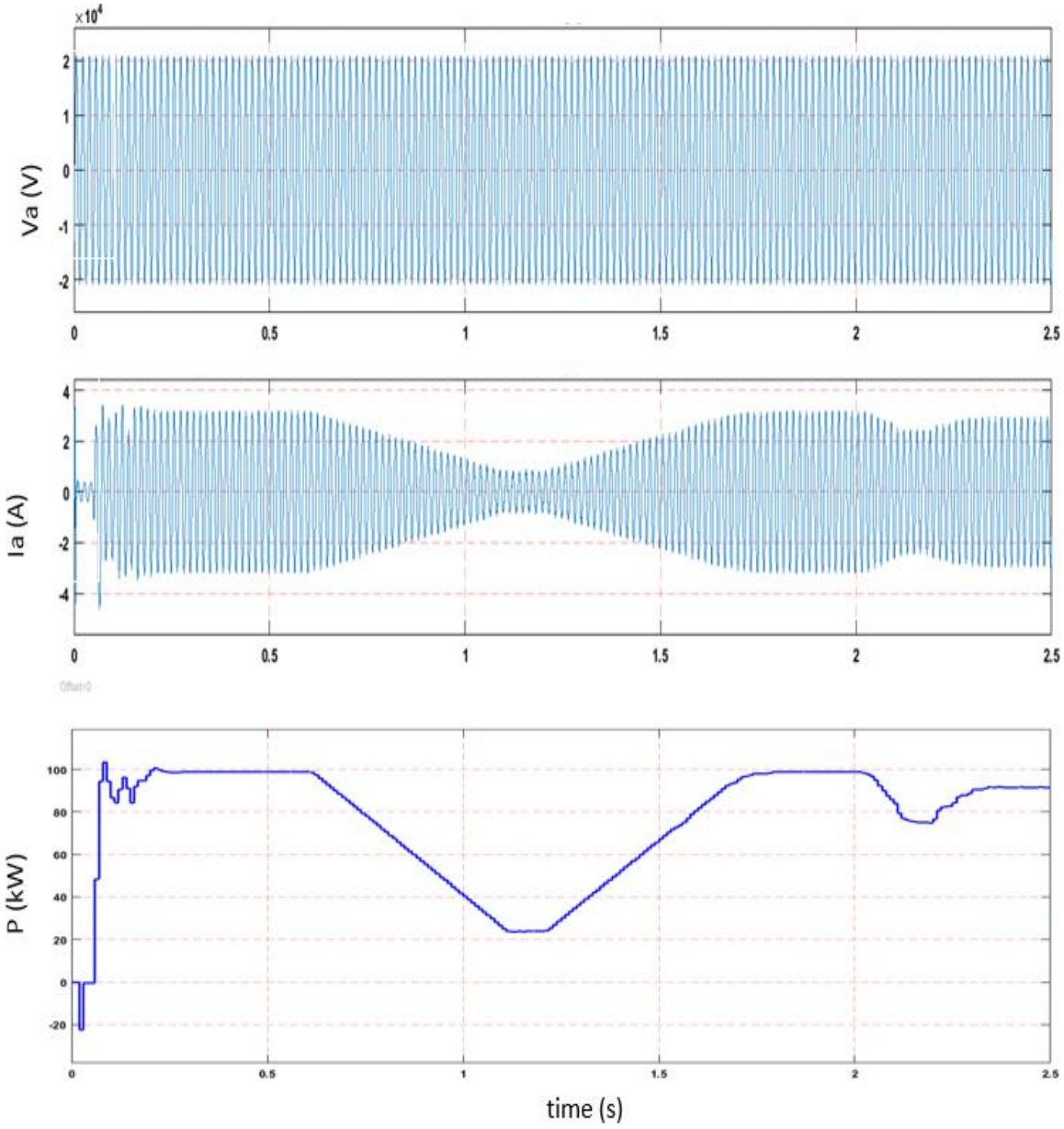

Figure 93. Voltage and current waveform of the power injected to the grid.

4. DISCUSSION

From the simulation results represented at Tables 8-9-10, we can obtain the results below.

Algorithm Change of Power (ΔP_{PV}) and Change of Voltage (ΔV_{PV}) as Inputs: This is a direct and easy method to track the MPP. Under changing irradiation and temperature levels with the symmetrical membership functions, the tracking efficiency is very low. This is because MPPT system was unable to track true MPP during fast environmental changes and at low irradiation levels. When asymmetrical membership functions were used the tracking speed and accuracy was increased to desired values and the tracking accuracy was 99,46 %.

Under unchanging irradiation/temperature levels and low irradiance levels, the tracking accuracy was about 98% when symmetrical MFs were used and about 99% when asymmetrical MFs were used.

When operating conditions were steady but the load was variable the tracking efficiency was about 91% with asymmetrical MFs. The settling time was about 0,333 seconds.

The main disadvantage of this method is that; the step size of the fuzzy controlling output could not be too high because of the oscillations around MPP. This causes a slower tracking speed.

Algorithm Change of Power (ΔP_{PV}) and Change of Current (ΔI_{PV}) as Inputs: This is a direct and easy method to track the MPP but inefficient under changing environmental conditions and low irradiation levels. Under changing irradiation and temperature levels with both symmetrical and asymmetrical membership functions, the tracking efficiency is high under the conditions defined in the simulations. But these results can misguide us because tracking accuracy was very low. Compared to other methods this method has the fastest tracking speed. So that using this method is advantageous when irradiation level increasing or stable.

Under unchanging irradiation/temperature levels and low irradiance levels, the tracking accuracy was about 34% when both symmetrical and asymmetrical MFs were used. This is because the MPPT system unable to track the MPP accurately.

When operating conditions were steady but the load was variable the tracking efficiency was about 76% with asymmetrical MFs.

The main disadvantage of this method is that; the step size of the fuzzy controlling output could not be too high because of the oscillations around MPP. This causes a slower tracking speed. During low irradiation levels the tracking accuracy is very low.

Algorithm P-V Slope and Change of Slope as Inputs: This is a direct and easy method to track the MPP too and change of slope is used to determine the approaching side to the MPP. Under changing irradiation and temperature levels with both symmetrical and asymmetrical membership functions, the tracking efficiency is about 88-89%. When both symmetrical and asymmetrical membership functions were used the tracking accuracy was about 99,5 %.

Under unchanging irradiation/temperature levels and low irradiance levels, the tracking accuracy was about 99,8% when symmetrical MFs were used and about 99,3% when asymmetrical MFs were used.

When operating conditions were steady but the load was variable the tracking efficiency was about 89,5% with asymmetrical MFs. The settling time was about 0,413 seconds.

This method was also used at the simulations when PV system was connected to the grid. During the simulations, the tracking efficiency was about 95%. MPPT system was able to track accurately and the tracking speed was at the desired level. This method is able to adapt to the high power applications.

5. CONCLUSION AND SUGGESTIONS

In this study a fuzzy logic based solar MPPT system, that provides the PV generators to operate at the maximum power point, was designed and different types of membership functions were used to optimize system's power generation performance. To achieve the goal of higher precision and fastest system responses to the changes of irradiation and temperature levels, different types of membership functions of inputs of fuzzy inference system were researched and compared with each other. The proposed system was used both standalone and grid connected PV systems and its disponibility was proved. The control output that was produced by the fuzzy controller was adaptive. That is, when the operating point was far away from the maximum power point the step size of the increment of control signal was bigger and when the operating point was near the maximum power point step sizes were smaller. By this way maximum power point was reached smoothly and fastly. And also the fluctuations were decreased to the lower levels.

It was revealed that the system performance at all operating conditions had been improved by using asymmetrical membership functions in the fuzzy logic controller. When we use symmetrical membership functions, we assume that all crisp values of the input variables get their degree of membership value symmetrically. But in practice the situation of symmetry at the distribution of the degree of memberships is not always possible. So that in order to improve the tracking accuracy and the tracking speed of the MPPT, we have to tune the membership functions that are used in the inference system. One of the biggest problem was that the tracking accuracy at low irradiation levels was lower. This accuracy was increased by using asymmetrical membership functions. There is one big advance of the proposed system; the buck-boost converter provides to track maximum point with all load values.

Different membership function tuning methods have been developed so far. In this study the tuning process was carried out by trial and error method. Trial and error method is an empirical method that uses the expert knowledge about the system. Implementation of this method is easy but it can take long time because of the repeated experiments to get the best results. From the results of simulations it can be inferred that the system performance is directly related with the optimization of the membership functions of fuzzy inference

system. This study also leads to the study of the designing methodology of optimization of asymmetrical membership functions for better system performance.

In practice partial shading situations of PV panels may occur. In such situations global maximum power points occurs. The proposed MPPT system would be improved to track these global maximum power points.

6. REFERENCES

1. International Energy Agency. Technology Roadmap: Solar Photovoltaic Energy, Paris, France, 2014.

2. Tomabechi, K., Energy Resources in the Future, Energies, 3 (2010) 686–695.

3. Femia, N., Petrone, G., Spagnuolo, G. and Vitellio, M., Optimization of Perturb and Observe Maximum Power Point Tracking Method, IEEE Trans. Power Electronics, 20, 4 (2005) 963–973.

4. Yong, T., Xia, B., Xu, Z. and Sun, W., Modified Asymmetrical Variable Step Size Incremental Conductance Maximum Power Point Tracking Method for Photovoltaic Systems, Journal of Power Electronics, 14, 1 (2014) 156–164.

5. Chin, C.S., Neelakantan, P., Yoong, H.P. and Teo, K.T.K., Optimisation of Fuzzy based Maximum Power Point Tracking in PV System for Rapidly Changing Solar Irradiance, Trans. Solar Energy Plan, 2 (2011) 130–137.

6. Radjai, T., Gaubert, P.J. and Rahmani, L., The new FLC-Variable Incremental Conductance MPPT Direct Control Method Using Cuk Converter, International Symposium on Industrial Electronics (IEIE), 2014, Istanbul, 2508–2513.

7. Rahmani, R., Seyedmahmoudian, M., Mekhilef, S. and Yusof, R., Implementation of Fuzzy Logic Maximum Power Point Tracking Controller for Photovoltaic System, American Journal of Applied Sciences, 10, 3 (2013) 209–218.

8. Shiau, J.K., Wei, Y.C. and Chen, B.C., A Study on the Fuzzy Logic Based Solar Power MPPT Algorithms Using Different Fuzzy Input Variables, Algorithms, 8 (2015) 100-127.

9. Ferret, F.A. and Simões, M.G., Integration of alternative sources of Energy, Wiley-Interscience IEEE Press, New Jersey, 2006.

10. Martín, C., Belver, Z., Lesaka, L. and Guerrero, Z., Modelling of Photovoltaic Module, International Conference on Renewable Energies and Power Quality (ICREPQ'10), March 2010, Granada, 1186-1190.

11. Pandiarajan, N. and Ranganath, M., Mathematical Modeling of Photovoltaic Module with Simulink, 1st International Conference on Electrical Energy Systems (ICEES), March 2011, California, 258-263.

12. Kashif I., Zainal S., Saad M. and Amir S., Parameter Extraction of Solar Photovoltaic Modules Using Penalty-Based Differential Evolution, Science-Direct, 99 (2012) 297-308.

13. Skoplaki E. and Palyvos J. A., On the Temperature Dependence of Photovoltaic Module Electrical Performance: A review of efficiency/power correlations, Science-Direct, 83 (2009) 614–624.

14. http://www.alternative-energy-tutorials.com/energy-articles/solar-cell-i-v characteristic.html Alternative Energy Tutorials, 22 February 2017.

15. Liu, B., Duan, S., Liu, F. and Xu, P., Analysis and Improvement of a Maximum Power Point Tracking Algorithm Based on Incremental Conductance Method for Photovoltaic Array, International Conference on Power Electronics and Drive Systems, November 2007, Bangkok, 637-641.

16. Yuvarajan, S. and Shoeb, J., A Fast and Accurate Maximum Power Point Tracker for PV Systems, Applied Power Electronics Conference and Exposition, May 2008, Texas, 167-172.

17. Femia, N., Petrone, G., Spagnuolo, G., and Vitelli, M., Optimizing Sampling Rate of P&O MPPT Technique, Power Electronics Specialist Conference, June 2004, Aachen, 1945-1949.

18. Pandey, A., Dasgupta, N. and Mukerjee, A., Design Issues in Implementing MPPT for Improved Tracking and Dynamic Performance, IEEE Conference on Industrial Electronics, April 2007, Paris 4387-4391.

19. Onat, N., Recent Developments in Maximum Power Point Tracking Technologies for Photovoltaic Systems, International Journal of Photoenergy, 2010 (2010) 1-11.

20. Coelho, R.F. and Martins, D.C., An Optimized Maximum Power Point Tracking Method Based on PV Surface Temperature Measurement, Sustainable Energy-Recent Studies, InTech, 2012.

21. Ghaisari, J., Habibi, M., and Bakhsahi, A., A MPPT Controller Design for Photovoltaic (PV) System Based on the Optimal Voltage Factor Tracking, IEEE Canada Electrical Power Conference, October 2007, Montreal, 359-362.

22. Tan, C. W., Green, T. C., and Hernandez-Aramburo, C. A., Analysis of Perturb and Observe Maximum Power Point Tracker Algorithm for Photovoltaic Applications, IEEE 2nd International Power and Energy Conference, December 2008, Johor Bahru, 237-242.

23. Askarzadeh, A., Voltage prediction of a photovoltaic module using artificial neural networks. International Transactions on Electrical Energy Systems, 24 (2014) 1715-1725.

24. Theocharis A.D. and Pyrgioti E.C., Development of a Linearized Photovoltaic Generator Model for Simulation Studies with Electromagnetic Transient Programs, International Transactions on Electrical Energy Systems, 25 (2014) 454-470.

25. Messai, A., Mellit, A., Massi, P.A., Guessoum, A. and Mekki, H., FPGA-Based Implementation of a Fuzzy Controller (MPPT) For Photovoltaic Module, International Journal of Energy Conversion Management, 52 (2011) 2695–2704.

26. Larbes, C., Ait Cheikh, S.M., Obeidi, T. and Zerguerras, A., Genetic Algorithms Optimized Fuzzy Logic Control for the Maximum Power Point Tracking in Photovoltaic System, Renewable Energy, 34 (2009) 2093–2100.

27. Messai, A., Mellit, A., Guessoum, A. and Kalogirou, S.A., Maximum Power Point Tracking Using a GA Optimized Fuzzy Logic Controller and its FPGA Implementation, Solar Energy, 85 (2011) 265–277.

28. Letting, L.K., Munda, J.L. and Hamama, Y., Optimization of a Fuzzy Fogic Controller for PV Grid Inverter Control Using S-function Based PSO. Solar Energy, 85,2 (2012) 1689–1700.

29. Kottas, T.L., Boutalis, Y.S., Karlis, A.D., New Maximum Power Point Tracker for PV Arrays Using Fuzzy Controller in Close Cooperation With Fuzzy Cognitive Networks, IEEE Transactions on Energy Conversion, 21, 3 (2006) 793–803.

30. Algazar, M.M., Al-Monier, H., El-Halim, H.A. and Salem, M.E.E.K., Maximum Power Point Tracking Using Fuzzy Logic Control, International Journal of Electrical Power and Energy Ssystems, 39, 1 (2012) 21-28.

31. Guenounou, O., Dahhou, B. and Chabour, F., Adaptive Fuzzy Controller Based MPPT for Photovoltaic Systems, Journal of Energy Conversion and Management, 78 (2014) 843–850.

32. Bendiba, B., Krimb, F., Belmilia, H., Almia, M.F. and Bouloumaa, S., Advanced Fuzzy MPPT Controller for a Stand-Alone PV system, Energy Procedia, 50 (2014) 383–392.

33. Altin, N. and Ozdemir, S., Three-Phase Three-Level Grid Interactive Inverter with Fuzzy Logic Based Maximum Power Point Tracking Controller, Journal of Energy Conversion and Management, 69 (2013) 17–26.

34. Mohd Zainuri, M.A.A., Mohd Radzi, M.A., Soh, A.C. and Rahim, N.A., Development of Adaptive Perturb and Observe Fuzzy Control Maximum Power Point Tracking for Photovoltaic Boost DC-DC Converter, IET Renewable Power Generation, 8 (2014) 183–194.

35. http://www.greenmatch.co.uk/blog/2014/11/how-efficient-are-solar-panels Greenmatch, 8 March 2017.

36. Ponce-Cruz, P. and Ramirez-Figueroa, F.D., Intelligent Control Systems with LabVIEW, Springer, London, 2010.

37. Kecman, V., Learning and Soft Computing Support Vector Machines, Neural Networks, and Fuzzy Logic Models, The MIT Press, London, 2001.

38. Ross, T.J., Fuzzy Logic with Engineering Application, Second Edition, Wiley, Sussex, 2004.

39. Holmblad, L.P. and Ostergaard, J.J., Control of Cement Kiln by Fuzzy Logic, Fuzzy Information and Decision Processes, 1982, Amsterdam, 389-399.

40. Er, M.J. and Sun, L.Y., Hybrid Fuzzy Proportional Integral Plus Conventional Derivative Control of Linear and Nonlinear Systems, IEEE Transactions on Industrial Electronics, 48 (2001) 1109-1117.

41. Wu, J.C. and Liu, T.S., A Sliding-Mode Approach to Fuzzy Control Design, IEEE Trans. On Control Systems Technology, 4, 2 (1996) 141-151.

42. Li, H.X. and Gatland, H.B., A New Methodology for Designing a Fuzzy Logic Controller, IEEE Trans. On Sys. Man, and Cybernetics, 25, 3 (1995) 505-512.

43. Yen, J. and Langari, R., Fuzzy Logic: Intelligence, Control, and Information, Prentice Hall, New Jersey, 1999.

44. Bai, Y., Zhuang, H. and Roth Z.S., Fuzzy Logic Control to Suppress Noises and Coupling Effects in a Laser Tracking System", IEEE Trans on Control Systems Technology, 13, 1 (2005) 113-121.

45. Wang, C., A Study of Membership Functions on Mamdani-Type Fuzzy Inference System for Industrial Decision-Making, MSc Thesis, Lehigh University, Bethlehem, 2015.

46. https://www.mathworks.com/help/fuzzy/what-is-fuzzy-logic.html Mathworks, 15 March 2017.

47. https://www.mathworks.com/help/fuzzy/building-systems-with-fuzzy-logic-toolbox-software.html Mathworks, 15 March 2017.

48. Liu, F., Duan, S., Liu, B. and Kang, Y., A variable step size INC MPPT method for PV systems, IEEE Transactions on Industrial Electronics, 55, 7 (2008) 2622–2628.

49. Adly, M., Ibrahim, M. and El Sherif H., Comparative Study of Improved Energy Generation Maximization Techniques for Photovoltaic Systems, Asia-Pacific Power and Energy Engineering Conference (APPEEC '12), March 2012, Shanghai, 1-5.

50. Wolfs, P. and Li, Q., A Current-Sensor-Free Incremental Conductance Single Cell MPPT for High Performance Vehicle Solar Arrays, IEEE Power Electronics Specialists Conference (PESC '06), June 2006, Jeju, 1–7.

51. Liu, C., Wu, B. and Cheung, R., Advanced Algorithm for MPPT Control of Photovoltaic Systems, Canadian Solar Building Conference, August 2004, Montreal, 53-61.

52. Al-Amoudi, A. and Zhang, L., Optimal Control of a Grid Connected PV System for Maximum Power Point Tracking and Unity Power Factor, International Conference on Power Electronics and Variable Speed Drives, September 1998, London, 80–85.

53. Suganya, J. and Mabel, M.C., Maximum Power Point Tracker for a Photovoltaic System, International Conference on Computing, Electronics and Electrical Technologies (ICCEET '12), March 2012, Kumaracoil, 463–465.

54. Ciabattoni, L., Grisostomi, M., Ippoliti, G. and Longhi, S., Neural Networks Based Home Energy Management System in Residential PV Scenario, IEEE Photovoltaic Specialists Conference (PVSC ’13), Tampa, June 2013, 1721–1726.

55. Sheraz, M. and Abido, M.A.,An Efficient MPPT Controller Using Differential Evolution and Neural Network, IEEE International Conference on Power and Energy (PECon ’12), December 2012, Kota Kinabalu, 378–383.

56. Elobaid, L.M., Abdelsalam, A.K. and Zakzouk, E.E., Artificial Neural Network Based Maximum Power Point Tracking Technique for PV Systems, 38th Annual Conference on IEEE Industrial Electronics Society (IECON ’12), October 2012, Montreal, 937–942.

57. Chiu, Y.H., Luo, Y.F., Huang, J.W. and Liu, Y.H., An ANN Based Maximum Power Point Tracking Method for Fast Changing Environments, Joint International Conference on IEEE Soft Computing and Intelligent System (SCIS ’12) and 13th International Symposium on Advanced Intelligent System (ISAIS ’12), November 2012, Kobe, 715–720.

58. Anitha, S.D. and Prabha, S.B.J., Artificial Neural Network Based Maximum Power Point Tracker for Photovoltaic System, International Conference on Sustainable Energy and Intelligent Systems (SEISCON ’11), July 2011, Chennai, 130–136.

59. Sreekumar, S. and Benny, A., Maximum Power Point Tracking of Photovoltaic System Using Fuzzy Logic Controller Based Boost converter, International Conference on Current Trends in Engineering and Technology (ICCTET ’13), July 2013, Coimbatore, 275–280,

60. Hossain, M.I., Khan, S.A., Shafiullah, M. and Hossain, M.J., Design and Implementation of MPPT Controlled Grid Connected Photovoltaic System, IEEE Symposium on Computers and Informatics (ISCI ’11), March 2011, Kuala Lumpur, 284–289.

61. Wang, Y., Yang, H., Li, A. and Wang, Y., Research of Photovoltaic and PHEV Hybrid Management System Based on Hierarchical Fuzzy control, 8th International Conference on Electrical Engineering, Computing Science and Automatic Control (CCE ’11), October 2011, M´erida , 1–5.

62. Chin, C.S., Chin, Y.K., Chua, B.L., Kiring, A. and Teo, K.T.K., Fuzzy Logic Based MPPT for PV Array Under Partially Shaded Conditions, International Conference on Advanced Computer Science Applications and Technologies (ACSAT ’12), November 2012, Kuala Lumpur, 133–138.

63. Kulaksiz, A.A. and Aydoğdu, O., ANN-Based Maximum Power Point Tracking of Photovoltaic System Using Fuzzy Controller, International Symposium on Innovations in Intelligent Systems and Applications (INISTA ’12), July 2012, Trabzon, 1–5.

64. Miyatake, M., Toriumi, F., Endo, T. and Fujii, N., A Novel Maximum Power Point Tracker Controlling Several Converters Connected to Photovoltaic Arrays with Particle Swarm Optimization Technique, Power Electronics and Applications (EPE ’07), September 2007, Aalborg, 1–10.

65. Phimmasone, V., Kondo. Y., Endo, T. and Miyatake, M., Improvement of the Maximum Power Point Tracker for Photovoltaic Generators with Particle Swarm Optimization Technique by Adding Repulsive Force Among Agents, Electrical Machines and Systems (ICEMS 2009), November 2009, Tokyo, 1-6.

66. Ishaque, K. and Salam, Z., A Deterministic Particle Swarm Optimization Maximum Power Point Tracker for Photovoltaic System under Partial Shading Condition, IEEE Transactions on Industrial Electronics, 60, 8 (2013) 195–206.

67. Ramaprabha, R. and Mathur, B.L., Genetic Algorithm Based Maximum Power Point Tracking for Partially Shaded Solar Photovoltaic Array, Int. J. Res. Rev. Inf. Sci. (IJRRIS), 2 (2012) 161–166.

68. https://www.mathworks.com/examples/simpower/mw/sps_product-power_PVarray_grid_det-detailed-model-of-a-100-kw-grid-connected-pv-array Mathworks, 2 May 2017.

CURRICULUM VITAE

Adem KOCABAŞ was born in 1985 in Trabzon. Completed his secondary and high school education at Akçaabat Anatolian High School. Received Bachelor of Science degree in electrical-electronics engineering from Karadeniz Technical University, Trabzon in 2007. Ranked first among the 2007 graduate students. At same year enrolled for Master of Science degree in Karadeniz Technical University Electrical-Electronics Engineering Department. Has been working in Türk Telekomünikasyon A.Ş. since 2007 as an access network operating senior engineer. Speaks fluent English.